A Three-dimensional Forward Dynamic Model of the Golf Swing

by

Daniel Johnson

A thesis

presented to the University of Waterloo

in fulfillment of the

thesis requirement for the degree of

Master of Applied Science

in

Systems Design Engineering

Waterloo, Ontario, Canada, 2015

I hereby declare that I am the sole author of this thesis. This is a true copy of the thesis, including any required final revisions, as accepted by my examiners.

I understand that my thesis may be made electronically available to the public.

Abstract

A three-dimensional (3D) predictive golfer model can be a valuable tool for investigating the golf swing and designing new clubs. A forward dynamic model for simulating golfer drives is presented, which includes: (1) a four degree of freedom golfer model, (2) a flexible shaft model based on Rayleigh beam theory, (3) an impulse-momentum impact model, (4) and a spin rate controlled ball trajectory model. The input torques for the golfer model are provided by parameterized joint torque generators that have been designed to mimic muscular inputs. These joint torques are optimized to produce the longest ball carry distance for a given set of golf club design parameters. The flexible shaft model allows for continuous bending in the transverse directions, axial twisting of the club and variable shaft stiffness along its length. The completed four-part model is used for examining the following parameters of interest in club design by performing simulation experiments: clubhead mass, clubhead centre of mass location, clubhead moment of inertia, shaft flexibility, and clubhead and shaft aerodynamics.

Analysis of the experiments led to the following recommendations for golf club design:

1. The clubhead mass should continue to be around 200g.

2. The centre of mass of the clubhead should be as close to the face as possible.

3. Shaft flexibility should be tuned for an individual golfer, depending on their particular swing.

4. Clubhead and shaft aerodynamic drag have a significant effect on the ball carry and clubhead orientation, and should be minimized during the club design process.

Finally, suggestions are made for future research which can be performed in this area.

Acknowledgments

Table of Contents

List of Figures

xi

List of Tables

Chapter 1

Introduction

Golf is a sport played by an estimated 80 million people worldwide on nearly 40000 courses [5]. Players and manufacturers spend billions of dollars on events, golf tourism, and equipment to play the game. To capture this market, golf equipment companies are constantly designing new clubs for players to use, promising gains in driving distance and accuracy, improved spin control, or other benefits to players who buy the latest technology. While it is clear that golf club technology has improved over the last 30 years [6], there is still a significant lack of understanding of the mechanisms behind this improvement. Golfers are left searching for answers within a haze of marketing information without clear scientific basis.

This thesis seeks to build our scientific understanding of the golf swing through modeling and simulation of golfers and their equipment. Along with improving our understanding of the golf swing, simulations can be used to help design and evaluate new golf clubs quickly and inexpensively.

1.1 Motivation and Goals

Computer simulations are used extensively in the design of multibody dynamic systems. In the past they have mostly been used for designing the mechanical and electrical components of systems, but improved techniques have allowed researchers to begin simulating humans interacting larger systems in biomechatronic models [7]. Simulations of the golf swing have been used since the 1970s to attempt to discover how to golf more effectively. By modeling the golf swing, we can gain insights into how golfers should swing and the best ways to design their equipment.

The goal of this project is to develop a biologically-motivated golf swing model including the golfer and club that can be evaluated based on its performance in striking the ball. The model should include variable parameters for golfer to allow for optimization of the swing and variable parameters for the golf club to test and evaluate different designs.

1.2 Project Outline

The project began with a review of existing golfer models that have been used to simulate the golf swing. The review focused on establishing what parts of the swing have been modeled and what opportunities exist for developing new golfer models. In addition, a review of manufacturer's claims for the capabilities of new golf clubs was performed to determine what questions the model could be used to answer. This review led to the conclusion that there was a need for a biologically-motivated golf swing model that could be used for evaluating golf clubs and the marketing claims made about them. This model should be able to swing clubs in an optimal fashion and capture the biomechanics relevant to the golf swing.

To easily evaluate golf clubs within the context of the model a four-step golfer model was proposed including the golfer, club, impact with the ball, and aerodynamics of the ball's flight. Different models were considered for each step, and the resulting selections combined together into a single simulation. This simulation of a golfer striking the ball is then optimized by changing the timing of the muscular torques that drive the model.

The final model was then used to perform several experiments on the claims made by manufacturers about new club designs. Club mass, club head moment of inertia, club head centre of mass position, and club flexibility are all examined within the context of the model. The effect of golfer strength was also investigated. Finally, the limitations of the model are addressed and some recommendations made for how to improve and expand its capabilities are made.

1.3   Contributions

- Overall contribution: A biological golfer model that can be evaluated using ball trajectories.

- Inclusion of a continuous flexible golf club model based on Rayleigh beam theory in a forward dynamic golfer and swing model.

- Method for providing joint torques that mimic those provided by muscles, including both passive and active biological contributions.

- A combined impact and aerodynamics model for predicting ball flight.

- An optimization technique for determining the best swing based on ball carry for a particular golfer and club combination.

- A clubhead aerodynamic model that can be used in forward dynamic simulation.

- A shaft aerodynamic model that can be used in conjunction with the flexible beam.

1.4   Document Structure

This document describes the process through which the four-part golfer model is created. Chapter 1 describes the goals and motivations for the project and the major contributions of this work. Chapter 2 has two goals: first, in Sections 2.1 and 2.2 to describe the basic biomechanics and physics which affect the golf swing and club design, and second in Section 2.3 to perform a literature review of the existing golfer models.

Chapter 3 describes the four-part golfer model created for this work. It is divided into four sections: Section 3.1 describes the golfer portion of the model including active and passive joint torques; Section 3.2 details the flexible club used, including aerodynamics on the clubhead and shaft; Section 3.4 describes the impulse-momentum based impact model; and Section 3.5 discusses the ball aerodynamic model.

In Chapter 4 the combined model is used to investigate the effect of golf club design decisions on the performance of golf clubs. Evaluations of the effect of a variety of golfer and club parameters on the success of the golf swing are performed and the results investigated. Limitations of the model are also addressed in this chapter.

Finally, in Chapter 5 the project is summarized and recommendations for future work are made.

Chapter 2

Background and Literature Review

In 1968, *Search for the Perfect Swing* by Cochran and Stobbs began the serious scientific study of the golf swing with a simple two-dimensional model of the swing based on a spring-powered double-pendulum [8]. They investigated the golfer's motion using strobe photography and developed simple models for the biomechanics of the swing, impact with the ball, and aerodynamic flight. Since then, the search has continued with ever more refined models to improve our understanding of the golf swing and the equipment golfers use.

This Chapter examines the basic mechanics of the golf swing, impact with the ball, and aerodynamics in Section 2.1. Section 2.2 then provides a short summary of the factors involved in designing a golf driver and the claims of manufacturers that are producing new clubs. Finally, in Section 2.3, a literature review of previous golfer and club models is provided. The conclusion of this review is that while a number of different golfer and club models have been created, there is no model available that is well-suited for evaluating club performance. No model exists that combines a biologically-motivated golfer model

with a sufficiently complex club model where ball strikes can be evaluated based on the success of the resulting drive. This is the gap which this project seeks to address.

2.1 Golf Swing

The golf swing is a complicated and precisely timed motion of the human body perfected by the best players with tens of thousands of repetitions. A successful swing results in striking the ball so that it flies to a desired location. For a drive, the goal is to hit the ball as far downrange as possible and to land in the fairway. The result of any particular swing depends on the behaviour of the golfer, club, impact with the ball, and the aerodynamics of ball flight. This section describes the basic physical principles which are necessary for describing and modeling the golf swing.

2.1.1 Biomechanics of the Golfer

The biomechanics of the swing can be broken down into three sections. First, during the backswing, the golfer lifts the club from the address position and coils their torso, shoulder, and wrist to position the clubhead for an accurate and powerful downswing. At the end of the backswing, a typical, right-handed, golfer will have rotated their shoulders more than 90 degrees [9], brought their left arm across the front of their body (abducted 75° to 90°) with the elbow fully extended, and maximally radially deviated their left wrist [10]. During the backswing, the club and arms generally travel within a single plane and the left hand (of a right-swinging golfer) is in control of the club.

During the downswing, which generally lasts between $0.2\,\mathrm{s}$ and $0.25\,\mathrm{s}$ [8], the left arm once again controls the club, providing the majority of the moment required to bring the

6

club to the ball. The downswing begins with the rotation of the torso by the pelvis and this motion generally begins before the backswing is complete [11]. The muscles of the torso activate as the club is accelerated downwards, the arm externally rotates as it comes across the body, and the wrist remains cocked as long as possible to maximize the speed of the clubhead. In general, the motions follow the kinetic chain from proximal to distal elements (torso, shoulder, arm rotation, and wrist uncocking) [12].

Finally, in the follow-through, the body and clubhead are decelerated using eccentric muscle action. The arm and club continue to swing through along the club plane. The golfer finishes their swing in a balanced position with the arms extended above the head.

Is the swing planar?

One question which has been examined by many researchers is whether the swing is planar and whether it is useful to model the swing as a planar motion. While it seems clear that many models have been able to obtain useful results from a planar swing, the question remains as to whether more useful information can be found from more complicated models.

In particular, Coleman and Rankin conducted a study in 2005 that challenged the assumption of a planar swing through experiment [13]. They used motion capture technology to capture the motions of 7 low-handicap golfers. When examining the planes of motion of the swing, they found that there was not a consistent plane throughout the downswing, and that more complex models should be developed. This idea is confirmed by Iwatsubo, who studied two link (planar) and four link (non-planar) models of the golf swing and concluded that four link models are better for evaluating golfer performance [14]. In particular, the joint torques that are required to actuate the model are more accurate in the four-link model.
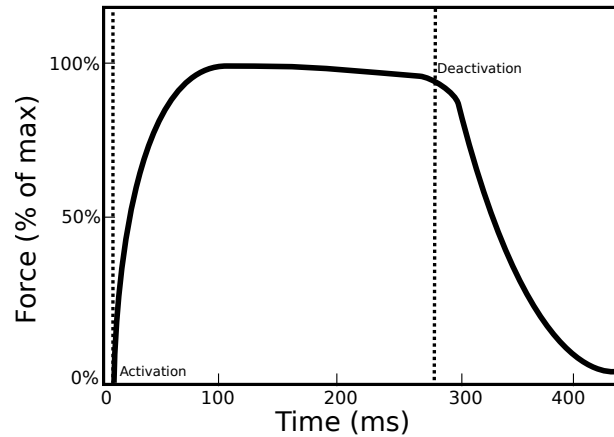
Figure 2.1: An illustration of muscle activation and deactivation dynamics [1].

2.1.2 Muscle Dynamics and Passive Joint Torques

An important aspect of the biomechanics of the golfer is the dynamics of the muscles that power the swing. How the golfer's muscles behave affect how the swing can be controlled and how much power can be generated.

Muscles are not able to produce instantaneous force at any level within their range of operation. After activation, it can take 5 ms to 10 ms for a single muscle fibre to reach its maximum tension and the recruitment of all the muscle fibres in a single muscle can take 100 ms to 200 ms [1]. The force provided by a single muscle approaches the maximum value over this period and is can be modeled using a first-order function. Similarly, when the muscle is relaxed, the force does not drop instantaneously, but ramps down over a longer time period. This phenomenon is illustrated in Figure 2.1.

In addition, there are two well-studied relationships which govern the amount of force that a well-rested muscle can produce relative to its maximum. The force-length and force-velocity curves for muscles are important in determining the amount of force that

8

any given muscle can produce at an instant and need to be considered in the development of biomechanical models. Other muscle characteristics, such as history dependence and fatigue, are ignored as the time scales involved in the golf swing are very short.

Force-Length Relationship for Muscles

First the force-length relation describes the relation between muscle length and the force the muscle can exert. The cross-bridge theory of muscle dynamics explains muscle force generation as the interaction between adjacent filaments in the muscle [1]. Depending on the amount of overlap between adjacent filaments more or less force can be generated. For each muscle, there is an optimal length region where maximum force can be generated. Beyond that region, the filaments overlap less and therefore less force is generated. At shorter lengths, the filaments interfere with each other and force generation is reduced. In addition, the force required to further deform the muscle at these lengths is increased and less force is available to be applied beyond the muscle. Figure 2.2 illustrates the shape of the force-length curve for active tensile strength of the muscle.

In addition to the active force-length relationship, there is a passive tensile force applied by the muscle when it is stretched beyond its rest length [1]. The passive force is small at first, but increases rapidly as the muscle reaches the limits of its flexibility as shown in Figure 2.3. At the limits of the muscle's range of motion, the passive force is often larger than the active force. The forces or torques inputted to a golfer model should try to take into account the force-length dynamics of human muscles. It's unlikely that the reduction in strength due to shortening occurs during the golf swing, but the passive tensile force becomes important as the golfer reaches the limits of their range of motion at the start of the downswing.
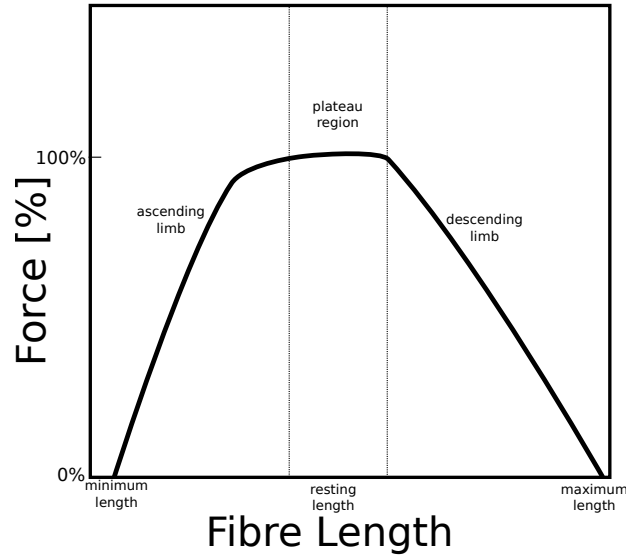
Figure 2.2: Force-length curve for active portion of a human muscle [1].

Force-Velocity Relationship for Muscles

The second factor which affects the force output of the muscle is the force-velocity relationship. In the most basic form, this relationship states that as the velocity of the muscle contraction increases, the force output decreases. Typically, this relation is described using the Hill muscle model [1],

$$F = \frac{(F_0 b - av)}{b + v} \tag{2.1}$$

where F is the instantaneous force, F_0 is the force produced in isometric (stationary) contraction, v is the current contraction speed, and a and b are constants. This relationship leads to the normalized force-velocity relationship shown in Figure 2.4. The exact properties of the curve change depending on the muscle's cross-sectional area, length, and proportion of fast-twitch and slow-twitch fibres, but the general form stays the same [1]. The force-velocity relationship has a significant effect on muscle output and should be accounted for in the development of the golfer model.

10
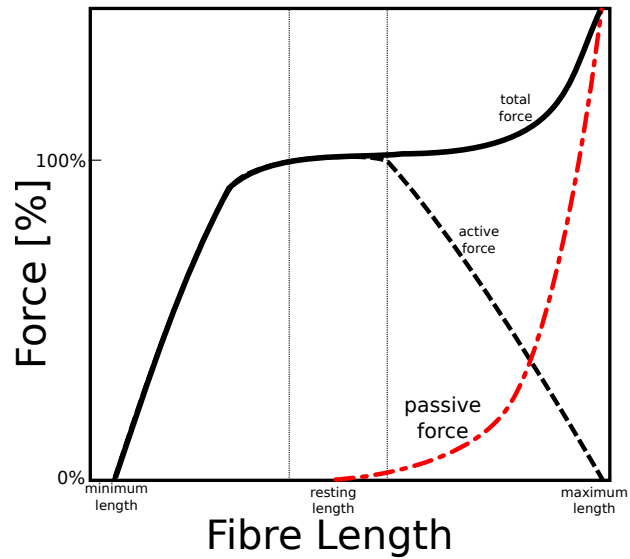
Figure 2.3: Full force-length curve for a muscle including passive and active components. The total force line shows how the combination of the passive and active components can produce larger forces than the active force alone. Both components of this force are important to include in the model. [1]
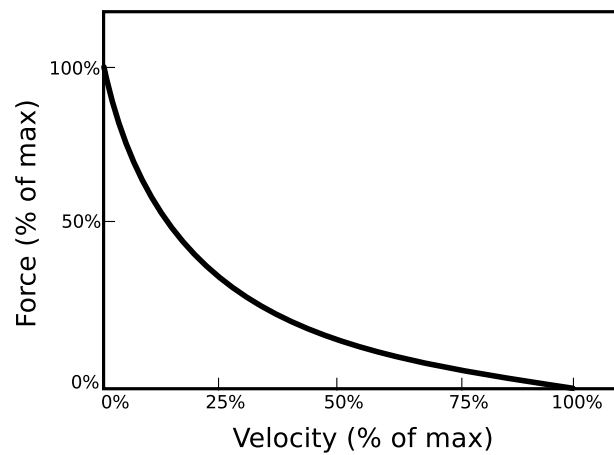
Figure 2.4: Normalized force-velocity curve for a typical muscle [1].

11

Passive Moments at Joint Limits

In combination with the passive muscle forces describe earlier, passive elastic structure (ligaments, joint capsules, skin, and other surrounding tissues) apply moments to joints to prevent them from leaving their normal range of motion. These passive forces can be very strong and have been shown to be important when modeling human gait [15]. The passive moment begins to affect joints near the limits of their range of motion and grow quickly as the joint goes beyond its normal range to prevent further bending.

Passive joint moments have been measured for many joints in the body and the general shape of the joint angle vs. torque curves is shown in Figure 2.5. The passive moment is small through the normal range of motion and quickly grows outside of those limits. The angle at which the moment is applied and rate of growth differs from joint to joint but the general shape of the applied torque remains the same.

Muscle Activity During the Golf Swing

Of these biological characteristics, the muscle activation dynamics described in Section and shown in Figure 2.1 are the most important factor in controlling the golf swing. They provide limits on the ability of the golfer to control the swing and make control strategies that involve turning muscles on and off frequently difficult. Since the golf drive is an activity where the goal is to achieve maximum distance, it is likely that the muscle groups used are activated for their maximum power production and the golfer's main role is to control the timing of these activations [16] and thus the timing of the swing.

The passive joint forces that provide limits on joint angles are also important to consider when modeling biomechanically possible swings. Especially at the wrist joint, the passive forces prevent the wrist from bending backwards into an anatomically impossible
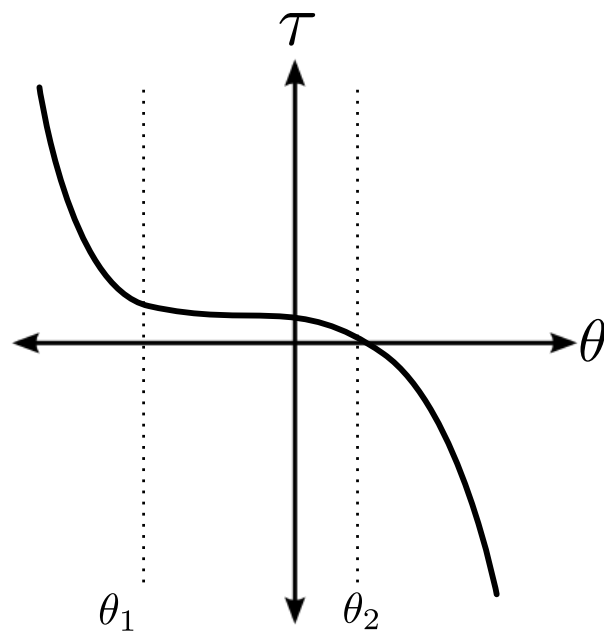
Figure 2.5: General shape of the passive joint moment [2]. τ is the passive moment and θ is the joint angle. θ_1 and θ_2 indicate the normal range of motion of the joint.

position during the early portion of the swing while the golfer's wrist muscles are not active. In addition, the passive forces are able to store strain energy accumulated during the backswing and provide more power to the swing. Passive forces are a significant part of the stretch-shorten cycle which allows golfers to generate more power in their swing [10].

The force-velocity relationship is also important for the muscles involved in the swing. As the golfer accelerates through the downswing, their muscles will be able to provide less torque to continue accelerating the club. The velocity of the swing is probably not large enough so that no torque can be provided, but the active torque applied is greatly reduced near the impact point.

The force-length relationship will not have a large effect on the muscles during the golf swing. For the range of motion required, the muscle sarcomere lengths will likely be within the optimal range [17].

2.1.3   Club Flexibility

Club flexibility plays an important role in generating clubhead velocity and greatly affects the presentation (orientation) of the clubhead at impact. During the downswing, the clubhead first lags the hands as strain energy is stored in the shaft before whipping forwards to contact the ball. By the time of impact, the club is usually bent forward, leading to increased loft angle of the club face, and possibly an increase in clubhead speed [18]. Figure 2.7 shows the expected flexing pattern for the club throughout the swing in the forward plane.

In addition to lead-lag flexing, the clubhead also droops during the swing to align the centre of mass with the plane of rotation of the swing. The centripetal acceleration of the clubhead tends to push the clubhead centre of mass downwards as the club accelerates.
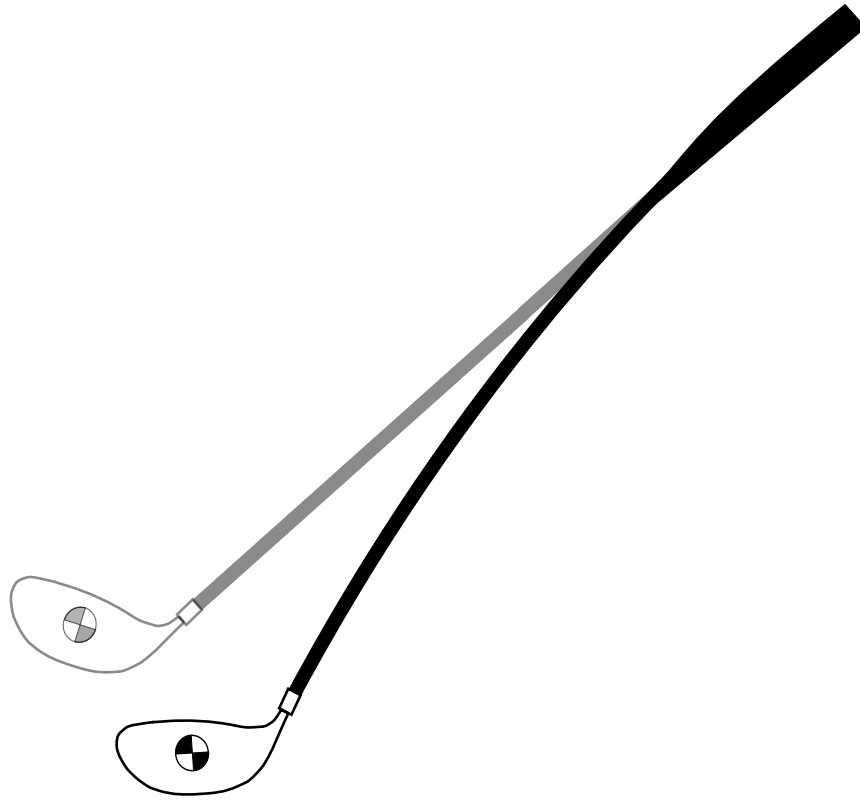
Figure 2.6: The clubhead droops as it accelerates, bringing the centre of mass closer in line with the plane of the swing and the hands of the golfer. The amount of droop is exaggerated in this Figure to better illustrate the effect.

This effect is illustrated in Figure 2.6. Finally, axial flexibility of the shaft introduces a small amount of lag between the rotation of the grip and the rotation of the clubhead about its vertical axis.

Flexible Club Models

Many attempts to model the flexible club have been made. In 1992, Milne and Davis [18] created a mathematical model for the shaft using a two-dimensional double-pendulum
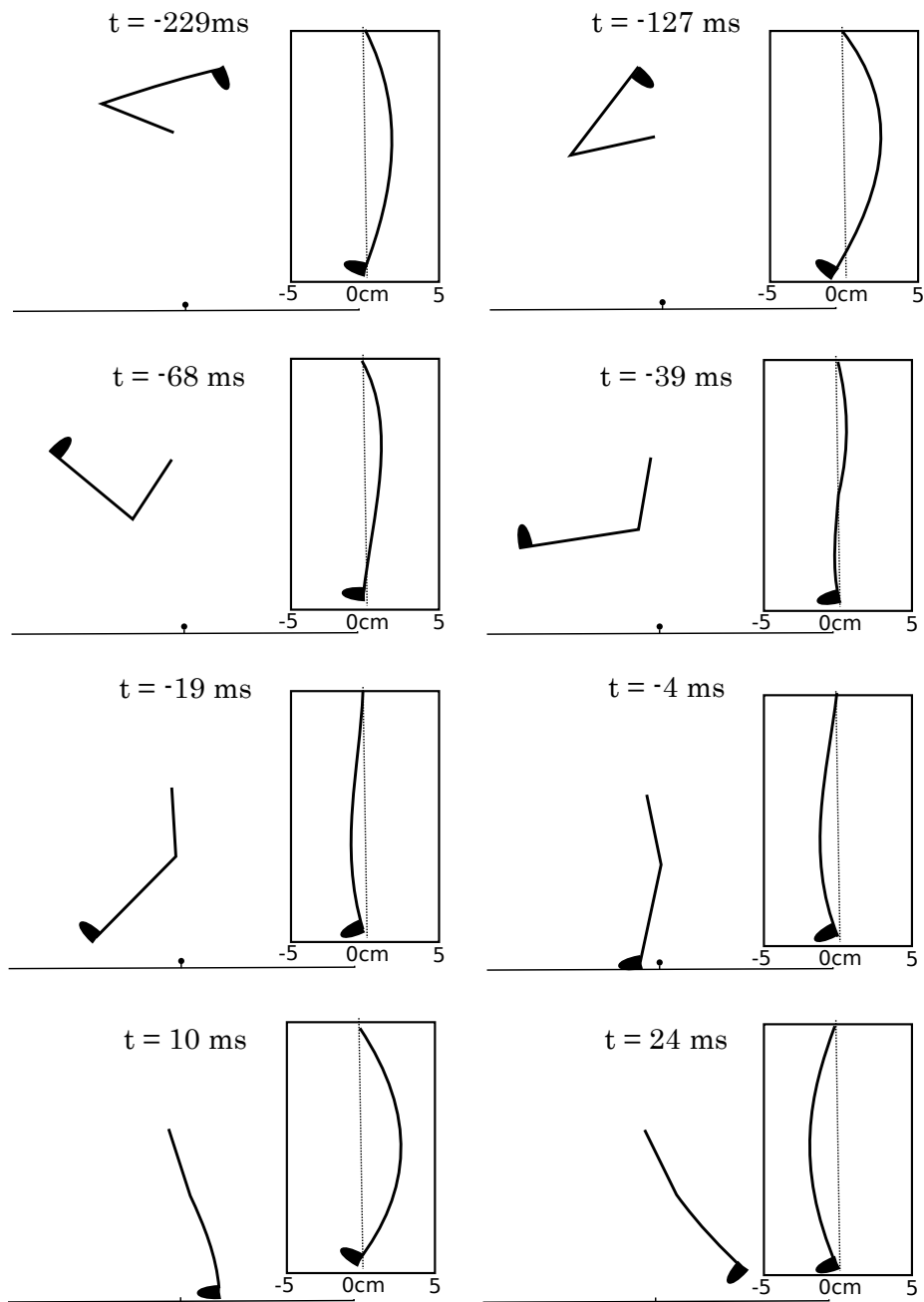
Figure 2.7: The typical flexing pattern of the club during the swing. The amount of shaft bending is magnified by 5 times in this image to make the bending patterns more obvious. Timing information and the amount of bending is taken from Milne and Davis [18].

model of the golf swing. This model used the principle of virtual work to derive a series of shape equations for the shaft. Three golfers' swings were tracked using optical markers and strain gauges were used to verify the results. The model was used simply to describe club flexing during the swing and it is not suitable for use in a forward dynamic simulation.

Another attempt to model the flexible golf shaft was made by Mackenzie as part of a larger 3-D golfer model [19]. The hands of the golfer, along with the shaft and clubhead (often considered as a single rigid body in many golfer and club models [20] [21] [22]) were divided into 4 subsections, each with its own set of inertial properties. These sections were connected with universal joints that allowed lead-lag and toe-down deflection. To approximate the shaft stiffness characteristics, each joint was fitted with a rotational spring and damper which provided a torque to the joint taking the form:

$$T = (-K\theta) - (C\omega) \tag{2.2}$$

where K was the stiffness coefficient, θ the angular displacement of the segment, C the damping coefficient, and ω the relative angular velocity of the segment. To find the K values, clubs were tested in a cantilever setup by suspending a 1kg weight at the hozel and measuring the shaft deflection. K values were selected by an optimization process that matched a simulated version of the test setup to the measured results. C values were selected that best matched experimental results. This model is able to account for some changes in stiffness characteristics along the length of the shaft but it cannot account for continuous bending of the shaft or any axial deformations (rotational or translational) that occur during the swing.

A more complete model of the flexible club was proposed by Sandhu et al. in 2010 [23]. This model uses Rayleigh beam theory to model the club and will be described in detail in Section 3.2. Using Rayleigh beam theory allows for continuous bending and continuously

17

varying stiffness properties along the length of the shaft. Sandhu used this model as part of a kinematically driven forward dynamic golf club model and was able to achieve good matches with the dynamic loft and droop of experimental results.

2.1.4 Impact

The impact portion of the golf swing is confined to a very short period of time (5 microseconds or less) so it is impossible for the golfer and shaft to have an effect on the clubhead during the impact time. Therefore, the shaft dynamics and the golfer's actions and dynamics can be ignored during the impact phase and the clubhead assumed to be moving freely during the impact [8]. The impact can be considered as an oblique impact between two 3-D bodies. The results of this impact, the initial conditions of the ball's velocity and spin during its flight, are dependent on the physical and geometric properties of the clubhead and ball, the orientation of the clubhead, the velocity of the clubhead, and the relative positions of the two bodies at impact. This Section will describe the impact of the golf club and the ball and explain how the mechanics of that impact are affected by changing these parameters.

Clubhead Orientation

The clubhead orientation changes two features of the impact. First, the dynamic loft of the clubface (the angle between the face of the club and a vertical plane at the point of impact) affects the vertical launch angle and the amount of backspin of the ball following the impact. Increasing the loft increases the launch angle and the amount of backspin. The dynamic loft is a combination of the nominal loft of the club (usually 9° to 11° for a driver) and the additional loft created by the flexing of the club shaft as described in

18
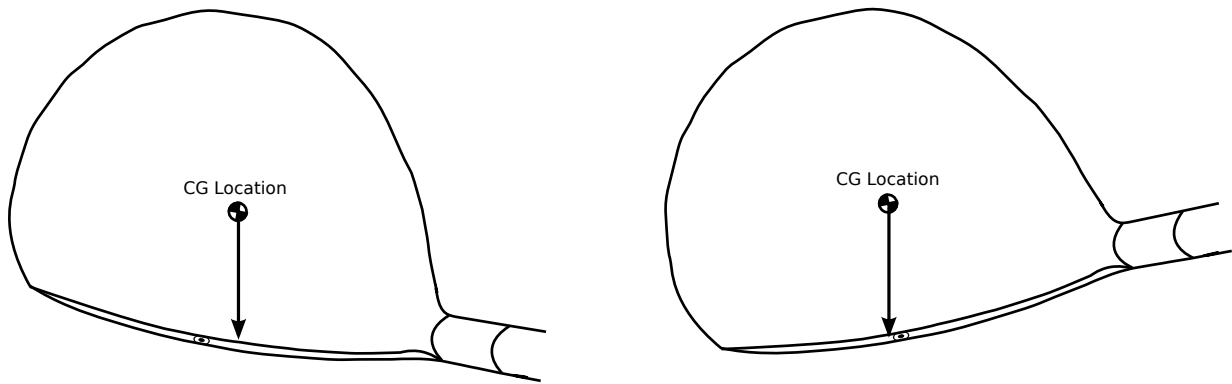
Figure 2.8: Top view of an open clubface orientation (left) and a closed clubface orientation (right).

Section 2.1.3. The dynamic loft can be adjusted by placing the ball further forward in the swing, selecting a club with greater nominal loft, or increasing the flexibility near the tip of the shaft. The amount of loft that is ideal depends on the individual swing and varies from golfer to golfer.

Second, the opening/closing angle of the club face has an important effect on the horizontal launch angle and the amount of side spin on the ball after impact. At impact, due to the moment of inertia of the club about the shaft axis, the clubface tends to be tilted backwards away from the golfer in an open position. This results in a slice spin on the ball and a horizontal launch angle away from the golfer. In similar fashion if the clubface is closed at impact, there is a resulting hook spin and launch angle towards the golfer. Since it is more common for a golfer to hit from an open position, golfers intentionally work to close the clubface at impact through the pronation of the arm. Ideally, the clubface is perpendicular to the ball at impact, resulting in a straight shot with minimal side spin. Figure 2.8 shows the open and closed clubface orientations.

Centre of Mass Alignment

The alignment of the centre of mass of the golf club with the centre of mass of the ball changes both the launch angles and the spin of the ball after impact. If the centre of masses are perfectly aligned with the velocity vector of the club, this is a perfect strike of the ball and the launch velocity will be entirely forward and upward with very little side spin.

More interesting is what happens when the ball is struck off-centre, with an eccentric impact imparting angular momentum to the clubhead and ball. The spin of the ball after such an impact comes from two sources: the tangential forces at the impact point, and the gear effect between the clubhead and ball. Figure 2.9 illustrates this scenario, showing a toe hit. In the figure, the impact location of the ball outside the centre of mass of the clubhead causes the clubhead to rotate clockwise as indicated. In a normal eccentric impact, this impact location would also lead to the ball spinning clockwise (opposite to the indicated direction) and for the shot to slice, but the gear effect changes the result. The contact point on the club face moves in the direction shown on the diagram and as the ball rolls on the face of the club, the ball is caused to spin in the opposite direction to the club. For a toed shot, there is resulting hook spin, and for a heeled shot, there is a resulting slice spin. This effect is known as the "gear effect" because the club face and ball act as two gears spinning in opposite directions.

The gear effect also affects the backspin of the ball for an impact that is out of alignment in the vertical direction. If the ball strikes high on the face the backspin is reduced and if the ball strikes low the backspin is increased.
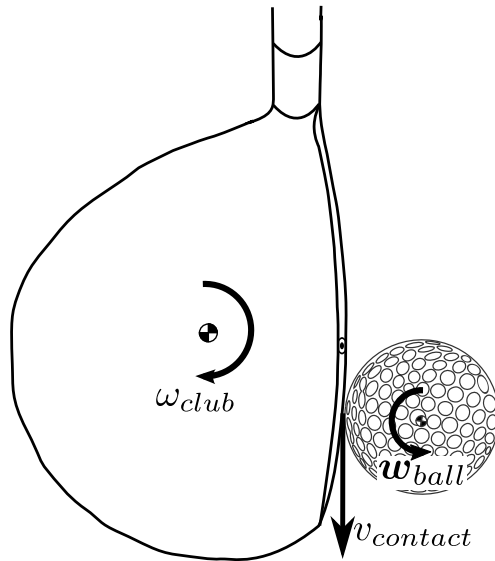
Figure 2.9: Illustrating the "gear effect" for a toed shot.

Clubhead Properties

Four properties of the clubhead have a significant effect on the impact and are therefore limited by the rules of the US Golf Association (USGA). The clubhead mass is important as it helps determines the amount of energy and momentum that is available during the impact. If the mass of the clubhead is increased and its velocity stays the same, the ball will be launched at greater speed following the impact. The mass of the clubhead is not directly limited by the USGA, but most drivers have a clubhead mass of about $200\,\mathrm{g}$.

The moments of inertia (MOI) of the clubhead have a more interesting role in determining the spin of the ball following impact. Because of the gear effect described above in Section 2.1.4 the amount of angular velocity imparted to the clubhead by an off-centre strike is important in determining the spin of the ball. By increasing the MOI about the vertical axis, the spin imparted to the club by an off-center hit is reduced and therefore

the side spin on the ball is reduced [24]. This helps reduce the hooking or slicing effect of an off-center hit. To prevent golf clubs with extremely high MOI from being produced, the USGA has limited the MOI of a golf club about its vertical axis through the centre of mass to $5900\,\mathrm{g\,cm^2}$ [25].

The elasticity of the club face controls the energy lost due to deformation when the ball and club collide. To increase the distance of the drive, club manufacturers try to increase the flexibility of the face so that the natural frequencies of the ball and club match as closely as possible to produce a "trampoline effect" that minimizes the energy lost [26]. To limit this effect, the USGA has also limited the elasticity of the clubface by limiting the contact time to $239 \pm 18\,\mathrm{\mu m}$ as measured by striking the club face with a particular mass and pendulum [25]. The measured contact time is directly related to the compliance of the clubface. Increasing the coefficient of restitution (CoR) by increasing the elasticity of the club face results in higher ball speeds after impact and longer drives.

Finally, the bulge and roll of the club face change the launch angles of the ball to produce straighter shots from off-centre hits. Since hitting the ball off-centre horizontally results in a slice or a hook spin due to the gear effect, the bulge of the clubface causes the ball to have an initial velocity in a direction opposing the motion that will be caused by that spin: e.g., for a toe hit which results in a hook spin the ball is initially launched with some velocity away from the golfer to reduce the effect of the hook. Similarly, the bulge of the club increases the vertical launch angle for hits above centre and decreases it for hits below centre.

Clubhead Velocity

By increasing the clubhead velocity, the ball will be launched at greater speeds. In fact, the clubhead velocity is the single greatest determining factor in the distance the ball will carry [20]. Increasing the clubhead velocity will make the effects of off-centre hits larger as the greater impulse in the collision leads to increased side spin.

2.1.5   Ball Aerodynamics

The aerodynamic flight of the golf ball is dependent on the initial velocity of the ball and the spin of the ball as it travels through the air. While the initial velocity is most important for the total distance the ball flies with greater velocity producing greater distance, it is the spin of the ball which has the most interesting effects on its flight path. The Magnus effect of the spin of the ball produces both lateral and upward lift forces during its flight [27]. In golf, these forces are influential in two ways.

First, the direction and amount of side spin (about the vertical axis of the ball) affects the sideways motion of the ball during its flight. As viewed from the top, clockwise spin causes the ball to 'slice' to the right and counter-clockwise spin causes the ball to 'hook' to the left [28] as shown in Figure 2.10. Sometimes side spin is intentionally applied to the ball to produce a particular trajectory but in general side spin has an undesirable effect on the shot and decreases the distance the ball will fly.

In contrast, backspin can increase the carry distance by providing lift to the ball during its flight. Increasing the backspin increases the amount of lift on the ball, but there is an upper limit to the amount of lift that can be usefully applied. If there is too little backspin on the ball, no lift is applied to the ball and the flight path is parabolic, like
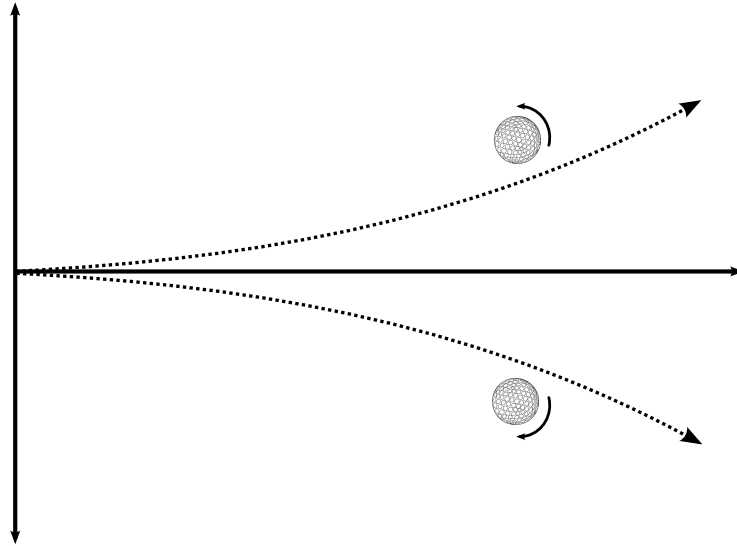
Figure 2.10: Top view of the effect of side spin on the flight of the golf ball. The top path is a 'hook' shot for a right-handed golfer and bottom path is a 'slice.'

that of non-spinning projectile as seen in Figure 2.11a. If there is too much backspin (see Figure 2.11b) the excess lift causes the flight path of the ball to balloon upwards, reducing the carry distance. In addition, this flight path leads to a higher angle of impact with the ground, reducing the distance the ball will roll. With the ideal amount of backspin (see Figure 2.11c) the ball rises on a high, boring, trajectory during its flight, carrying further downrange. The ideal amount of backspin depends on the launch velocity and angle of the ball, but in general higher velocity trajectories require less backspin to maintain the optimal trajectory [29]. One club manufacturer has stated that the optimal amount of backspin is 1700 rpm [30].
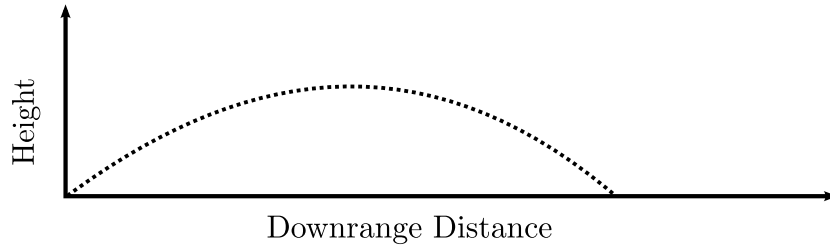
(a) Typical flight path of the golf ball for a low backspin shot. Notice how it follows a parabolic path. There is no lift provided by the spin.
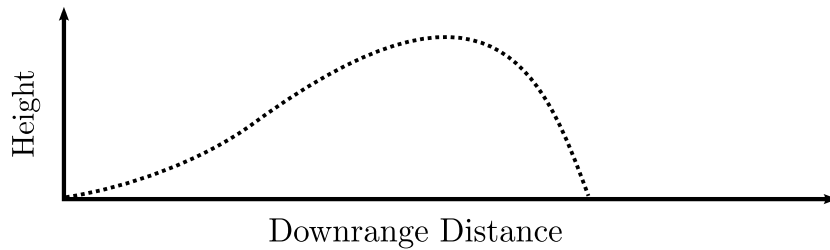
(b) Typical flight path of the golf ball for a high backspin shot. Too much lift causes the flight path to balloon upwards, reducing the carry and reducing the roll after hitting the ground.
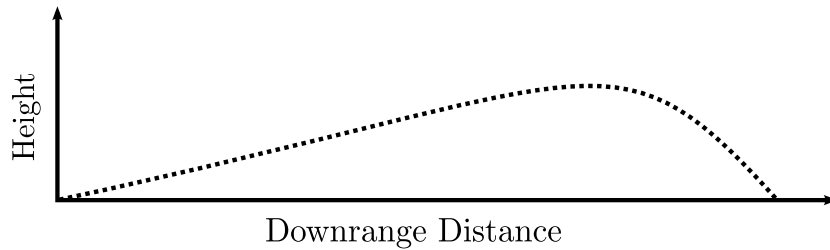
(c) Typical flight path of the golf ball for a shot with a good quantity of backspin. Note the boring trajectory that leads to a non-parabolic flight path and the increased carry distance.

Figure 2.11: Flight paths of the ball illustrating the effect of backspin on the flight of the golf shot.

25

2.2 Golf Driver Design

Designing a golf driver requires the balancing of many factors within the framework dictated by the rules of the US Golf Association (in the USA and Mexico) and the R & A (worldwide). While the rules of the game provide hard constraints on several aspects of the design of the club, there remain many trade-offs to be made in the design process. Each year, club manufacturers release new clubs and make new claims about the scientific improvements they have made that will allow golfers to hit the ball further and straighter. In this section, several different design decisions and manufacturers claims will be described along with the possible and expected outcomes of those decisions. These decisions and claims will be revisited and analyzed within the context of the model presented in Chapter 3 in Chapter 4.

2.2.1 Club Mass

One of the more recent claims of golf club manufacturers is that a lighter club would result in longer drives [31]. The claim made was that by decreasing the club mass 10 g, the golfer would be able to swing the club 1 mph (0.45 m/s) faster, resulting in longer drives. The trade off here is that by decreasing the club mass, the momentum of the club is not necessarily increased overall by an increase in clubhead speed and the momentum of the clubhead before impact that controls the amount of energy that can be transferred to the ball. It is likely that there is a sweet spot for club mass for each individual golfer and finding that spot is one of the challenges in designing a club.

2.2.2 Clubhead Moment of Inertia

Due to the gear effect of the ball interacting with the club (see Section 2.1.4, the amount of angular velocity imparted to the clubhead during impact is important in determining the side-spin of the ball. By increasing the moment of inertia (MOI) of the clubhead, the angular velocity of the clubhead is reduced and the amount of spin imparted to the ball is similarly reduced. By increasing the MOI of the clubhead about its vertical axis, manufacturers have created drivers that can hit the ball straighter for off-centre impacts on the club. This led to the creating of a rule by the USGA that no club may have a MOI greater than $5900\,\mathrm{g\,cm^2}$ [25].

Even without this rule, improvements to the club made by increasing the clubhead MOI were shrinking as the increase in MOI makes it more difficult for the golfer to close the clubface at impact. Since the MOI is larger, more torque is required from the forearms and hands to rotate the club to the appropriate angle. There is clearly a tradeoff between increasing the MOI to reduce the spin and decreasing the MOI to increase the controllability of the club.

2.2.3 Clubhead Centre of Mass Position

The ideal centre of mass position of the clubhead is also a matter of debate. While most people agree that then the centre of mass of the clubhead should be low, to decrease the amount of backspin on the ball, it is unclear whether it should be low and close to the clubface or low and far from the clubface. In particular the TaylorMade SLDR driver released in 2013 claimed that a low and forward centre of mass location would provide better launch conditions.

The centre of mass should be low so that the gear effect of the ball striking above the centre of mass reduces the backspin of the ball as most golfers tend to hit with too much backspin for an optimal flight (see Figure 2.11b). Striking above the centre of mass causes the clubface to rotate upwards and reduces the backspin on the ball. Moving the centre of mass forward or backwards normal to the clubface should not change this effect as the moment arm of the impact force will not change. It's unclear whether this movement might have other effects and this should be further investigated. Moving the centre of mass forward horizontally relative to the ground should reduce the backspin as the moment arm of the impact will be increased.

2.2.4 Shaft Flexibility

The shaft of the golf driver bends forward at impact so that the clubhead strikes the ball while angled slightly upwards. This can help to reduce the backspin of the ball and increase the launch angle to improve the carry. The common wisdom is that a golfer with a faster swing speed needs to use a stiffer club and a golfer with a slower swing speed should use a more flexible club. It's important for a golfer to select the correct shaft flexibility for their particular swing and this selection is one of the parts of a traditional shaft fitting performed by a golf pro.

While shaft flexibility does not involve design trade offs in the traditional sense the selection of the appropriate shaft can be difficult and deserves consideration. Any single shaft is unlikely to be correct for all golfers, but the question of fitting a shaft for a particular golfer is an interesting one. In a world where more goods will be personally manufactured for individual consumers the possibility of designing the shaft flexibility directly for one particular golfer using a computer model is attractive. While the model

presented in this paper is not subject-specific it can be used for testing different flexible shafts and optimizing the stiffness.

2.3 Golfer Models

2.3.1 Early Golfer Models

Cochran & Stobbs

Search for the Perfect Swing, first released by Cochran and Stobbs in 1968, was the first serious scientific study of the golf swing [8]. They developed a planar double-pendulum model for describing the golf swing where each of the joints is powered by a rotational spring that is loaded during the backswing and released during the downswing. They were the first to propose the idea that the relative timing of the torques applied to each link in the kinematic chain of the golf swing was crucial to a successful, powerful, swing and the importance of swinging in a planar manner. They compared their model to stop-motion photography of golfers and found that it was a reasonable fit for real golf swings. In the same study, Cochran and Stobbs also analyzed a number of other scientific aspects of golf such as shot strategy and putting, but these are not relevant for this work.

Lampsa - Golf Swing Optimization

One of the earliest attempts to optimize the golf swing was made by Lampsa in 1975 [20]. Lampsa made use of a planar double-pendulum model of the golf swing to investigate the optimal control aspect of the golf swing. By applying Pontryagin's Minimum Principle to the joint torques applied to the double-pendulum model, Lampsa attempted to optimize

the golf swing for maximum clubhead speed while maintaining biologically feasible joint angles. The joint torques found through the optimization were dissimilar from those found from inverse dynamics. Lampsa concluded that it should be possible to hit the ball much further without increasing the golfer's strength and that the key to longer drives would be to delay uncocking the golfer's wrists as long as possible to generate greater clubhead speed. Lampsa's study also performed a sensitivity analysis of changes to the club, varying the mass of both the clubhead and shaft by 10% to determine the effects on the optimal swing. The conclusion was drawn that changing these parameters has little effect on the optimal torques and results in at most a 1.3% change in the optimal clubhead speed at impact.

2.3.2   Modern Golfer Models

Sharp - Parameterized Joint Torques

A more recent influential model of the golf swing was proposed by Sharp in 2009 [22]. Sharp compared the typical rigid double-pendulum model of the golf swing with a rigid triple-pendulum model and concluded that including the rotation of the torso and shoulders as part of the swing allowed for a significant improvement in matching captured experimental data. In particular, the triple pendulum model allows for more range of motion in the backswing and a fuller golf motion during the downswing. Sharp concluded that the double-pendulum model of Lampsa was insufficient and created a new forward dynamic model for the swing.

One of the main innovations of this model was the inclusion of parameterized joint torques as inputs to the model to allow some flexibility for the inputs while simplifying the optimization of the swing. The shapes of the torque functions were selected to provide

reasonable matches to inverse dynamics results obtained through testing of a few highly skilled golfers. Three joint torques were required and a different form was used at each joint. The torque provided to rotate the shoulders was

$$T_s = T_{s_{max}} \tanh\left(\lambda t\right) - \tau_{s_2}(t - t_s)H(t - t_s) \tag{2.3}$$

where $T_{s_{max}}$ is the maximum exertion level, τ_{s_2} defines the linear drop-off in torque, t_s is the drop off start time, and $H(x)$ is the Heaviside step function. The torque to rotate the arm about the shoulder was given by

$$T_a = \min(\tau_{a_1}t, T_{a_{max}}) - \tau_{a_2}(H(t - t_a)(t - t_a)) \tag{2.4}$$

where $T_{a_{max}}$ is the maximum exertion level, τ_{a_1} defines the linear increase in the torque at the start of the swing, and τ_{a_2} defines the linear decrease in the torque after time t_a. Finally the wrist torque was defined as

$$T_w = T_{w_{max}} \tanh(\lambda(t - t_w)) \tag{2.5}$$

giving a negative maximum torque $(T_{w_{max}})$ at the start of the simulation, followed by a switch to a positive maximum torque after time t_w.

Sharp also included passive joint torques in the form of linear spring-dampers at extreme joint angles. The passive joint torques are 0 until the limits are reached and are then activated.

By optimizing the parameters in the joint torque functions, Sharp was able to fit the triple pendulum golfer model to real swings of 3 different highly skilled golfers with good agreement. He then tried optimizing the swing to produce the maximum clubhead speed. Contrary to Lampsa's earlier results, the optimal torque did not show a holding-back phase for the wrist. Changing the strength of the golfer did not change the general patterns of the swing, but did increase the clubhead speed at impact.

31

Mackenzie - A Biomechanical Model

Mackenzie's golfer model, published in 2009 also used the concept of parameterized joint torques to improve the feasibility of optimizing the golf swing [16]. He also introduced a version of the triple-pendulum model that allows for 3-dimensional motion during the swing. Instead of just swinging in a single plane, Mackenzie added an extra degree of freedom along the long axis of the golfer's left arm to allow supination and pronation of the wrist during the swing and added a separate plane of rotation for the shoulders and arms during the swing. Mackenzie's parameterized joint torques will be described in detail in Chapter 3 but in short, they allow for the same biologically-motivated parameterized torque to be used at each joint.

In Mackenzie's model, the shaft of the club was split into four sections with a spring and damper at each joint to model the flexibility characteristics of the shaft. A number of golf clubs were subjected to a flexing test and the stiffness parameters selected to best match the shape of the club as measured in the test. This approach allows for flexing of the shaft at a few points along its length, but cannot model continuously varying shaft properties or bending.

Like Sharp, Mackenzie also used parameter optimization to attempt to find the best possible swing. Genetic algorithms were used to pick the best possible activation and deactivation times for the muscles using the clubhead speed as the objective function. Penalties were added to avoid improper clubhead presentation. The final maximum clubhead speed achieved by Mackenzie was 41.7m/s.

2.3.3   Other Golfer Models of Interest

Other golfer models created over the last 50 years with many different goals and purposes were examined during this work. A few of them with interesting details will be described in this section. Many of these models included ideas that were incorporated into the final model proposed in this paper.

Reyes and Mittendorf applied the fixed double-pendulum golfer model to the swing of a long drive champion [21]. Unlike other studies, instead of just studying clubhead velocity, an impact and carry model was used along with the golfer model to determine possible changes to the swing to improve the distance. Increasing the backswing angle, wrist angle, or changing to a lighter clubhead were the areas identified by the model as offering the greatest change in clubhead speed. Ball carry was not affected by using a lighter clubhead as the effect of using the lighter club on the impact reduced the carry.

Nesbit [32] and Serrano [33] created a full-body model of a golfer and used inverse dynamics to study the swings of 1 female and 84 male golfers. He found significant subject to subject variation in the swing, even among skilled golfers. More skilled golfers are able to increase their club speed not by applying greater force, but through increased range of motion. They do more work during the swing, and have a higher peak power output during the swing. Power peaks slightly before impact during the swing and most of the power output is provided by the torso and shoulder rather than the wrists or hands. The amount of strain energy stored by the club is minimal compared to the total work.

Betzler's thesis [34] examined the effects of changing the staff stiffness on the biomechanics of the swing using a motion capture system. Two different levels of club flexibility were tested by a group of twenty skilled golfers. Decreasing the flexibility of the shaft increased the clubhead speed significantly, due to increased recovery of the stiffer shaft

from lag bending. The face angle and impact location were unaffected by shaft flexibility. Similar tests were performed with a golf robot and the results confirmed. It seems that golfers are able to adapt to different club flexibilities to hit the ball well but there may be some difference in the distance of shots achieved.

Kenny [35] created a full-body golfer model with 42 degrees of freedom that was driven by experimental data from a single golfer. This golfer-specific model was used to analyze the kinetic energy of the kinematic chain of the golf swing. He found that the while the kinetic energy increased from proximal to distal body segments, there was no sequential ordering to the peaks in each body segment. Kenny concluded that each individual golfer would likely have a unique profile to their golf swing. It will be important to accommodate this variability into any golfer model produced.

Hauefle [36] investigated the effect of changing the mass of the club through simulation and experiment. Using the double-pendulum model of Pickering [37] with two different club models, it was found that increasing the club mass by 22g resulted in a swing that was 1.7% slower. In contrast, experimental results for actual golfers did not show a predictable change in club speed with a heavier club. This showed the golfers respond to changes in the golf club by changing they way that the club is swung, instead of swinging the same way with every club.

2.4   Opportunities

Despite all of the work already done in this field, there remain significant opportunities for creating an improved golfer model that allows for new questions to be asked and answered. In particular a model which can include the following features would be valuable:

- Forward dynamic model capable of answering 'what-if' questions regarding changes to the club and golfer.

- Golfer model including a non-planar model of human motion, active joint torques that act similarily to human muscle, and passive joint torques that mimic the storage of energy during the backswing of the golfer.

- Flexible club model capable of predicting droop, dynamic loft, and clubface presentation.

- Impact model and aerodynamic model for evaluating each swing.

- Optimization strategy that allows the model to swing optimally in a variety of configurations.

Such a model would be able to answer questions that have been asked recently about club design including how to distribute flexibility along the length of the shaft, whether a lighter club can really hit the ball further, and where the centre of mass of the clubhead should be positioned.

The model presented in Chapter 3 of this thesis accomplishes the goals stated here and the experiments in Chapter 4 try to answer some of the questions posed. These questions represent just the first of many that could be answered using this model.

Chapter 3

Golfer Model

To simulate the golfer and club and take advantage of the opportunities described in Section 2.4 a four-part model was constructed. The parts are

1. Biomechanical golfer model with parameterizable joint torques

2. Flexible club model including club aerodynamics

3. Impact model of the club and ball

4. Aerodynamic model of ball flight

This Chapter will describe each portion of the model and its implementation in detail.

3.1 Biomechanical Golfer Model

The golfer portion of the mathematical model consists of three rigid bodies representing the torso, left arm, and left hand of the golfer. There are four degrees of freedom for the

golfer. The first degree of freedom is the rotation of the torso. This represents the rotation of the shoulders during the golf swing and is activated by the power of the muscles of the legs and core. The second degree of freedom allows transverse flexion and transverse adduction of the shoulder across the front of the body. The third degree of freedom allows supination and pronation of the arm and the final degree of freedom allows for ulnar and radial deviation of the wrist. These four degrees of freedom are illustrated in Figure 3.1. This golfer model, based on the work of Mackenzie [16] was considered to be sufficient to apply the correct kinetics to the golf shaft throughout the swing. A discussion of the limitations of the model can be found in Section 4.8.

Four degrees of freedom are sufficient to provide the model golfer with the range of motion required for the swing. The golfer begins the swing with the torso rotated backwards (away from the target), the shoulder maximally adducted, the wrist maximally deviated towards the radius, and the arm pronated so that the club extends over the golfers right shoulder towards the target. During the swing, the torso rotates forward, the arm extends across the body, the wrist fully deviates towards the ulna and the arm supinates to square the face of the club towards the ball. A three body-model of the golfer is sufficient to capture the main dynamics of the swing.

The mass and inertia properties for the torso and arm of the golfer were taken from the work of Mackenzie [17] and are shown in Table 3.1. The mass and moment of inertia of the hand also takes into account the mass of the grip of the shaft and is also shown in Table 3.1. The segment geometries are shown in Table 3.2. Finally, the golfer's torso was inclined from the vertical by 30 degrees and the swing plane of the arms was inclined 50 degrees. Separate planes of rotation for the shoulder and arm rotation are better able to mimic the swing of a human golfer than single-plane models [14].
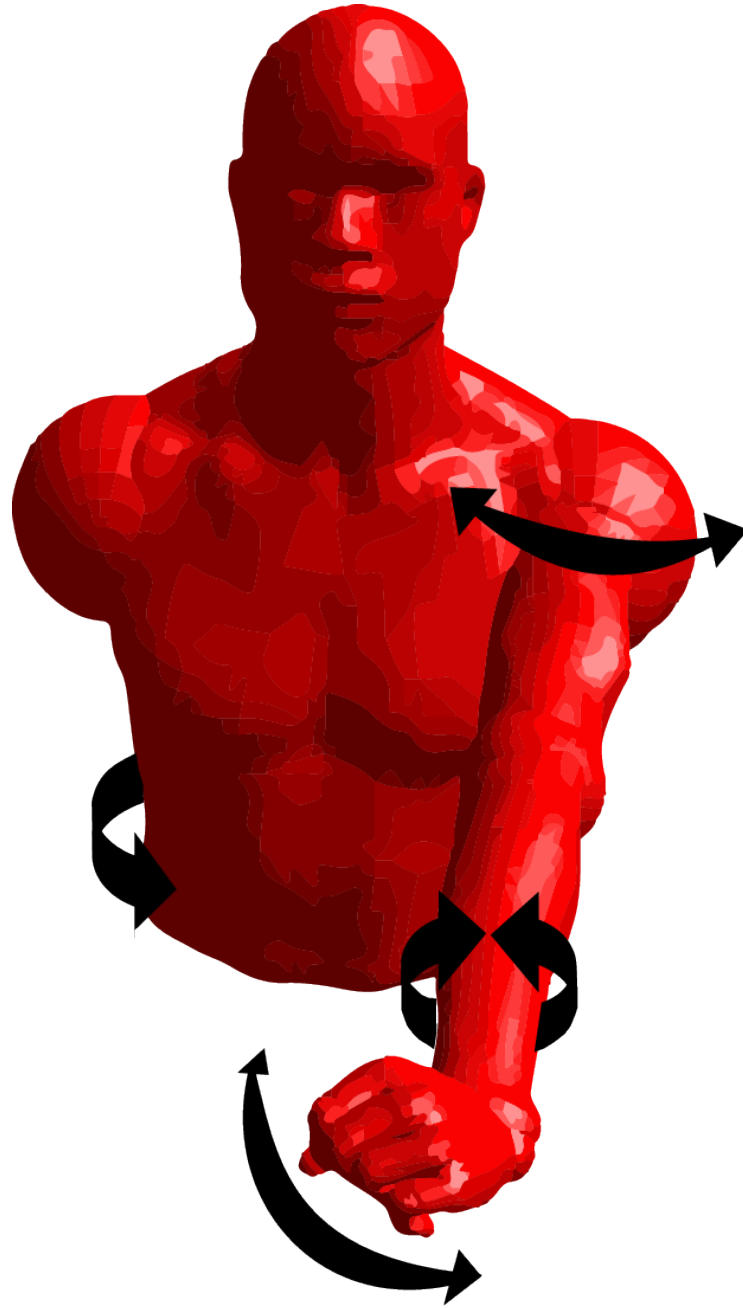
Figure 3.1: Golfer model with four degrees of freedom indicated

Segment	Mass (kg)	I_{xx} (kg cm^2)	I_{yy} (kg cm^2)	I_{zz} (kg cm^2)
Torso	34.61	...	3655	...
Arm	3.431	1076	1096	58.06
Hand & Grip	0.6	10.24	10.24	6.04

Table 3.1: Segment mass properties of the golfer.

Segment	Length (cm)	$CMLoc_x$ (cm)	$CMLoc_y$ (cm)	$CMLoc_z$ (cm)
Torso	20	0	0	0
Arm	60	0	0	26.1
Hand & Grip	20.0	0	0	9.0

Table 3.2: Segment geometry properties of the golfer.

3.1.1   Active Muscle Torques

Inputs are provided to the model at each degree of freedom in the form of parameterized joint torques. When designing these input torques, a number of factors were taken into account. The goals for the selection of these torques were:

- To provide realistic biologically-inspired inputs to the model;

- To capture the relevant muscle dynamics (described in Section 2.1.2) in producing the torques;

- To contain the inputs within biological limits;

- To parameterize the inputs so that the optimal control of the swing can be performed easily; and

- To use the same form for the torque at each degree of freedom.

To accomplish these goals, the parameterized torque functions proposed by Mackenzie were chosen as the active inputs to the model [38].

In this method, a two step calculation is used. In the first step, it is assumed that the golfer attempts to apply a maximum joint torque instantaneously for some time and then stops applying that torque. As muscles are unable to produce instantaneous torque due to the dynamics discussed in Section 2.1.2 the applied torque ramps up and ramps down as it is activated and deactivated. The equation used to describe step 1 is

$$T_{pre}(t) = T_m(1 - e^{\frac{t_{on}}{\tau_{act}}}) - T_m(1 - e^{\frac{t_{off}}{\tau_{deact}}}) \tag{3.1}$$

where T_m is the maximum possible applied torque, τ_{act} is the time constant of activation, and τ_{deact} is the time constant of deactivation. t_{on} and t_{off} are the amount of time that has passed since the torque was activated and deactivated respectively and are calculated as piecewise ramp functions.

$$t_{on}(t) = \begin{cases} 0 & : t < t_{activate} \\ t - t_{activate} & : t > t_{activate} \end{cases} \tag{3.2}$$

$$t_{off}(t) = \begin{cases} 0 & : t < t_{deactivate} \\ t - t_{deactivate} & : t > t_{deactivate} \end{cases} \tag{3.3}$$

where $t_{activate}$ is the time at which the joint torque is activated and $t_{deactivate}$ is the time at which it is deactivated.

The second step in generating the active torque component is to perform scaling based on the current velocity of the muscles involved. The scaling performed is based on the Hill muscle model described in Equation 2.1. By manipulating this equation, we can reach a
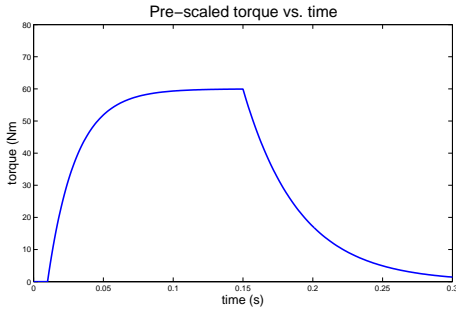
(a) Joint torque from Equation 3.1   (b) Experimental Activation Curves [39]
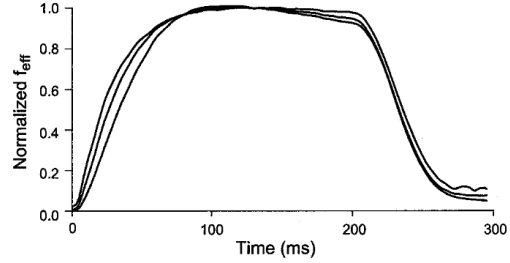
Figure 3.2: A comparison of muscle torques generated by Equation 3.1 to a typical muscle activation curve.

point where all of its components are easily determined biologically.

$$F = \frac{(F_0 b - av)}{b + v}$$

$$F = F_0 \frac{b - \dfrac{a}{F_0}}{b + v} \tag{3.4}$$

$$F = F_0 \frac{\dfrac{F_0 b}{a} - v}{\dfrac{F_0 b}{a} + \dfrac{F_0}{a}v}$$

This seems more complicated, but each of the inner fractions can be replaced with a more descriptive, biologically relevant, form. First $\frac{F_0 b}{a}$ can be replaced by v_{max}, the maximum velocity at which the muscle is still able to exert force [1]. And second, the inverse of the second fraction, $\frac{a}{F_0}$, has been measured in experiments to be close to 0.25 for mammalian skeletal muscles [1]. Replacing $\frac{F_0}{a}$ with the parameter Γ, we arrive at a scaling equation for the muscle force.

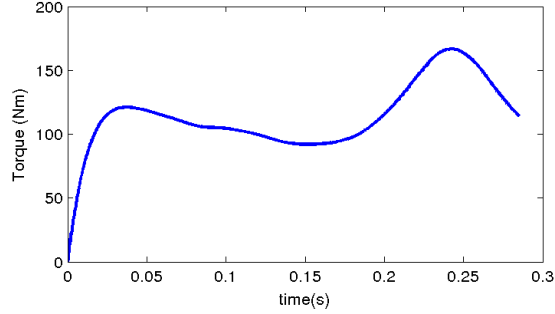$$F = F_0 \frac{v_{max} - v}{v_{max} + \Gamma v} \tag{3.5}$$

41

Figure 3.3: Sample joint torque curve incorporating velocity scaling

Assuming that we can transform this equation from the translational (muscle force) to the rotational (joint torque) domain using constant length moment arms, and including the activation curves from Equation 3.1, the active portion of the joint torque is then generated in the same manner as Mackenzie [16].

$$T(t, \omega) = T_{pre}(t) \frac{\omega_{max} - \omega}{\omega_{max} + \Gamma \omega} \tag{3.6}$$

A sample curve showing the active portion of the joint torque for the torso during a swing can be found in Figure 3.3.

This approach was selected because it accounts for both the activation dynamics and the force-velocity relationship for the muscles while keeping the number of control parameters small. Since the maximum torque, activation constants, and shape parameters remain constant across swings, only the activation timings need to be determined for each torque generator in the model. This results in 8 muscle parameters that must be chosen during the optimization process, a manageable number.

For each joint, the maximum torque provided (T_m) and the maximum angular velocity (ω_{max}) must be selected. The parameters for each joint are shown in Table 3.3.

42

Generator	T_m (N m)	τ_{act} (s)	τ_{deact} (s)	ω_{max} (rad/s)	Γ
Torso	200	0.02	0.04	30	4.0
Shoulder	160	0.02	0.04	30	4.0
Forearm	90	0.02	0.04	60	4.0
Wrist	90	0.02	0.04	60	4.0

Table 3.3: Parameters for the four active joint torque generators.

3.1.2 Passive Muscle Torques

To account for the torques applied to the golfer's joints at the limits of their range of motion (e.g., at the start of the downswing) and to keep the joints of the model within the normal range of human motion, passive joint torques are applied to each degree of freedom at the limits of its acceptable range. Passive joint torques are included for the torso, shoulder and wrist, and represent the energy stored during the backswing. To model this sort of passive force, Yamaguchi [2] proposed the use of Equation 3.7.

$$T_{passive}(\theta, \dot{\theta}) = k_1 e^{-k_2(\theta - \theta_-)} - k_3 e^{-k_4(\theta_+ - \theta)} - c_1 \dot{\theta} \qquad (3.7)$$

This function is able to approximate the restoring moment at both extremes of the joint range of motion and offer a smooth transition in joint torque from the normal range of motion, where very little torque is applied, to the large moments applied at the edges. The constants k_1 and k_3 govern the magnitude of the force at the breakpoints (θ_- and θ_+) while k_2 and k_4 govern the sharpness of the break. For this form, θ_- and θ_+ should be set well within the range of motion of the joint.

For each joint with a passive component, the values k_1, k_2, k_3, k_4, θ_- and θ_+ must be found. A careful search of the literature found explicit values of these parameters for
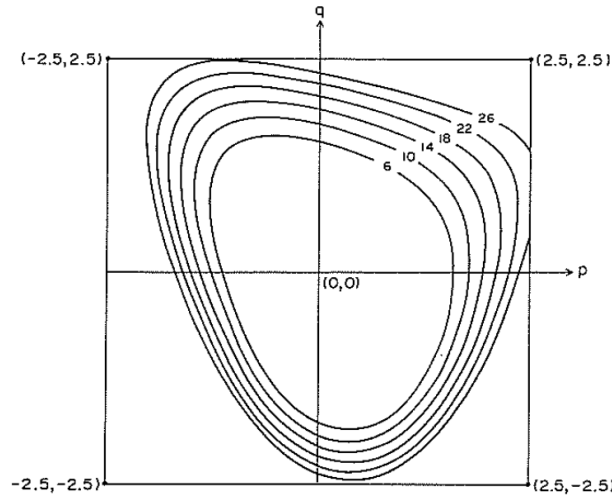
Figure 3.4: Contour plot illustrating the passive torques for the shoulder joint [3].

ankle, knee, and hip moments [2] [15] [40] but no values for the upper body were found. Instead, the parameters were determined from experimental data.

Engin [3] performed experiments to determine the passive moments of the shoulder complex for its full range of motion resulting in a contour plot like Figure 3.4. To find the parameters for Equation 3.7 a point for each contour in Figure 3.4 was extracted at the appropriate sagittal angle and the Matlab command `nlinfit` used to find the appropriate values. The same process was repeated for the wrist joint using data from [41], for the torso using data from [42], and for the forearm pronation/supination using data from [43]. The damping coefficient c_1 was set to 0.1 as suggested by Yamaguchi [2].

Plots showing the experimental data and the fitted curves using Equation 3.7 are shown in Figure 3.5 and the extracted parameters are given in Table 3.4.
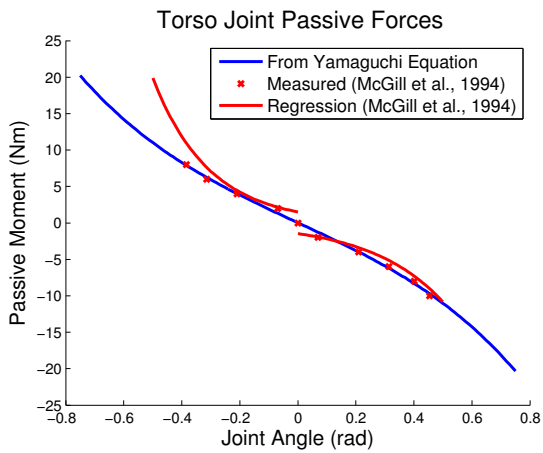
(a) Torso passive torque
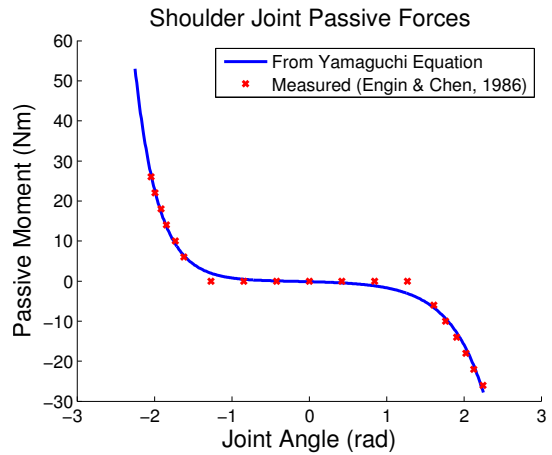
(b) Shoulder passive torque
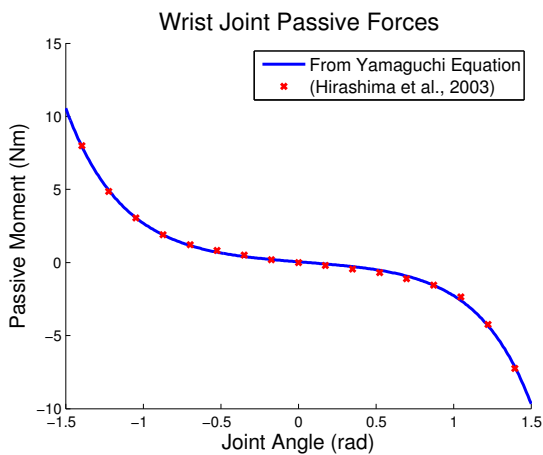
(c) Wrist passive torque
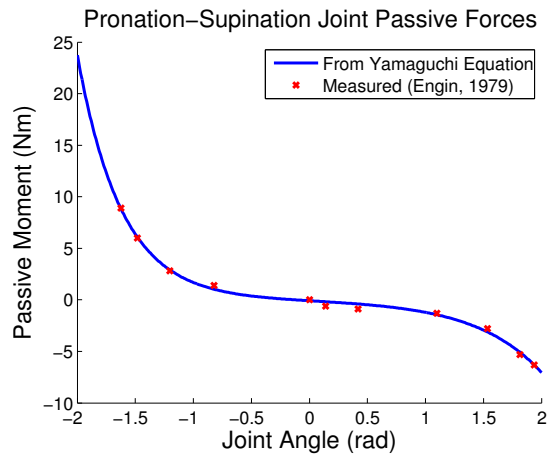
(d) Forearm passive torque

Figure 3.5: Fitting curves for the passive forces at each joint in the golfer model. In each graph, the measured experimental torques are shown in red and the fitted curve used in the model in blue. For the torso in (a), the experimental paper also provided a regression equation for the passive torques and this was also plotted for comparison.

Joint	θ_- (rad)	θ_+ (rad)	k_1	k_2	k_3	k_4	c_1
Torso	0.0618	-0.693	3.898	2.082	3.814	2.098	0.1
Shoulder	-1.289	1.210	2.111	3.354	2.704	2.241	0.1
Wrist	-1.171	1.185	4.301	2.732	3.895	2.891	0.1
Forearm	-1.237	1.340	3.206	2.624	2.216	1.752	0.1

Table 3.4: Parameters for passive joint torques at the torso, shoulder, and wrist joints

3.1.3 Control of the Swing

By replacing the golfer's muscle dynamics with parameterized joint torque functions in the form proposed by Mackenzie [38], control of the swing can be achieved by selecting appropriate values for $t_{activate}$ and $t_{deactivate}$ in equations 3.2 and 3.3. It is assumed that the swing is short enough that the golfer cannot turn their muscles on and off multiple times during the swing and that the golfer attempts to swing with maximum power. By modifying the relative timings of the joint torque activations, different swings can be achieved. The process for selecting the optimal swing parameters for a particular club will be discussed in detail in Section 3.6.

3.1.4 Validation

The golfer model was validated by Sasho Mackenzie by using the model to generate a swing similar to that of a live golfer [16]. The model was found to be able to produce angular displacement curves for the torso, shoulder, arm, and club that well matched the swing of the real golfer given the same initial starting configuration. This matching was performed by using the 8 control parameters for the joint torques along with a scale factor for the maximum joint torque values and angular velocities for each joint. The passive joint

torques added to Mackenzie's model were validated against experimental data as they were added to the model. The passive torque curves are shown fitted against the experimental data in Figure 3.5.

3.2 Flexible Club Model

3.2.1 Flexible Shaft

The club model consists of two parts, the flexible shaft and the clubhead. The flexible shaft used in the model is based on the work of Sandhu et al. [23]. The model uses a flexible Rayleigh beam [4] to describe the flexing and twisting of the club as it is swung. The approach makes use of a complete second-order elastic rotation matrix for a Rayleigh beam and has been implemented in the simulation package MapleSim. Shear due to bending and warping due to torsion are neglected, but the model can account for large deflections in the transverse directions that occur during the golf swing. The model can also account for changing stiffness, size, and density of material along the length of the shaft by defining each as a function of the distance from the bottom of the grip, x. Figure 3.6 shows the types of deformations that can be modeled using this type of beam.

In general, any particle of the flexible shaft can be located using four deformation variables: $u(x,t)$ for axial deformation, $v(x,t)$ and $w(x,t)$ for bending in the two transverse directions, and $\phi(x,t)$, the angle of twist about the centroidal axis. Deformation of the beam in each of these directions is approximated using Taylor series polynomials for the spatial variations, combined with a certain number of time-varying elastic coordinates for each of the four deformation variables. In this project, one elastic coordinate was used for the twist and for bending in each of the transverse directions. As a consequence $\phi(x,t)$,
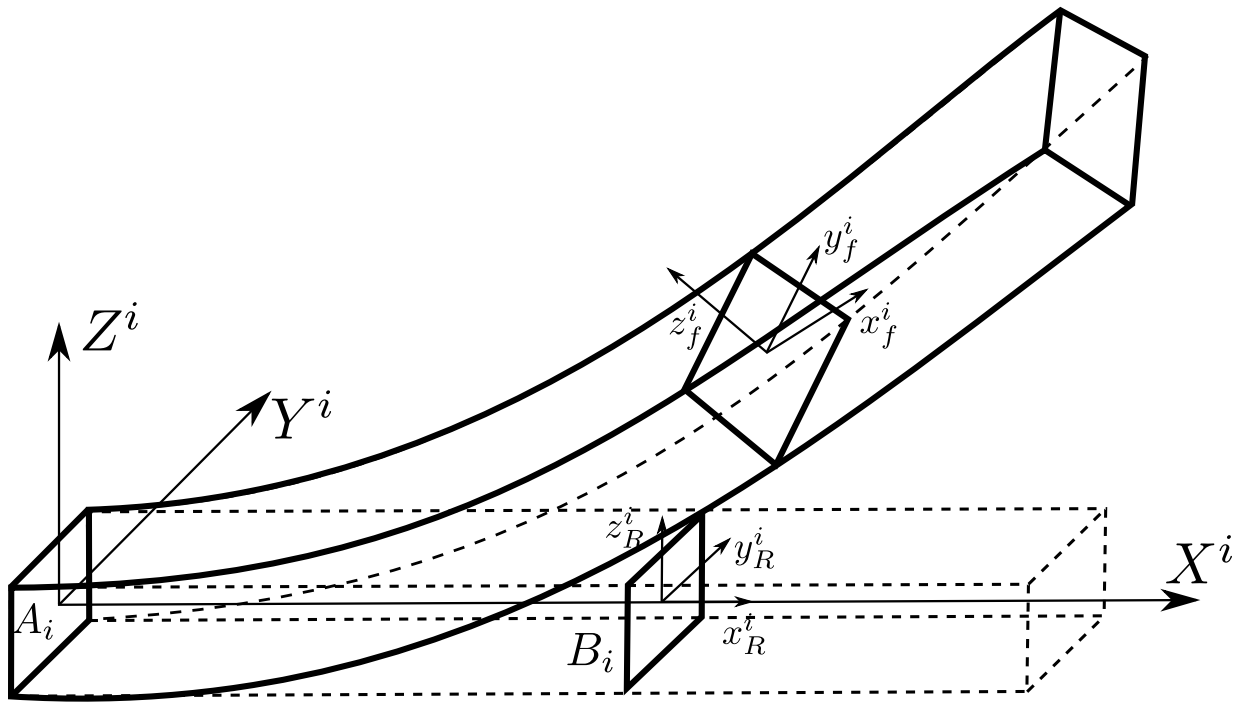
47

Figure 3.6: Flexible beam model as proposed by Shi et al. [4].

$v(x,t)$ and $w(x,t)$ are spatially approximated with 2nd order polynomials. No axial strain, measured by $u(x,t)$, was included in the model to improve computation times. To locate any point on the flexible shaft within 3-D space its position can be written as the location of the base frame of the shaft (in this model, the hands of the golfer), added to some function of the elastic coordinates detailed in [44]. Using short hand notation, we can rewrite this function as the position of the point with respect to the base frame, $\mathbf{r_{P/b}}$.

$$\mathbf{r}_p(x,t) = \mathbf{r}_b(0,t) + \mathbf{r}_{P/b}(x,t) \tag{3.8}$$

This equation can be used to calculate the position in 3-D space of any point on the flexible beam.

Flexible Club Parameters

Four different club shafts and their material properties, measured using a custom cantilever test rig, were provided by a manufacturer. The cross-sectional area, Young's modulus, shear modulus, and second moment of cross-sectional area vary along the length of the club and are approximated using sixth-order polynomials. Sixth-order polynomials were chosen to achieve a good fit for the data found in Appendix A. Normalized plots of the four clubs stiffness properties are shown in Figure 3.7. Non-normalized data cannot be shown due to an agreement with the manufacturer. Examining this figure, we can say that the green and orange shafts have a smooth transition of club stiffness and have likely not been tuned. The red, and in particular the blue, shafts have sharp changes in their stiffness profiles or are more heavily tuned. The density ($1510\,\mathrm{kg/m^3}$) and length of the shaft below the hands ($0.91\,\mathrm{m}$) are also required parameters for the model.

Sandhu et al. [23] validated the flexible club model with experimental testing and a finite element model of the shaft. This testing found good agreement between the dynamic
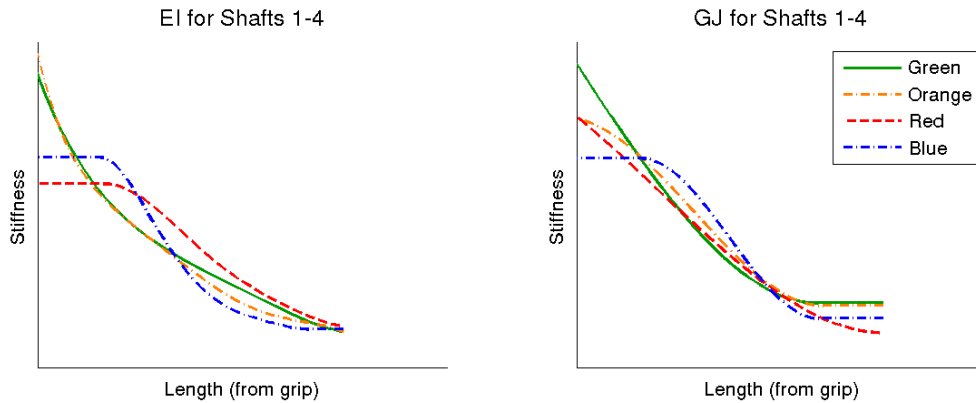
Figure 3.7: Flexible club properties provided by a club manufacturer. The specific units and values cannot be shown.

ΔX (mm)	ΔY (mm)	ΔZ (mm)	$Mass$ (g)	I_{yy} (g cm^2)
40.42	13.2	56.0	200	4200

Table 3.5: Clubhead geometry and mass properties

loft, droop, and clubhead speed at impact, showing that the model is suitable for use in forward dynamic simulation.

3.2.2 Clubhead

The clubhead is modeled as a rigid body fixed to the end of the flexible shaft. The most important parameters for the clubhead are the location of the centre of mass, mass, and moment of inertia of the clubhead about the vertical axis. These properties were measured for a set of clubheads as part of a different project and one clubhead was selected for initial use in this work. The properties of the selected clubhead are shown in Table 3.5. To interpret these properties, look at Figure 3.8 for the relevant frames of reference.
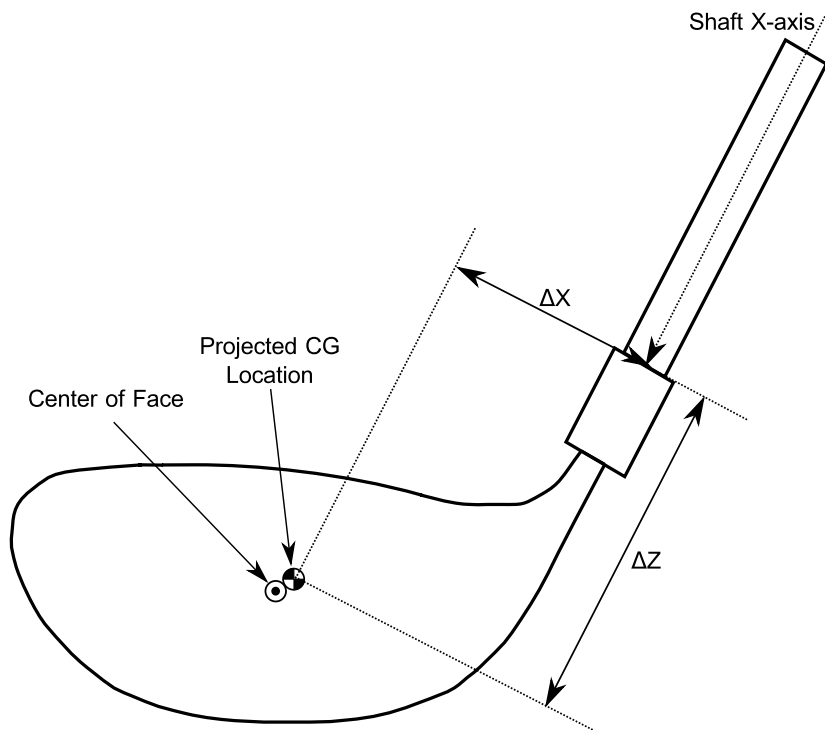
(a) Front view of clubhead model.
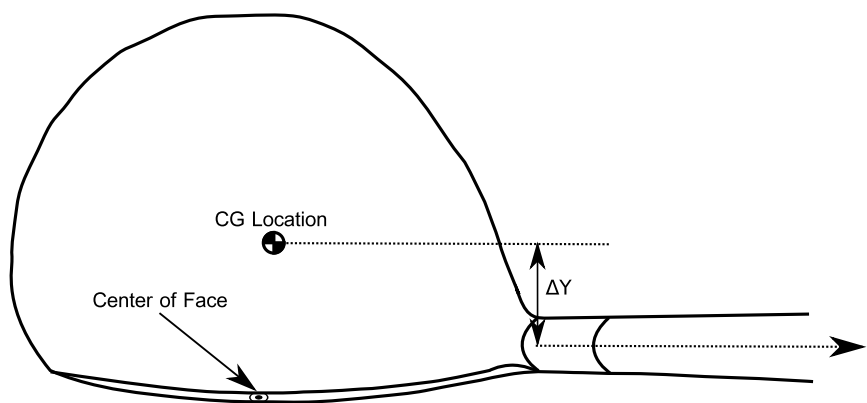
(b) Top view of clubhead model.

Figure 3.8: Diagram illustrating the frames of reference and measurements for the rigid body clubhead.

3.2.3   Clubhead and Shaft Aerodynamics

Clubhead Aerodynamics

The aerodynamics of the clubhead have a small, but not insignificant effect on the swing. Recently, several golf club companies (Ping and TaylorMade) have claimed that they are able to reduce the drag on their clubheads through the addition of small turbulators that change the way the airflow affects the club [45]. To account for aerodynamic effects, drag on the clubhead is included in the model using the standard drag equation:

$$\mathbf{F_d} = -(\frac{1}{2}\rho A C_d |\mathbf{V_{club}}|^2)\hat{\mathbf{V}}_{\mathbf{club}} \tag{3.9}$$

where ρ is the density of the air, A is the cross-sectional area of the clubhead, and C_d is the aerodynamic coefficient of the clubhead.

Experimental measurements of C_d were provided from experiments performed in a wind tunnel. A club was placed in the tunnel and rotated from a heel-first presentation to a face-first presentation at a variety of wind speeds. The C_d value for the clubhead was found to vary with both the presentation angle of the clubhead and the wind speed. The C_d values for each yaw angle at high clubhead speeds (greater than 33.5 m/s) are shown in Table 3.6. At lower speeds, C_d increases and it was found that the values are 50 % higher at 22.5 m/s. There is a linear transition zone between the high low speed values and the lower high speed values. Figure 3.9 shows a linear interpolation of the values of C_d for a large range of values of the yaw angle and clubhead speed.

Since the C_d value is dependent on both the yaw angle and the velocity of the clubhead relative to the air, we need to define these two variables within the context of the model. This requires the definition of a new coordinate system which is body-fixed in the clubhead with the X-axis pointing out of the face, the Y-axis upward along the shaft of the club, and
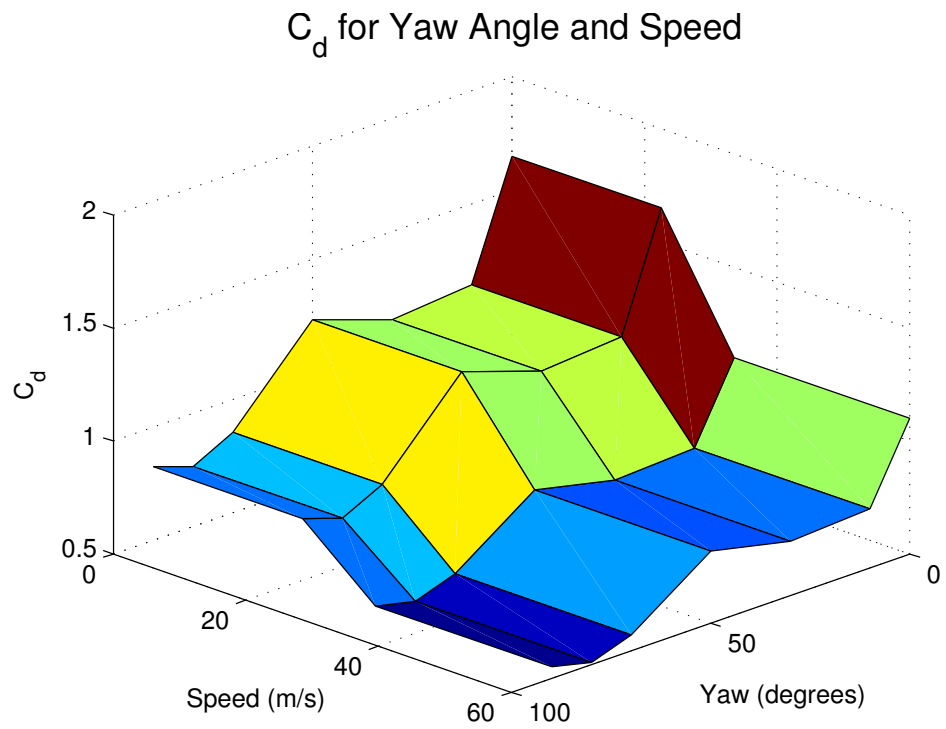
Figure 3.9: C_d values for the clubhead as modeled for different combinations of clubhead speed and yaw angle.
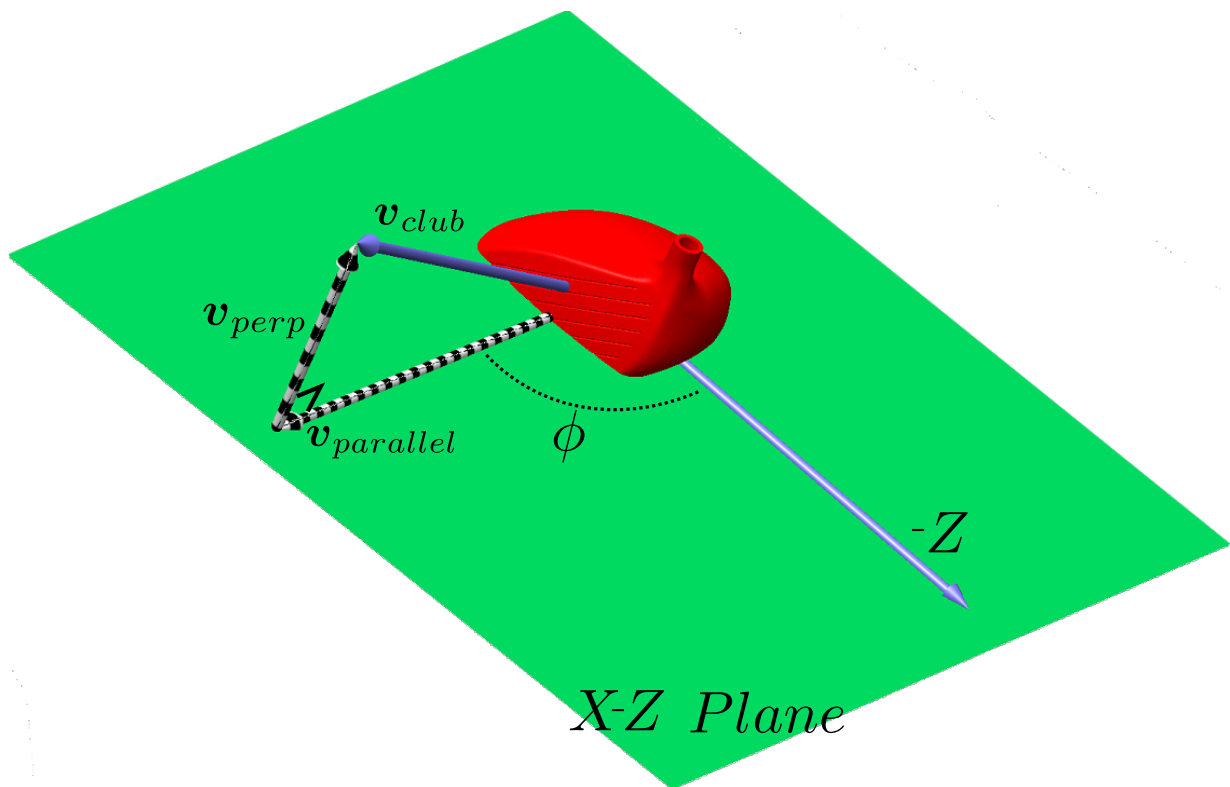
Figure 3.10: An illustration of the relevant frames and velocities for calculating the aerodynamic loads on the clubhead.

Yaw Angle (deg)	C_d
0	1.10
10	0.76
30	0.74
50	0.82
70	0.57
80	0.51
90	0.55

Table 3.6: Measured values of C_d for a variety of yaw angles at high clubhead speeds. A yaw angle of 0 degrees corresponds to a heel-first clubhead presentation (e.g., top of the backswing) while a yaw angle of 90 degrees corresponds to a face-first presentation (e.g., at impact).

the Z-axis tangent to the club face. We use this coordinate system to define the $X-Z$ plane in which the yaw angle of the club is calculated. To calculate the yaw angle, the velocity of the club is split into two components, $\mathbf{v}_{parallel}$ in the $X-Z$ plane, and $\mathbf{v}_{perpendicular}$ normal to the plane. The yaw angle is the angle between $\mathbf{v}_{parallel}$ and the $-Z$ axis. The speed of the airflow used in the calculation of $\mathbf{F}_d$ is then $\mathbf{v}_{parallel}$. Figure 3.10 illustrates the both the yaw angle and $\mathbf{v}_{parallel}$. The value of C_d at each moment is determined using a two-dimensional look up table based on ϕ and $|\mathbf{v}_{parallel}|$. Using this information, we can rewrite our aerodynamic equation as

$$\mathbf{F}_d = -(\frac{1}{2}\rho A C_d(\phi, |\mathbf{v}_{parallel}|)|\mathbf{v}_{parallel}|^2)\hat{\mathbf{v}}_{parallel}. \tag{3.10}$$

Finally, the effective cross-sectional area of the club was provided as a constant $A = 0.004805$ m^2 and the density of the air used in the simulations was $\rho = 1.1839$ kg/m^3.

Shaft Aerodynamics

Shaft aerodynamics were also included in the club and golfer model using the same standard aerodynamic equation as the basis of the analysis. This work was performed by Dr. Joydeep Banerjee, and the resulting model included in the golfer model developed for this project. The aerodynamics of the shaft are based on the aerodynamics of a cylinder moving through the air. Since different portions of the length of the shaft will be moving at different speeds, the standard aerodynamics equation is written in differential form as a function of the distance along the length, x.

$$d\mathbf{F}_d(x) = -\frac{1}{2}\rho(A(x)C_d(x)|\mathbf{V}_{shaft}(x)|^2)\hat{\mathbf{V}}_{shaft}(x) \tag{3.11}$$

To calculate the aerodynamic force, the values of $C_d(x)$, $A(x)$, and $\mathbf{V}(x)$ must be defined along with a method for applying the calculated force back to the model. $C_d(x)$ is defined as a constant, 1.2 [46], and $A(x)$ is simply the diameter of the shaft, D. $\mathbf{V}_{shaft}(x)$ is more complicated as the flexing of the shaft must be taken into account. To define the position of any point along the length of the shaft recall Equation 3.8 which adds the position of the flexible coordinates of the shaft, $\mathbf{r}_{p/b}$ to the position of the base frame, $\mathbf{r}_b$ (defined as the position of the golfer's hands).

$$\mathbf{r}_p(x) = \mathbf{r}_b + \mathbf{r}_{p/b}(x) \tag{3.12}$$

This equation is then differentiated to determine the velocity of the beam along its length.

$$\mathbf{V}_{shaft}(x) = \dot{\mathbf{r}}_p(x) = \dot{\mathbf{r}}_b + \mathring{\mathbf{r}}_{p/b}(x) + \boldsymbol{\omega}_{shaft} \times \mathbf{r}_{p/b}(x) \tag{3.13}$$

where $\mathring{r}_{p/b}$ is the velocity of the point of interest on the shaft with respect to the base frame and ω_{shaft} is the angular velocity of the base frame.

Once $C_d(x)$, $A(x)$, and $\mathbf{V}(x)$ have been defined, the total aerodynamic force applied to the shaft can be calculated by integrating Equation 3.11 along the length of the shaft.

$$\mathbf{F}_d = -\frac{1}{2}\rho C_d \int D(x)|\mathbf{V}_{shaft}(x)|^2\hat{\mathbf{V}}_{shaft}(x)\mathrm{d}x \tag{3.14}$$

Similarly, the moment applied by the aerodynamic force can be calculated by the integration of

$$\mathbf{M}_d = \int r_{p/b} \times \mathbf{dF}(x) \tag{3.15}$$

Unfortunately, MapleSim was unable to handle the integration of these equations symbolically, so instead a numerical integration was performed by dividing the shaft into 13 discrete sections. The number of sections was selected using a convergence study. To perform the integration numerically, the diameter which represented the area term has to be multiplied by the length of the segment.

$$A(x) = D(x)\frac{L}{N} \tag{3.16}$$

where L is the length of the shaft and N is the number of sections into which it was divided.

3.2.4   Validation

The flexible shaft model was validated by Sandhu [23]. A motion capture experiment was performed with four golfers in order to capture both the grip kinematics and the motion of the clubhead. The grip kinematics were then given to the flexible model of the club and the dynamic loft, droop, and clubhead speed compared between the analytical model, a finite element model, and the experimental data. The analytical model was able to achieve good agreement with the finite element model throughout the swing and good agreement with the experimental results during the impact phase of the swing. The clubhead aerodynamics

were compared to experimental data from [45] and found to be in good agreement. The shaft aerodynamics have not been validated experimentally for this work, but the C_d value for a cylinder in turbulent flow is well known [46].

3.3   Combined Club and Golfer Model

The combined club and golfer model is created by connecting the shaft of the flexible club to the hand of the golfer with a weld joint. Figure 3.11 shows the combined model.

3.4   Impact Model

As one of the goals of this work was to develop a golfer model that could be evaluated based on ball carry distance, it was important to include an impact model. The impact model should be able to determine the ball launch conditions based on the speed and orientation of the clubhead at impact and should result in slice and hook shots for hits with non-ideal clubhead conditions. The impact model should also be fast as it needs to be used many times within each simulation to determine the optimal location within the swing to hit the ball.

The impact model selected was based on the work of Petersen and McPhee [24] and is a three-dimensional impulse-momentum based approach. The equations which describe the impact are based on five assumptions that allow an efficient and simple model to be created:

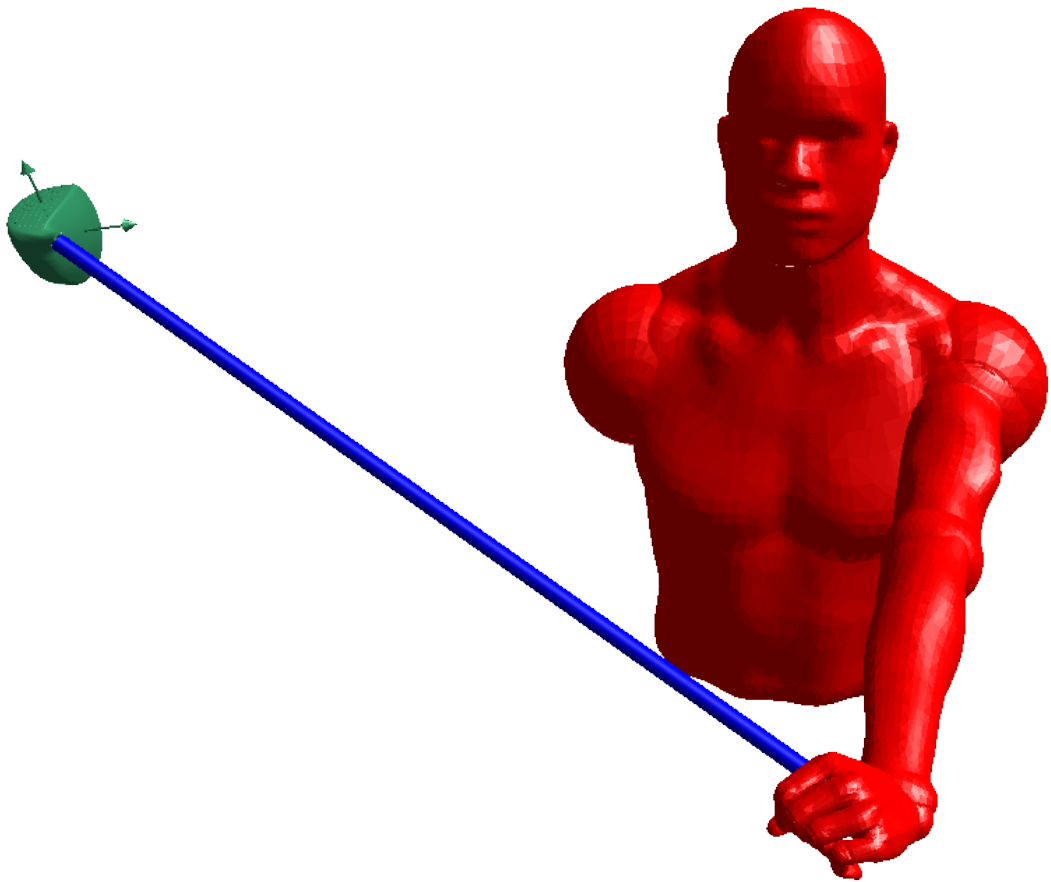1. Contact occurs at a single point between the clubhead and the ball.

Figure 3.11: The combined golfer and club model in the early part of a swing. The wrist has yet to break.

2. Contact occurs in a short period of time.

3. The velocity change of both the club and the ball happens instantaneously at the moment of impact.

4. There is negligible displacement during impact.

5. The ball rolls without slipping on the clubface (the gear effect as described in Section 2.1.4)

The impact model is used to determine the ball launch conditions based on the clubhead speed and orientation.

System of Equations

The ball and the clubhead each have 6 degrees of freedom (3 translational and 3 rotational) and therefore each have 6 velocity components following the impact. The three impulses of the impact are also unknown and are defined as the integrals of the contact forces over the length of the impact.

$$\mathbf{P}_n = \int \mathbf{F}_n \, dt \qquad \mathbf{P}_z = \int \mathbf{F}_z \, dt \qquad \mathbf{P}_y = \int \mathbf{F}_y \, dt \qquad (3.17)$$

In total there are 15 unknowns which must be solved for by the model, 12 velocity components and 3 impulses.

To solve for 15 unknowns, 15 equations are required and they can be formulated in the following groups:

- 6 equations for linear impulse and momentum (3 for each body)

- 6 equations for angular impulse and momentum (3 for each body)

60

- 1 equation for normal restitution

- 2 equations from the kinematic constraint of the the ball rolling without slipping on the clubface (stiction)

Impulse and Momentum Equations

Figure 3.12 and Figure 3.13 shows the free body diagram and frames of reference used for developing the impulse and momentum equations for the clubhead and the ball. There are four relevant reference frames. The first is the global frame (X, Y, Z) in which the clubhead velocity is inputted and the ball velocity is calculated. The term X is the downrange direction, Y is upwards, and Z is outwards away from a right handed golfer. The second reference frame (x_c, y_c, z_c) is the clubhead frame which is the coincident with the global frame when the club is at address position and is body fixed in the club at the centre of mass. The third reference frame is the ellipsoid frame $(x_{ell}, y_{ell}, z_{ell})$ which is used to define an analytical shape for the face of the clubhead. This frame has its origin at the center of an ellipsoid defined by the clubhead's bulge and roll and is inclined from the clubhead frame by the loft angle (α) of the club so that the x_{ell} axis passes through the centre of face of the club normal to the surface. The final frame of reference is the impact frame $(x_{imp}, y_{imp}, z_{imp})$ which is normal to the clubface at the point of impact. The angles γ and β between the ellipsoid frame and the impact frame are caused for an off-centre impact by the bulge and roll of the club and are calculated using the ellipsoid which approximates the surface of the clubface. Throughout this section, the final subscript of each variable will indicate the frame of reference in which it is defined.

The system equations are written in the impact frame. By applying the principle of impulse and momentum to the bodies involved, the equations for the clubhead can be

written as

$$m_c \mathbf{V}_{c_{imp}} - m_c \mathbf{v}_{c_{imp}} = -\mathbf{P}_{\mathbf{imp}} \tag{3.18}$$

$$\mathbf{I}_c \cdot \boldsymbol{\Omega}_{impc} - \mathbf{I}_c \cdot \boldsymbol{\omega}_{c_{imp}} = \mathbf{r}_{imp} \times -\mathbf{P}_{\mathbf{imp}} \tag{3.19}$$

and the equations for the ball can similarly be written

$$m_b \mathbf{V}_{b_{imp}} - m_b \mathbf{v}_{b_{imp}} = \mathbf{P}_{\mathbf{imp}} \tag{3.20}$$

$$\mathbf{I}_b \cdot \boldsymbol{\Omega}_{b_{imp}} - \mathbf{I}_b \cdot \boldsymbol{\omega}_{b_{imp}} = \mathbf{r}_{ball} \times \mathbf{P}_{\mathbf{imp}}. \tag{3.21}$$

In these equations, and throughout this section, capital letters will stand for the velocity and spin of the ball and club before impact and lowercase letters will be used for the velocity and spin before impact. Also, m_c, $\mathbf{I}_c$, m_b, and $\mathbf{I}_b$ represent the mass and inertia tensors for the club and ball respectively. $\mathbf{P}$ is the combined vector of the three impulses, $\mathbf{P}_n$, $\mathbf{P}_z$, and $\mathbf{P}_y$. $\mathbf{r}_{imp}$ is the vector from the center of mass of the club to the impact point in the impact frame, and $\mathbf{r}_{ball}$ is the vector from the center of mass of the ball to the impact point in the impact frame.

Restitution Equation

The coefficient of restitution (CoR) is the factor which accounts for energy loss in the impact of the ball and the club. By rule, e is restricted for golf clubs to be less than 0.83 [25]. In equation form, e is defined as the ratio of the final to initial velocities of the colliding bodies in the impact frame, normal to the plane of contact between them.

$$e = \frac{V_{c_{x_{imp}}} - V_{b_{x_{imp}}}}{v_{c_{x_{imp}}} - v_{b_{x_{imp}}}} \tag{3.22}$$

e implicitly accounts for the energy lost during the impact due to the deformation of the ball and the vibration of the clubhead.
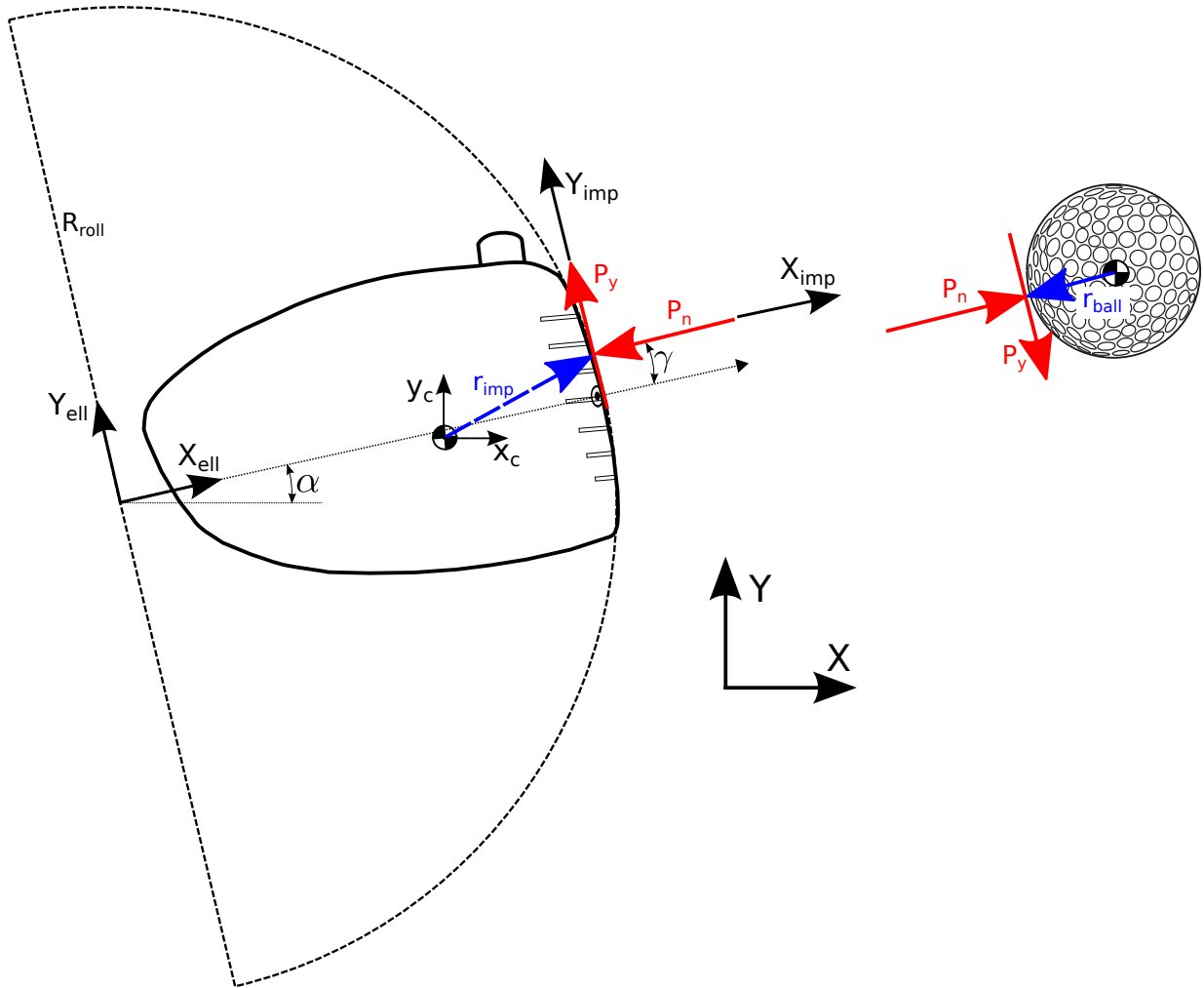
Figure 3.12: Side view of the impact model illustrating impulses, frames of reference, and the clubhead ellipsoid.
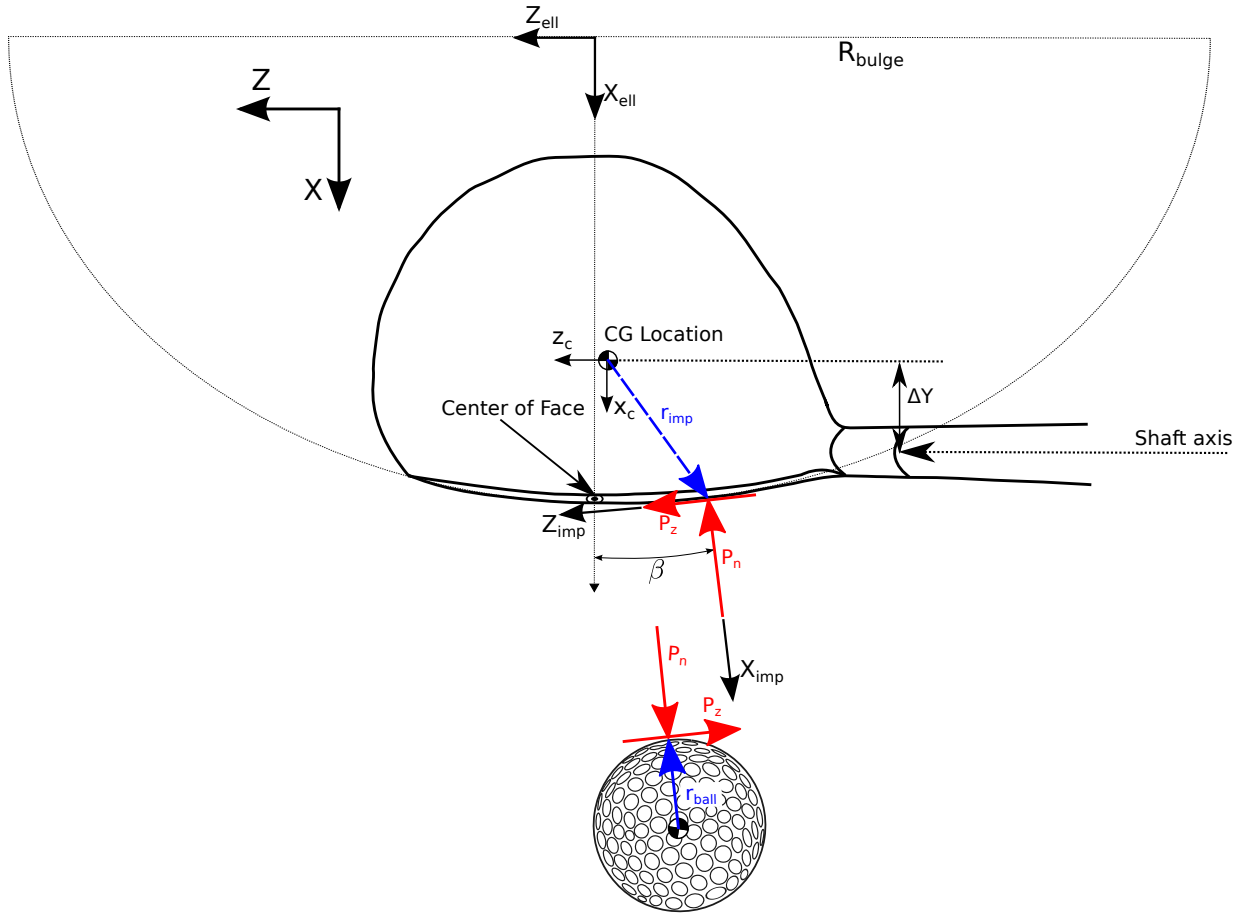
Figure 3.13: Top view of impact mode illustrating impulses, frames of reference, and the clubhead ellipsoid.

Kinematic Stiction Constraint (Gear Effect)

Due to the gear effect, before the ball leaves the club face it is assumed to have reached the state of rolling without slipping. Hence, two kinematic constraints can be added to the system of equations to solve to find the impact conditions. In each of the tangential directions, the point in contact between the ball and the club must be moving in the same direction at the same speed after the impact.

$$V_{c_{y_{imp}}} - V_{b_{y_{imp}}} = 0 \tag{3.23}$$

$$V_{c_{z_{imp}}} - V_{b_{z_{imp}}} = 0 \tag{3.24}$$

Equations 3.18 through 3.24 constitute the 15 equations required to solve for the 15 unknowns in the impulse-momentum balance. The velocity and spin of the ball and clubhead pre-impact are known along with the orientation of the clubhead and these are used to calculate the change in the velocity and spin of the ball and club after impact in the impact frame. A transformation matrix is found using the angles α, β, and γ to transform this velocity back into the global frame.

Rotation Transformations Between Frames of Reference

As the inputs to the impact model are given in the inertial frame and the calculations occur in the impact frame, a rotation transform between these frames is required to calculate the appropriate values of the clubhead velocity and spin before impact and the ball velocity and spin after impact. This rotation transform is calculated using the orientation of the clubhead (the rotation matrix R_{club}), the loft angle (α), and the impact location on the face of the club relative to the centre of face (a two element vector defined in the ellipsoid frame $[\Delta Y \ \Delta Z]$).

First, the impact location is used to calculate the angles β and γ and the value of the x-coordinate of the impact location. Since the clubface is defined as an ellipsoid the location of any point on the surface can be calculated using just the provided coordinates ΔY and ΔZ using the ellipsoid equation,

$$x = \frac{\sqrt{b^2 c^2 - b^2 \Delta Z^2 - c^2 \Delta Y^2} ab}{c} \tag{3.25}$$

where a is ellipsoid radius in the x direction, b is the ellipsoid radius in the y direction (roll), and c is the ellipsoid radius in the z direction (bulge).

The angles β and γ can then be calculated by taking the inverse tangent of the derivatives of x with respect to y and z.

$$\tan \beta = \frac{\mathrm{d}x}{\mathrm{d}z} = \frac{ab\Delta Z}{\sqrt{b^2 c^2 - b^2 \Delta Z^2 - c^2 \Delta Y^2} c} \tag{3.26}$$

$$\tan \gamma = \frac{\mathrm{d}x}{\mathrm{d}y} = \frac{ac\Delta Y}{\sqrt{b^2 c^2 - b^2 \Delta Z^2 - c^2 \Delta Y^2} b} \tag{3.27}$$

A number of different useful rotation matrices are defined in terms of α, β, and γ. First a rotation from the ellipsoid frame to the impact frame is calculated:

$$[R_{ell \to imp}] = \begin{bmatrix} \cos \beta & 0 & -\sin \beta \\ 0 & 1 & 0 \\ \sin \beta & 0 & \cos \beta \end{bmatrix} \begin{bmatrix} \cos \gamma & \sin \gamma & 0 \\ -\sin \gamma & \cos \gamma & 0 \\ 0 & 0 & 1 \end{bmatrix} \tag{3.28}$$

The rotation from the centre of mass frame of the club to the ellipsoid frame is just a simple rotation about z_{CoM} using the loft angle:

$$[R_{CoM \to ell}] = \begin{bmatrix} \cos \alpha & \sin \alpha & 0 \\ -\sin \alpha & \cos \alpha & 0 \\ 0 & 0 & 1 \end{bmatrix} . \tag{3.29}$$

66

And then finally the rotation matrix from the inertial frame to the impact frame is the product

$$[R] = [R_{club}][R_{CoM \rightarrow ell}][R_{ell \rightarrow imp}]. \tag{3.30}$$

The inverse of this matrix $[R]^T$, provides the inverse transformation needed after the ball velocity is calculated.

Parameters for the Impact Model

The clubhead and ball parameters that are required for the impact model are shown in Tables 3.7 and 3.8. For the clubhead, these parameters were taken from measurements of a Ping i15 driver while the ball parameters are standard values.

Parameter	Value
$Mass$ (g)	200
I_{xx} (g cm^2)	3000
I_{yy} (g cm^2)	4200
I_{zz} (g cm^2)	2200
$Bulge$ (cm)	30
$Roll$ (cm)	30

Table 3.7: Required clubhead parameters for the impact model.

3.4.1 Validation

Validation of the impact model was performed as part of the work of Petersen and McPhee [24]. In this work, the results of impulse-momentum impact model were compared to the

Parameter	Value
Mass (g)	45.93
Radius (cm)	2.1336

Table 3.8: Required ball parameters for the impact model.

results from a finite element model of the ball and club impact. For an impact at the sweet spot of the club, the velocity of the ball after impact was within 6% of the finite element model.

3.5   Ball Aerodynamics

After the ball launch velocity and spin has been calculated, the ball flight is computed using an aerodynamic model to allow for comparisons of impacts. This model takes into account the lift, drag, and gravitational forces on the ball in flight. It also includes a decay term for the spin of the ball. A free body diagram of the ball in flight is shown in Figure 3.14. The aerodynamic model used is based on the work of Quintavalla [47] which provides equations and coefficients for calculating the forces on the ball in flight. It also includes the ability to include wind conditions and elevation data for the tee, but these factors were not included in the model.

The model is simple and uses the usual aerodynamic equations for the forces on the ball. The gravitational force $\mathbf{W}$ is just the weight of the ball acting in the negative Y direction.

$$\mathbf{W} = m_{ball}\mathbf{g} \tag{3.31}$$

The drag force $\mathbf{D}$ acts opposing the direction of motion of the ball and is proportional to

68
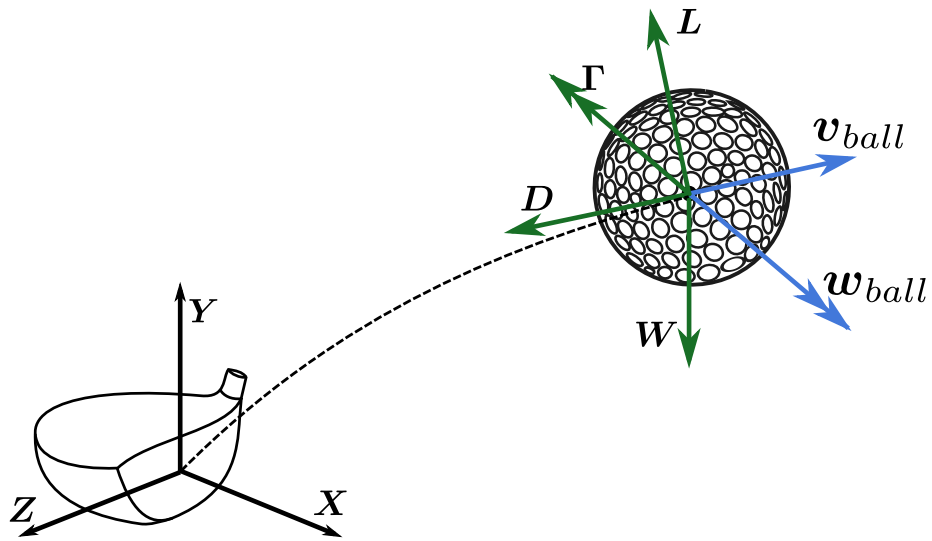
Figure 3.14: Free body diagram of the ball in flight.

the square of the velocity.

$$\mathbf{D} = \frac{1}{2}\rho A_{ball}|\mathbf{v}_{ball}|^2 C_D(-\hat{\mathbf{v}}_{ball}) \tag{3.32}$$

The lift force $\mathbf{L}$ acts perpendicular to the velocity of the ball ($\mathbf{v}_{ball}$) and perpendicular to the spin ($\boldsymbol{\omega}_{ball}$) in the direction of $\boldsymbol{\omega}_{ball} \times \mathbf{v}_{ball}$.

$$\mathbf{L} = \frac{1}{2}\rho A_{ball}|\mathbf{v}_{ball}|^2 C_L(\hat{\boldsymbol{\omega}}_{ball} \times \hat{\mathbf{v}}_{ball}) \tag{3.33}$$

The final force Γ that acts on the ball is a torque that opposes the spin of the ball and slows it down throughout its flight. The direction of the spin does not change.

$$\Gamma = \frac{1}{2}\rho A_{ball}|\mathbf{v}_{ball}|^2 C_M D_{ball}(-\hat{\boldsymbol{\omega}}_{ball}) \tag{3.34}$$

The coefficients C_D, C_L, and C_M are determined experimentally and the values were found to be dependent on the spin rate of the ball S_p.

$$S_p = \frac{\omega_{ball}\frac{D_{ball}}{2}}{V} \tag{3.35}$$

And the coefficients calculated as follows:

$$
\begin{aligned}
C_D &= 0.171 + 0.62S_p \\
C_L &= 0.083 + 0.885S_p \\
C_M &= 0.0125S_p
\end{aligned}
\tag{3.36}
$$

These values were provided for imperial units so a careful unit conversion was performed before the aerodynamic calculations were performed.

Once the values of the aerodynamic coefficients were determined, the equations of motion for the ball were found by projecting the force equations onto the XYZ coordinate system. The resulting equations of motion for the ball are numerically integrated within Matlab.

3.5.1 Validation

Validation of the ball trajectory model was performed by comparing the results to robot testing data. In this comparison, ball launch conditions from 10 different swings were inputted into the aerodynamic model and compared to their actual trajectories from robot testing. The mean carry distance was found to be $3.23\,\mathrm{m}$ less than the robot testing data with the mean dispersion distance being only $0.36\,\mathrm{m}$ different. The ball model used in this work is from older ball data and could be updated to include modern coefficients if they were available. This would help to resolve the discrepancy between the model and the robot testing results.

3.6 Optimal Control

In order for the simulated golfer to adapt to different situations, it is important to optimally control the swing to produce the best swing for each set of simulation parameters used. A real golfer would modify their swing when given a different club, and the simulated golfer should similarly adjust as required. The optimal control of the golf swing is a difficult problem to solve directly, as there are many inputs and biological constraints on the inputs so instead of using conventional optimal control techniques (e.g., Pontryagin's Minimum Principle or dynamic programming) the control of the model was achieved by the selection of parameters for the muscle torque generators.

The optimal control of the golfer model was performed through the activation and deactivation timing of the four torque generators in the biomechanical model. From equations 3.1 to 3.3, each torque generator is controlled by the timing parameter $t_{activate}$ and $t_{deactivate}$. By proper selection of these two parameters, the action of the muscles is con-

trolled. Through the use of these parameterized torque functions, the optimal control of the swing is reduced from a free optimal control problem with arbitrary torques throughout the duration of the swing to a parameter optimization problem.

To solve the parameter optimization, the Matlab routine `patternsearch` was used to search the possible parameter space for the optimal swing. Two different objective functions were developed to determine which one produced the best results.

3.6.1   Objective Function One: Maximum Clubhead Velocity

The first objective function developed attempts to maximize the clubhead velocity while applying penalties to the swing based on the orientation and direction of motion of the clubhead at impact. The function is simple

$$M = V_{club} - W_a|\Delta\Theta_a| - W_{ha}|\Delta\Theta_{ha}| - W_c|\Delta\Theta_c| - W_l|\Delta\Theta_l| \tag{3.37}$$

and requires the definition of the following parameters:

- V_{club} : clubhead speed

- $\Delta\Theta_a$: deviation of the attack angle from the range of 2-6 degrees

- $\Delta\Theta_{ha}$: deviation of the horizontal attack angle from 0 degrees

- $\Delta\Theta_c$: deviation of the face angle from 0 degrees

- $\Delta\Theta_l$: deviation of the dynamic loft from the range of 7-15 degrees

- W_i : weighting terms.
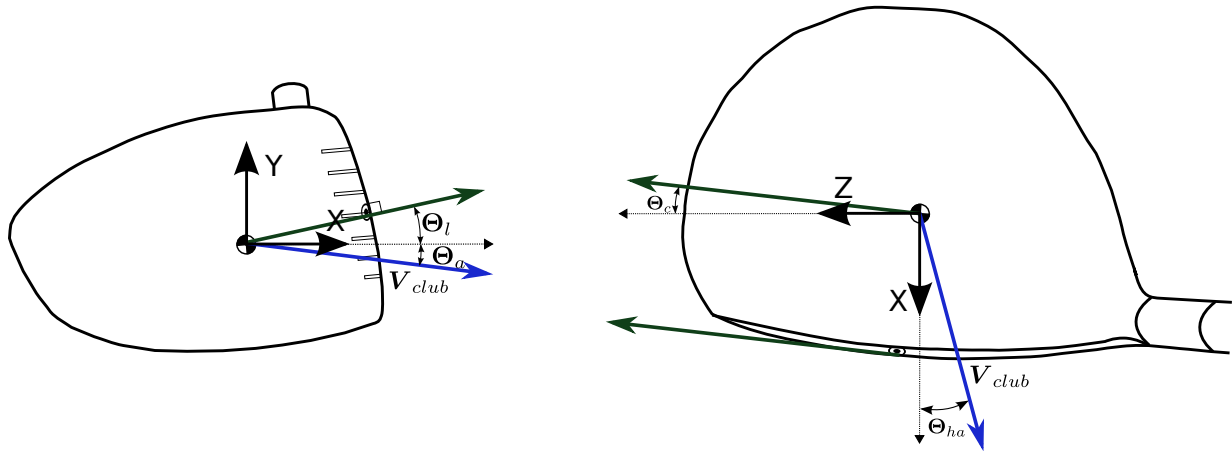
Figure 3.15: Illustrating the required angles for calculating the penalties in objective function 3.37. The blue arrow indicates the direction of the velocity of the clubhead, which is required for calculating the attack angle, Θ_a, and the horizontal attack angle, Θ_{ha}. The green arrow on the left is normal to the clubface and the green arrows on the right are tangent to the clubface. They are used to calculate the dynamic loft, Θ_l, and face angle, Θ_c, at impact.

Figure 3.15 illustrates the definitions of these parameters. When using this objective function, it is necessary to select appropriate values for the ranges of acceptable values for each of the penalty terms. It is straightforward to select the ideal value for the horizontal attack angle and face angle of the club as 0 degrees, but it is more difficult to select the correct values for the dynamic loft and the vertical attack angle. Instead, a range of acceptable values was selected.

This objective function was used to produce some preliminary results, but it was difficult to decide if the swings produced were optimal in terms of the ball launch conditions. Hence, the impact and aerodynamic model described above were created to allow the definition of a second, more intuitive, objective function.

3.6.2 Objective Function Two: Ball Carry

The goal of the second objective function is to use the most intuitive method for evaluating a swing by examining the flight path of the ball. The goal is to maximize the distance the ball carries while minimizing the lateral deviation of its flight. The objective function is designed to allow for a small amount of lateral deviation without a significant penalty to simulate the ball landing in the fairway, but larger deviations are heavily penalized to simulate landing in the rough or out of bounds. The equation is

$$M = X - We^{Z^2/Z_{max}^2} \tag{3.38}$$

where X is the downrange carry, Z is the lateral deviation, Z_{max} is the maximum acceptable deviation, and W is a weighting term. Figure 3.16 shows how this function behaves for constant X and a range of values for Z. It's clear from the Figure that for deviations greater than Z_{max} (10 yards), the calculated goodness of the swing (M) is greatly decreased.

The objective function based on ball carry was used to evaluate swings for the remainder of the project.

Striking the Ball

One important question remains in choosing the optimal parameters for the swing: "Where should the ball be placed by the golfer?" or more accurately within the context of the model: "Where within the swing should the golfer strike the ball?"

To determine the best position within each swing for striking the ball, the simulation examines a range of points within the swing and tests them all to determine which ball position results in the best flight. For every point where the clubhead is within 7 cm of its lowest, the impact and aerodynamic analysis is performed and the value of the objective
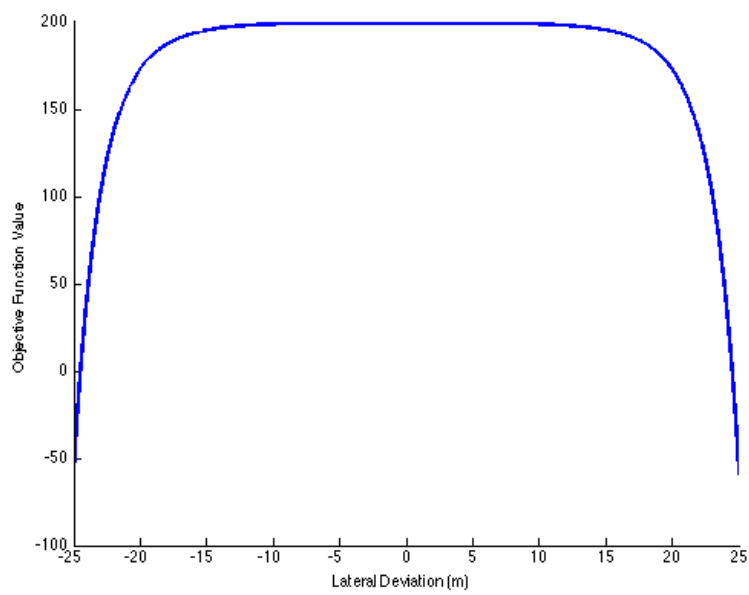
Figure 3.16: A plot of objective function 3.38 for constant $X = 200$ with $Z_{max} = 10$. The function is flat across the acceptable range from -10 to 10, but steeply penalizes shots with larger lateral deviations.

function (Equation 3.38) calculated. The point with the highest value is selected as the ideal point of contact for that swing, and that ball carry and objective function value are considered to be the value for that particular swing. For all impact calculations, the ball is assumed to strike the center of the clubface.

3.7   Complete Model

The completed golf model includes all the sub-models described so far. The combined golfer-club model provides the clubhead position, velocity, and orientation to the impact model, the impact model calculates the initial conditions for the ball flight, and the trajectory model calculates the carry distance for the ball. Figure 3.17 show the inputs, outputs, and parameters for each part of the model. The entire model is then controlled through parameter optimization of the joint torque activation timings to maximize the ball carry.

3.8   Implementation

The golfer and club model was implemented in MapleSim 6.4 [48]. This software product has the capability of easily and quickly generating the equations for multibody dynamic systems. After implementation, the generated equations were then exported to create a C-function which is able to calculate the velocity and orientation of the clubhead throughout the swing given the muscle activations and initial conditions for the golfer's joints. This function was compiled into a `.mex` function in Matlab [49] where the optimization process was performed.

A number of different optimization techniques were experimented with in Matlab including `fminsearch`, `patternsearch`, and genetic algorithms (`ga`). The best and most
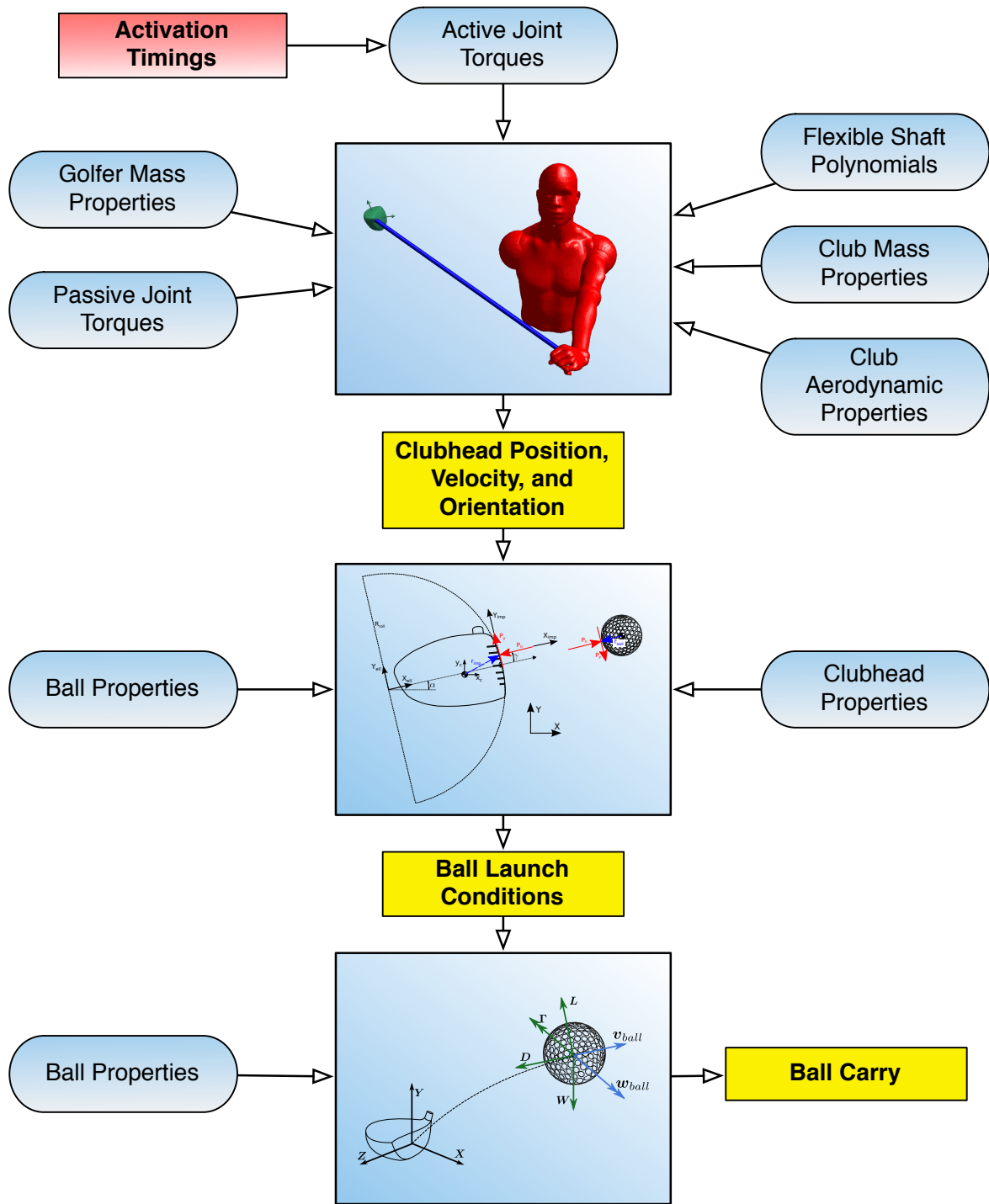
Figure 3.17: The complete golfer-club, impact, and carry model.

consistent results were obtained using `patternsearch`. The `patternsearch` algorithm works by direct search starting from an initial guess for the optimal solution. The objective function is evaluated at the initial guess and then at a surrounding mesh of points a certain distance away within vector space which contains acceptable variable values. The search distance is initially 1 but changes as the algorithm progresses. If a surrounding point is found to have a better objective function value, the center of the search is moved to that point and the search distance increased. If there is no better point found, the search distance is decreased and the closer points checked. The algorithm terminates when the search distance is sufficiently small and there is no point evaluated which improves the value of the objective function beyond a certain tolerance.

Within the optimization, the activation times of the various torque generators were optimized simultaneously with the starting joint angles for the golfer. This meant that there were 11 variables within the optimization. These variables along with their constraints are shown in Table 3.9. In addition, the activations of the muscles were constrained to occur before the deactivations.

Variable	Initial Guess	Min. Value	Max. Value
Torso Activation	0 s	-0.1 s	0.1 s
Torso Deactivation	0.22 s	0.1 s	$simLength$ s
Shoulder Activation	0.004 s	-0.05 s	0.1 s
Shoulder Deactivation	0.18 s	0.05 s	$simLength$ s
Forearm Activation	0.13 s	0.05 s	$simLength$ s
Forearm Deactivation	0.22 s	0.05 s	$simLength$ s
Wrist Activation	0.04 s	0 s	0.15 s
Wrist Deactivation	0.12 s	0.1 s	$simLength$ s
Initial Shoulder JA	70°	68°	72°
Initial Forearm JA	90°	88°	92°
Initial Wrist JA	110°	108°	112°

Table 3.9: List of the 11 variables that are optimized by the `patternsearch` and their initial values and constraints. $simLength$ means the end of the simulation time.

Chapter 4

Results and Discussion

Results from the model will be discussed in the following order. First a detailed discussion of the results from a swing with the default parameters can be found in Section 4.1. This Section will provide an example of the results that can be obtained from the model and will describe a normal swing obtained by the optimization process. Following in sections 4.2 through Section 4.7 will be a series of experiments performed using the model. These will explore the effects of changing a variety of club parameters. The results shown in these sections will highlight the differences from those in Section 4.1 and will try to explain those differences both qualitatively and quantitatively. This Chapter will conclude with a discussion of the usefulness of the model and its limitations in Section 4.8. Throughout this chapter, a vertical line through a time plot will indicate the moment of impact. Since the impulses of the impact are not applied back to the golfer model, results for the club and golfer after impact are not plotted. For each impact, the ball is struck at the centre of the driver face. For all the following plots unless otherwise specified, the X direction is downrange, the Y direction is upwards, and the Z direction is pointed away from the

golfer.

4.1   Results for the Default Parameters

After running the optimization procedure outlined in Section 3.6, the results from a single swing were obtained. These results are presented here as a baseline for comparison to the experiments that follow in Sections 4.2 to 4.7. The model used for this simulation is the model presented in Chapter 3 using the default parameters and the Green shaft. The following plots show the large range of swing characteristics that can be examined using this model.

First, for the default parameters, the optimized ball carry is 214 yards with a lateral deviation of 2 yards. After impact the ball has 3280 rotations per minute (RPM) of backspin, a launch angle of 18.1°, and a ball speed of 60.8 m/s (136 mph). The trajectory results can be found in Figure 4.1 and show a trajectory without upward ballooning as discussed in Section 2.1.5. The backspin is a little high for the ball speed resulting in higher than optimal trajectory but overall the swing leads to a reasonable ball flight for the clubhead speed.

The clubhead speed is shown in Figure 4.2. Peak clubhead speed is reached slightly before impact and the clubhead speed at impact is 41.5 m/s (92.8 mph). The clubhead speed at impact is slightly slower than the peak clubhead speed to achieve better impact conditions with the ball. By delaying the impact slightly, the club has started to move upwards improving the attack angle of the swing and increasing the launch angle.

Figure 4.3b shows this delay illustrating how the club is moving upwards at impact. Increasing the delay further decreases the benefit since the clubhead is slowing down and
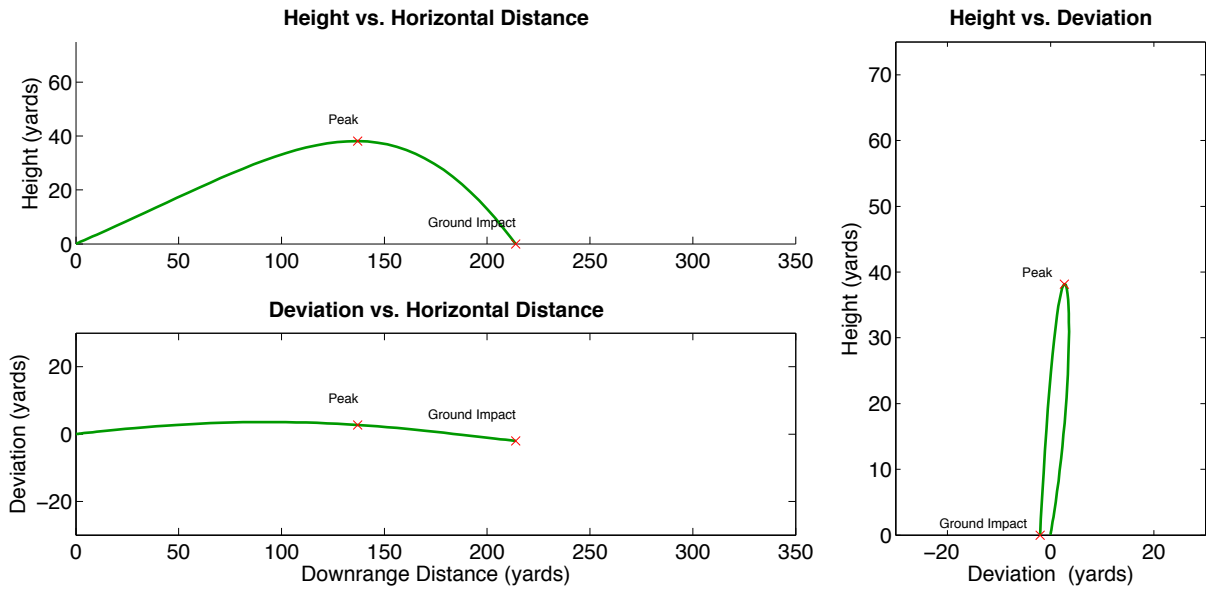
Figure 4.1: Ball trajectory for swing with default parameters.
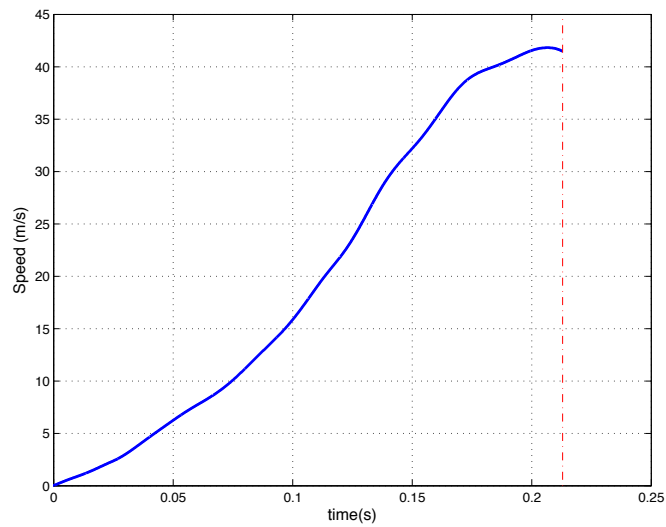
Figure 4.2: Clubhead centre of mass speed for swing with default parameters.

82

clubhead speed is the most significant factor in the ball carry distance. The ball is struck near the low point of the swing at a position about 1 m along the z-axis in front of the golfer's torso. The ball is struck 1.7 cm above the low point of the swing at a legal tee height. This positioning can be seen in Figure 4.3a by comparing the low point of the y-direction clubhead position with the impact point.

The golfer's kinematics are also available from the model. The joint angles are shown in Figure 4.4. This Figure clearly illustrates the kinematic sequencing of the swing. At $t = 0$, the torso starts its forward motion, followed by the shoulder around $t = 0.05$, the wrist at $t = 0.1$ and finally the forearm around $t = 0.15$. This progression from the proximal to distal joints is similar to those found in experimental results [12] and previous modeling results [19]. The forearm is a bit of special case as it is not more distal than the wrist. Instead, it waits for the wrist to start rotating since the rotation of the wrist brings the club in line with the arm reducing the moment of inertia of the arm-club complex. Once the club is in line with the arm, it is easier for the pronation of the arm to occur.

The active joint torques for the default golfer can be found in Figure 4.5a. For the shoulder and forearm, the joint torque is activated slightly before the motion begins, providing the main impetus for the motion. For the wrist and torso the wrist joint and torso joint, a large passive moment (due to coiling at the top of the backswing) provides the torque which starts the motion before the active torque fires. The passive torques can be found in Figure 4.5b. The passive torque in the pronation and supination of the arm is small since that joint does not reach the limits of the normal range of motion for the arm. The combination of the passive and active torques for each joint is shown in Figure 4.6. This Figure shows the joint torque at each joint peaking as the motion begins and falling off as the joint is accelerated.

The model is especially sensitive to changes in the timing of the forearm torque as it
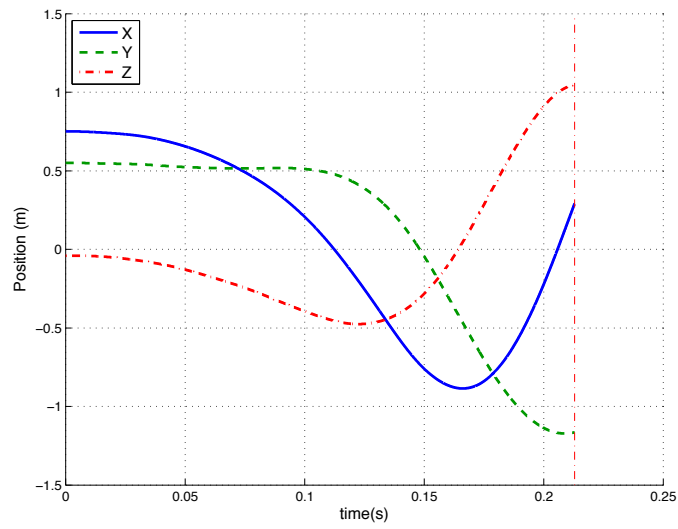
(a) Centre of mass position
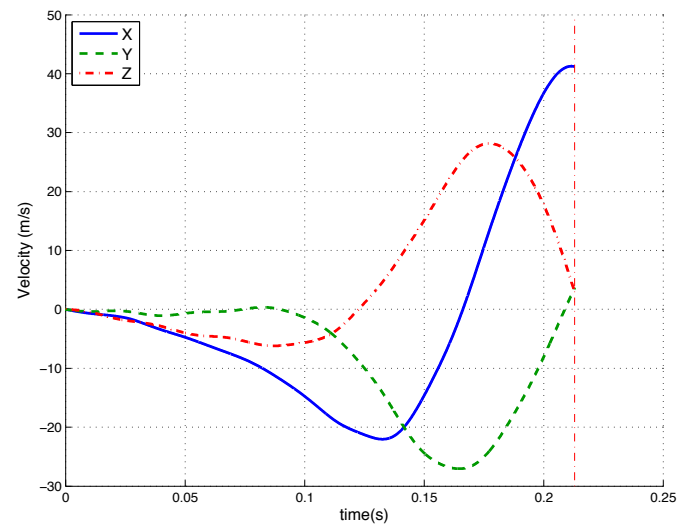
(b) Centre of mass velocity

Figure 4.3: Clubhead kinematics for swing with default parameters.
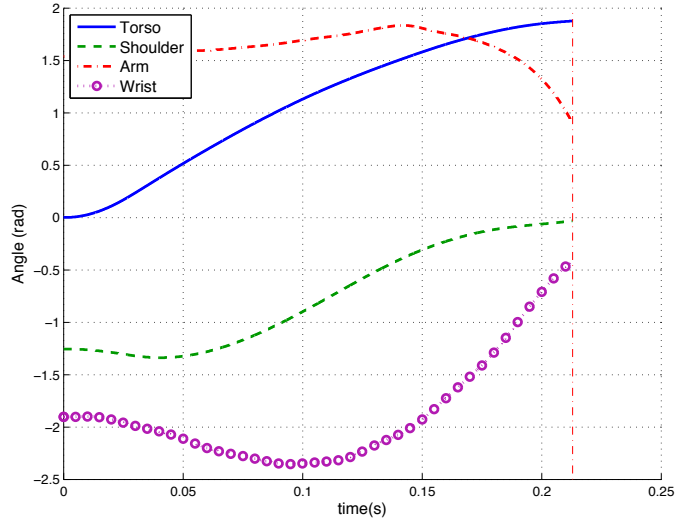
Figure 4.4: Golfer joint angles for swing with default parameters.

is difficult to square the face of the club at impact without precise timing of the forearm torque. Too early a torque will close the face at impact and too late a torque will open the face at impact and both of these scenarios lead to large lateral deviations in the ball trajectory. This effect will be examined more closely when experimenting with the clubhead MOI in Section 4.5.

The clubhead aerodynamic drag force, which is a novel feature of this forward dynamic model of the swing, is shown in Figure 4.7. Recall from Section 3.2.3 that the C_d value for the clubhead is calculated using a 2-D look up table based on clubhead speed and yaw angle. The clubhead speed has already been examined in Figure 4.2 and the magnitude of the yaw is shown in Figure 4.7a. At the beginning of the swing (when there is little clubhead velocity) the yaw angle cannot easily be calculated since it is measured between the direction of the velocity vector and the z-axis of the club. Once the club starts moving ($t = 0.02$) the yaw angle of the club remains close to 0 (heel-first presentation) until late in
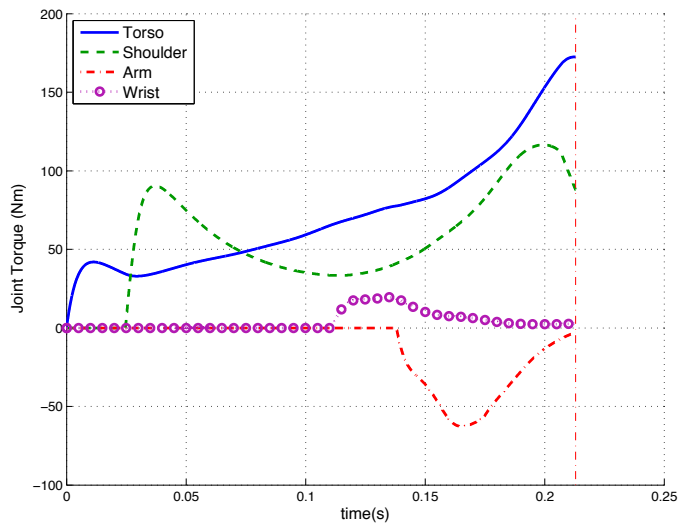
(a) Active torques
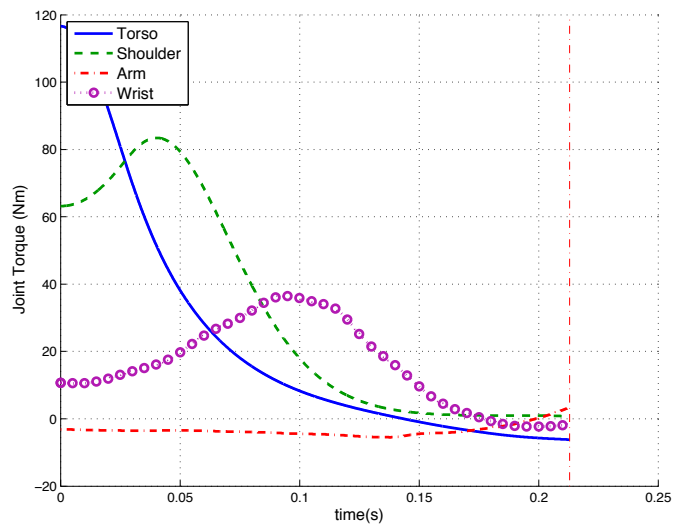
(b) Passive torques

Figure 4.5: Golfer joint torques for swing with default parameters.
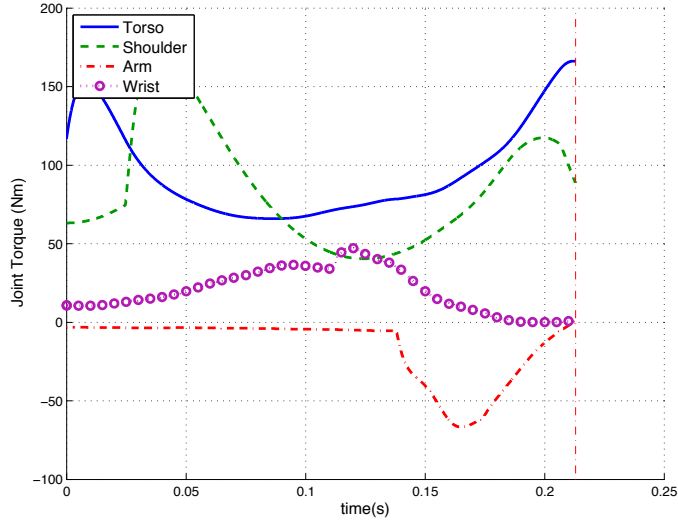
Figure 4.6: Total golfer joint torques for swing with default parameters.

the swing when the face is squared to meet the ball. The yaw angle is nearly 90° at impact indicating that the club velocity is normal to the face at impact. The C_d value calculated from the yaw and the clubhead speed is shown in Figure 4.7b. This plot is spiky because of the sharp upward trend as the yaw approaches 0° in the surface of the look up table shown in Figure 3.9. An improved representation of the clubhead C_d value would lead to a more realistic smoother curve. The final calculated drag force is shown in Figure 4.7c. Peaking at 5 N for the clubhead speeds encountered is very similar to the values found in the literature [45]. At higher clubhead speeds, higher drag forces would be expected.

Finally, the model is able to incorporate the flexing and bending of the shaft during the swing. This is easiest to see in Figure 4.8. The forward and backward flexing of the shaft clearly shows the club bend backwards during the swing and then flex forward for impact. This is the expected result as shown in Figure 2.7. For the default golfer with the green shaft, the club is bent forward 4 cm at impact. The droop oscillates more than

87
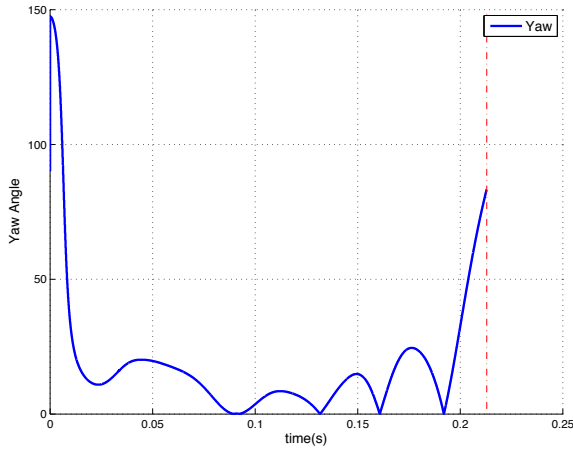
(a) Yaw angle
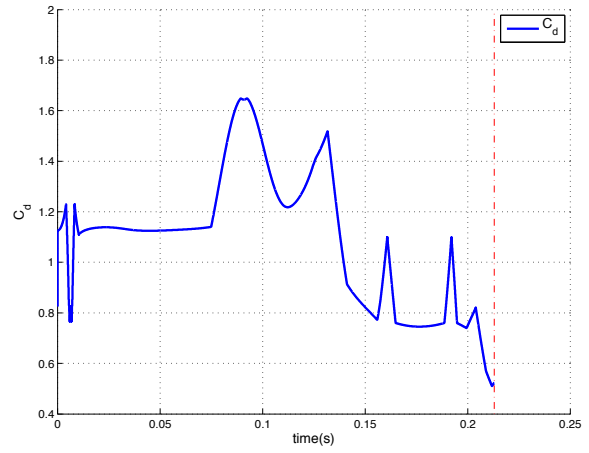
(b) C_d value
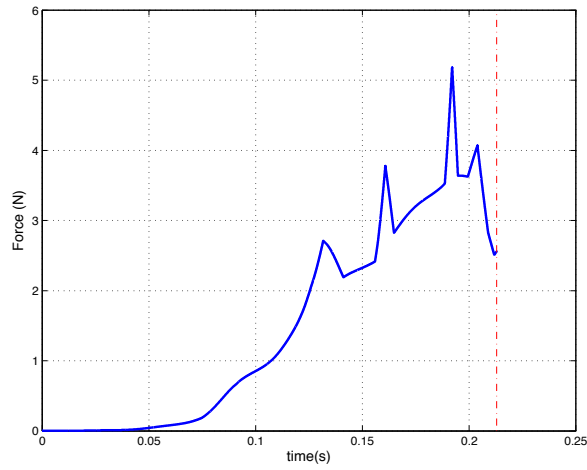
(c) Drag force

Figure 4.7: Clubhead aerodynamics plots for swing with default parameters.
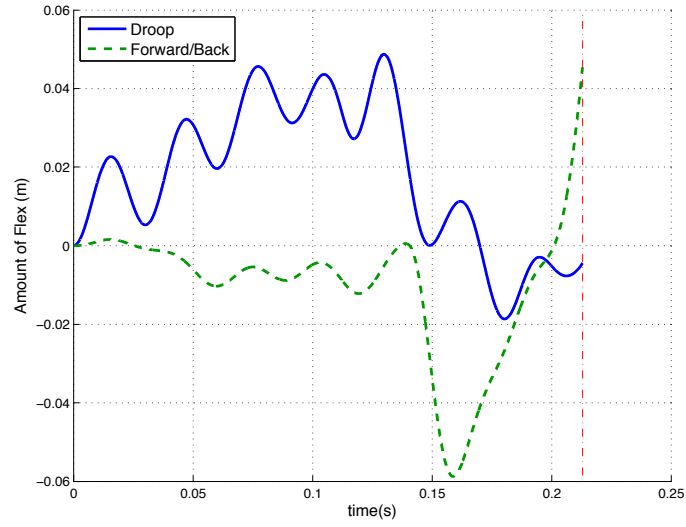
Figure 4.8: Club flexing as measured from the grip.

expected but does exhibit downward bending (negative droop) at impact. This compares favourably with the experimental results obtained by Sandhu et al. [23] which showed a similar trend in the club droop.

4.2   Effect of Golfer Strength

To demonstrate the ability of the model to adapt to different swing conditions, the strength of the golfer was varied by scaling all of the active muscle torques by a factor from 0.9 to 1.7 times their default values. The expected result here was that a stronger golfer would be able to generate increased clubhead speed and therefore increased carry distances. The optimization process would have to change the timing of the muscle activations in order to produce good swings with the new muscle characteristics. Both of these effects were observed. First in Figure 4.9, the carry distances are plotted against the strength factor showing a clear progression from a low strength golfer hitting the ball around 200 yards to a high strength golfer hitting the ball over 250 yards. This change in carry distance is caused by an increase in the peak clubhead speed from $40.5\,\mathrm{m/s}$ (90.5 mph) to $49.5\,\mathrm{m/s}$ (110.7 mph) as shown in Figure 4.10. There appears to be slightly diminishing returns from increasing the golfer strength as the slope of the curve is decreasing as we reach the top of the range of golfer strengths tested.

The golfer's torque activation timings varied significantly from the low-strength golfer to the high-strength golfer. As one would expect, the high strength golfer requires earlier timings as the faster clubhead speed needs earlier motion from the wrist and forearm to snap the wrists and square the clubface. The active portion of the joint torques is shown in Figure 4.11. The activation timings, and therefore the torques, follow the same patterns as before since the goal of the swing is still the same, but the stronger golfer swings both earlier and with more strength. This experiment showed two things. First the obvious conclusion that a stronger golfer is able to hit the ball further. And second, that the optimization scheme used to pick 'good' swings is able to adapt the swing to different simulation conditions.
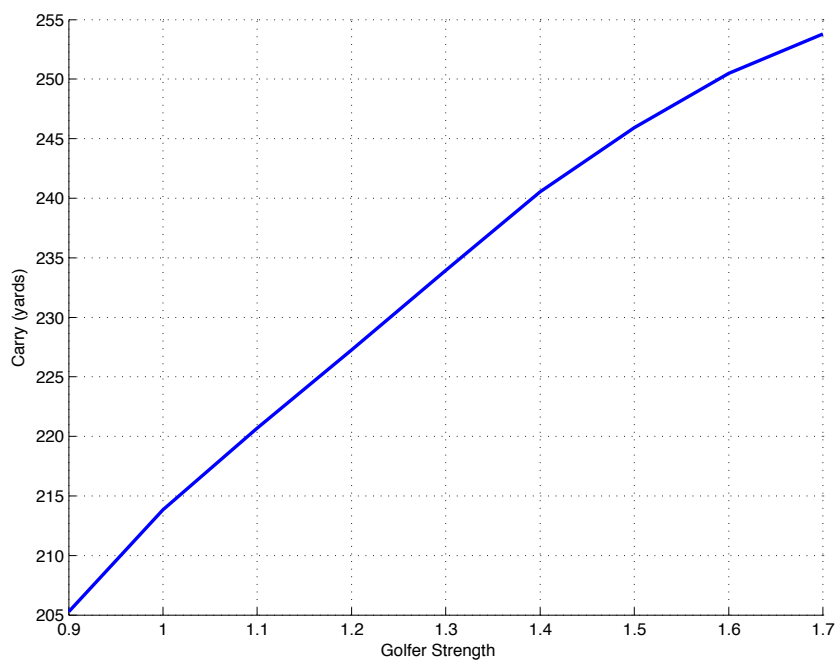
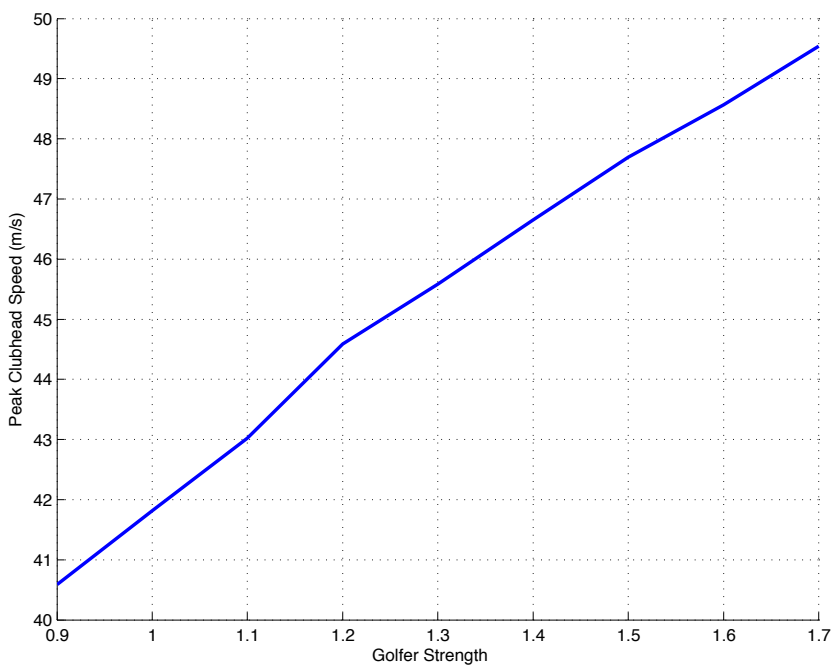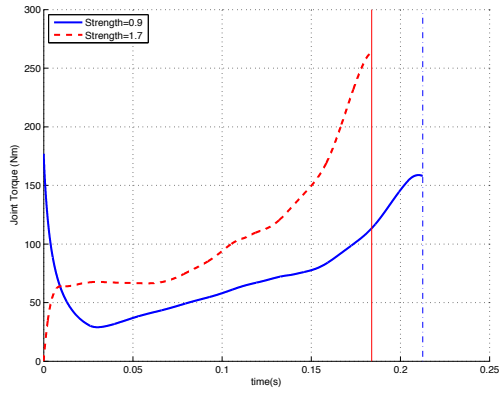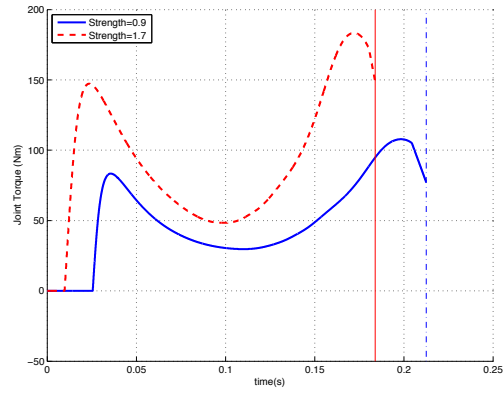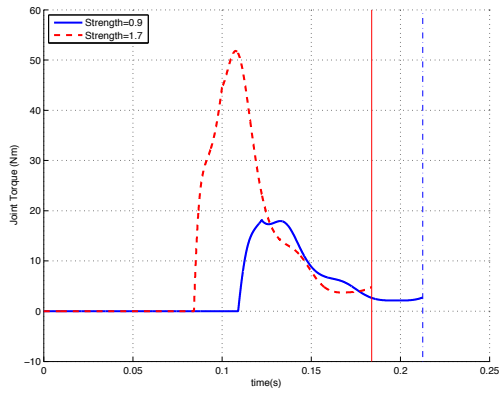Figure 4.9: Ball carry plotted against golfer strength factor.

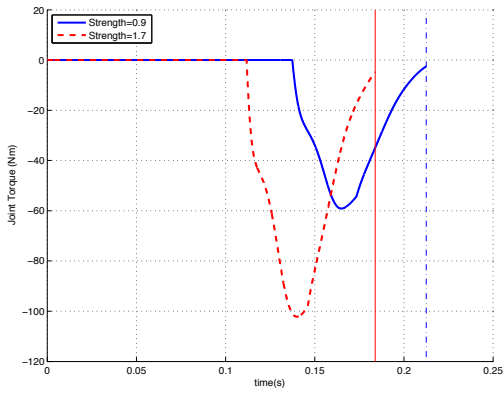Figure 4.10: Clubhead speed plotted against golfer strength factor.

(a) Torso Torque

(b) Shoulder Torque

(c) Wrist Torque

(d) Forearm Torque

Figure 4.11: Active joint torque comparison across golfers of different strength.
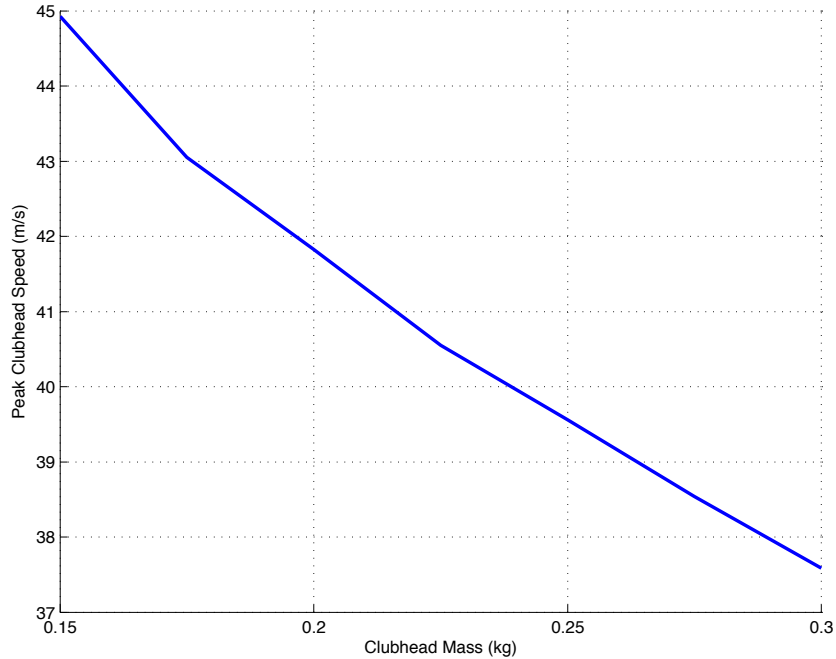
Figure 4.12: Clubhead speed plotted against clubhead mass.

4.3 Effect of Clubhead Mass

The second effect tested was the effect of the clubhead mass on the golf swing. Changing the mass of the clubhead is expected to have two effects. First, as the clubhead becomes heavier, the golfer will not be able to swing the club as fast, leading to slower peak clubhead speeds. This effect is shown in Figure 4.12. Due to the increasing clubhead mass from 150 g to 300 g, the clubhead speed is decreased from 45 m/s (100 mph) to 37.5 m/s (83.9 mph). The slower clubhead speed is expected to decrease the carry distance.

But, by increasing the clubhead mass, the clubhead has more momentum at the same speed so when it strikes the ball more speed is imparted to the ball. Holding clubhead speed constant and increasing the mass of the club would lead to longer drives so there
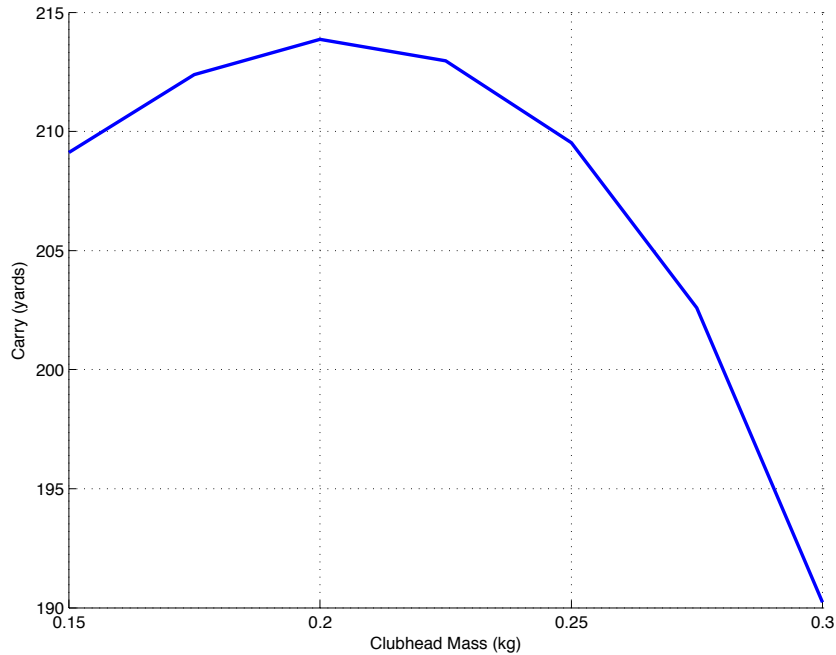
Figure 4.13: Ball carry plotted against clubhead mass.

is a tradeoff to be made between decreasing the clubhead mass to increase the clubhead speed and increasing the clubhead mass to improve the impact. Figure 4.13 illustrates this tradeoff clearly. At very low clubhead masses, the carry of the ball is small despite the high clubhead speeds shown in Figure 4.12. Similarly at high clubhead masses, the ball carry is small despite the favourable mass balance in the impact between the ball and the club. These results show that current clubheads (weighing around 200 g) are appropriately weighted for the golfer modeled.

Examining the torques of the golfer when comparing the swing with different clubhead masses, it was found that the golfer started the active torque for the torso much earlier when swinging with a heavier club to try to compensate for the higher clubhead inertia.
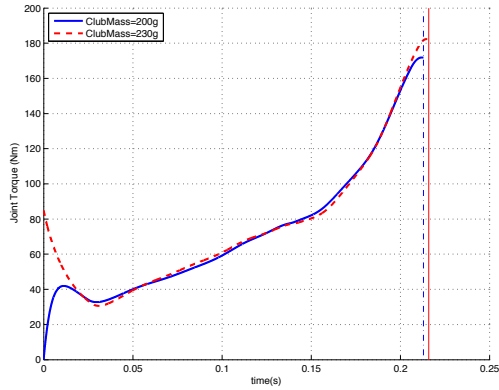
(a) Active Torso Torque
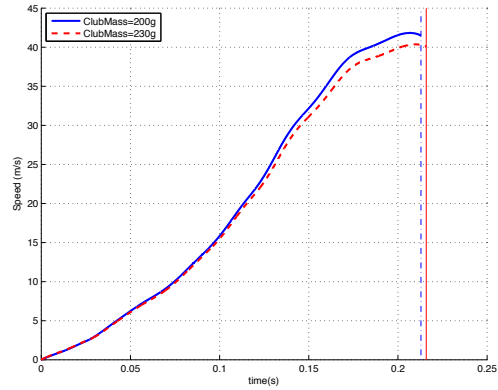
(b) Clubhead Speed

Figure 4.14: Comparison between golfer swinging the default club and swinging a club with increased clubhead mass.

This change was not enough to counteract the heavier mass and increase the clubhead speed. These results are shown in Figure 4.14.

To further examine this effect and get a better sense of what mass the clubhead should be, the range of masses from 170 g to 230 g were simulated in 5 g increments. The resulting plot is shown in Figure 4.15. The observed effect is less smooth and the optimal carry point remained at 200 g. The results around 200 g are relatively flat, so any clubhead mass between 190 g to 205 g would be appropriate. This result should not be interpreted as indicating that all clubheads should be in this range as it could change depending on the strength of the golfer, mass and flexibility of the shaft, or any of the other factors studied in this project. But it is a strong indicator that each individual golfer and shaft will have a particular clubhead mass that would be ideal for them and also that the selected clubhead mass should be around 200 g.
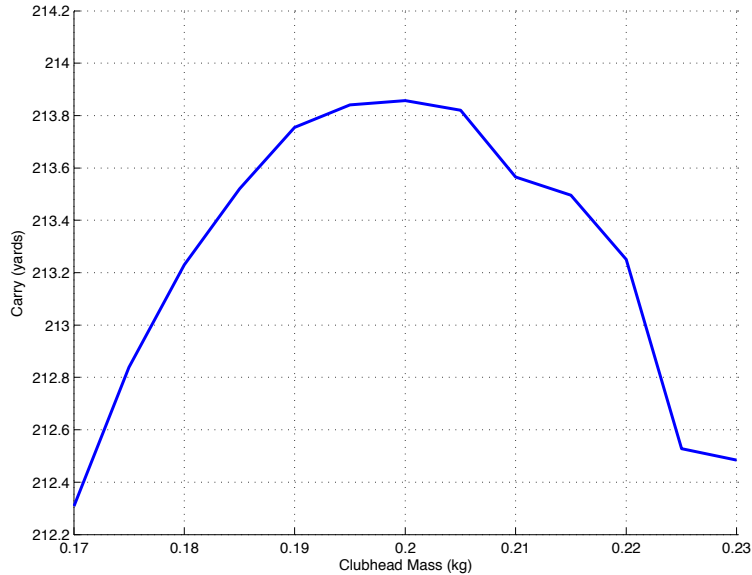
Figure 4.15: Ball carry plotted against clubhead mass on the range of 170 g to 200 g.

4.4   Effect of Clubhead Centre of Mass Position

The third experiment performed using the model was to shift the centre of mass position backwards and forwards along the Y-axis shown in Figure 3.8b. This axis is not normal to the clubface but for a perfectly squared clubface would be parallel to the downrange axis with the origin fixed in the hozel of the club. Shifting the center of mass along this axis then shifts the relative position to the ellipsoid axis shown in Figure 3.12, changing the impact conditions for the ball and club. Moving the centre of mass will also have an effect on the effective moment of inertia for the clubhead, may affect the ability of the golfer to close the face of the club, and may change the amount of dynamic loft at impact. The assumption made here is that we can change the centre of mass position without changing the moments of inertia inherent to the clubhead.
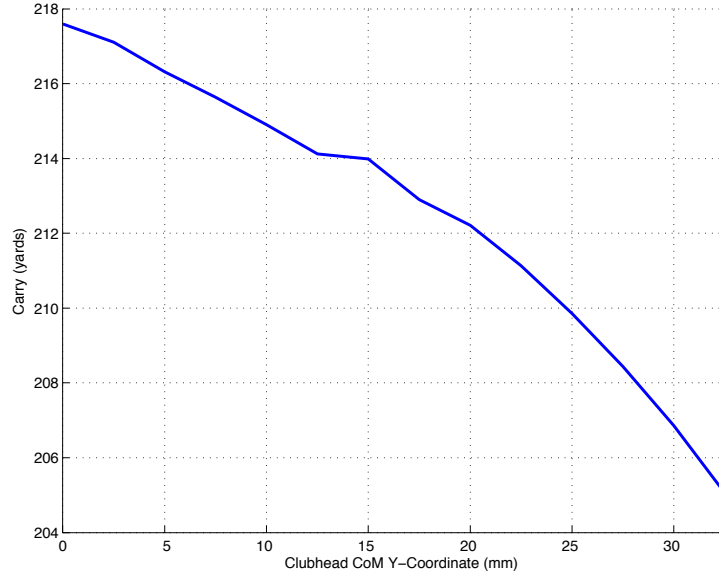
97

Figure 4.16: Ball carry plotted against clubhead centre of mass y-coordinate.

As can be seen in Figure 4.16, shifting the centre of mass away from the face of the club has a small negative effect on the carry distance. Moving the centre of mass from 0 cm from the hozel to 3 cm from the hozel reduced the carry from 218 yards to 205 yards. This effect is almost entirely due to the change in the impact model as the clubhead speed does not change significantly across these simulations. Figure 4.17 shows that the clubhead speed remains close to 41.7 m/s for all simulations varying the centre of mass position.

The golfer kinematics are nearly identical across the swings in this experiment. As we can see in Figure 4.18 across all four joints, the swing is not affected by the change in the centre of mass position of clubhead. The effect of the clubhead centre of mass position on the golfer's swing is small enough to be disregarded as part of this analysis.

Turning instead to the ball launch characteristics, there is a significant trend in the
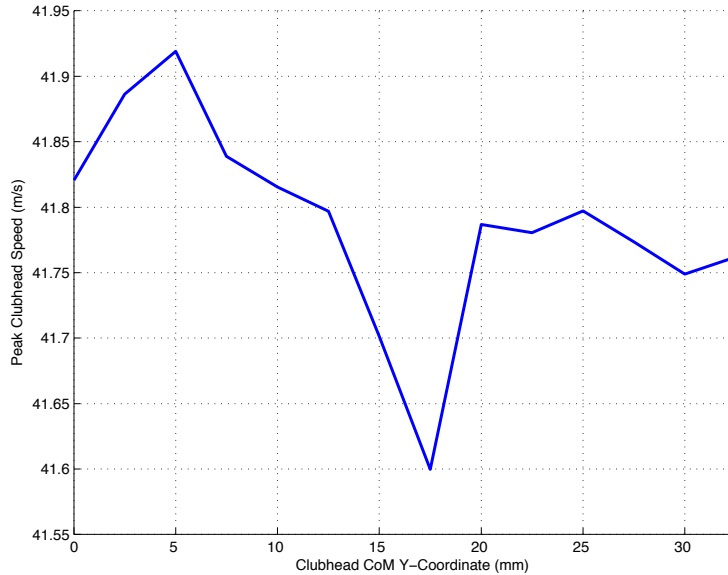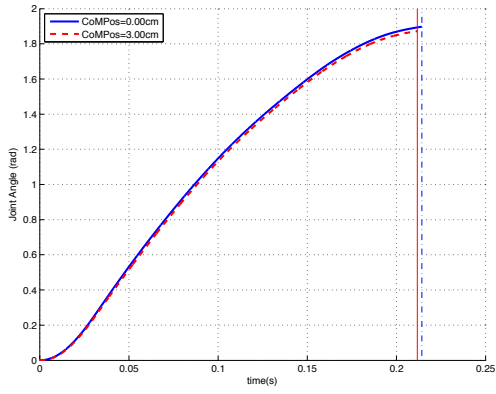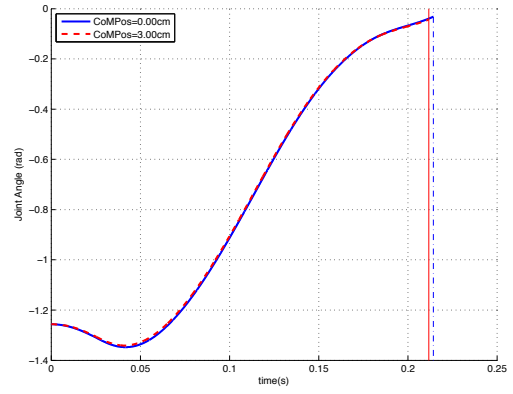
Figure 4.17: Clubhead speed plotted against clubhead centre of mass y-coordinate.

backspin imparted to the ball across these simulations. As can be seen in Figure 4.19 the backspin of the ball increases from 3250 RPM to 3700 RPM as the centre of mass moves further from the face of the club along a horizontal axis. The increase in spin changes the trajectory of the ball and and prevents it from traveling as far downrange. This effect can be seen in the carry diagram shown in Figure 4.20. Therefore the clubhead centre of mass position should be kept as close as possible to the face of the club to reduce the backspin and increase the range. How close the centre of mass can be to the face may be limited by other considerations including clubhead MOI, club strength, and the materials selected.
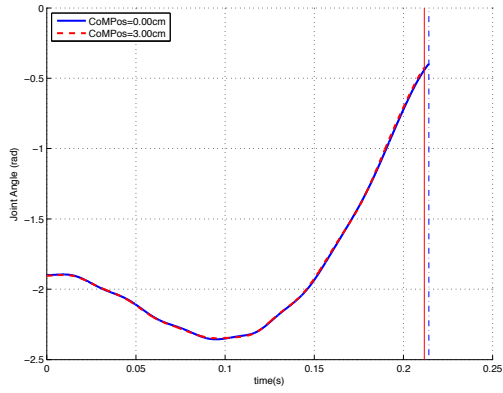
The change in the ball launch conditions comes partly from the changes which occur in the impact model and partly from a change in clubhead presentation. Moving the centre of mass closer to the face increases the perpendicular length of the moment arm of the impact
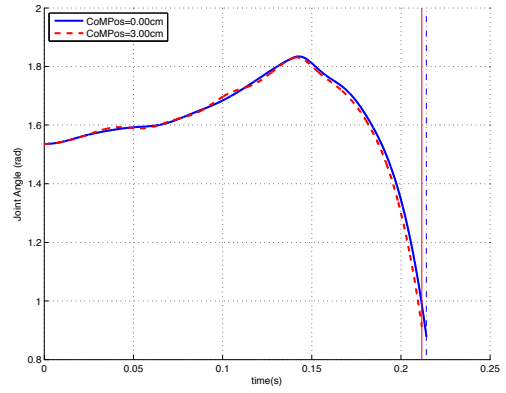
(a) Torso Angle

(b) Shoulder Angle

(c) Wrist Angle

(d) Forearm Angle

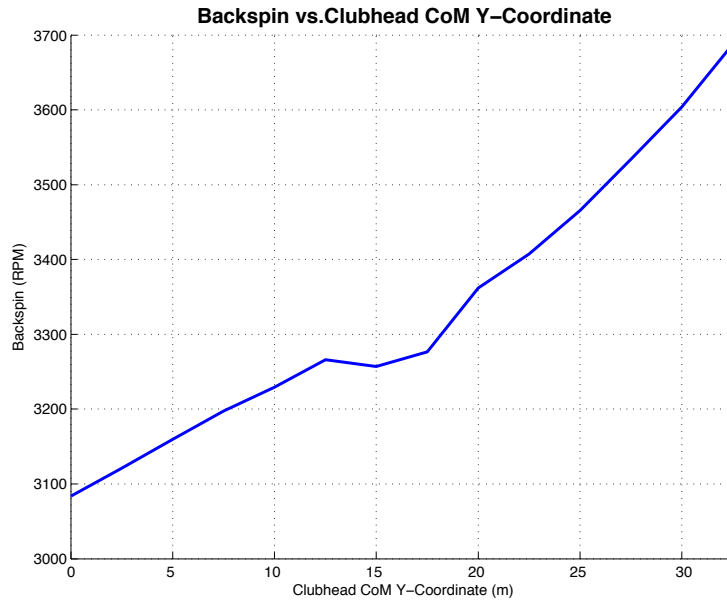Figure 4.18: Joint angle comparison across swings with different clubhead centre of mass positions.

Figure 4.19: Launch backspin plotted against clubhead centre of mass y-coordinate.
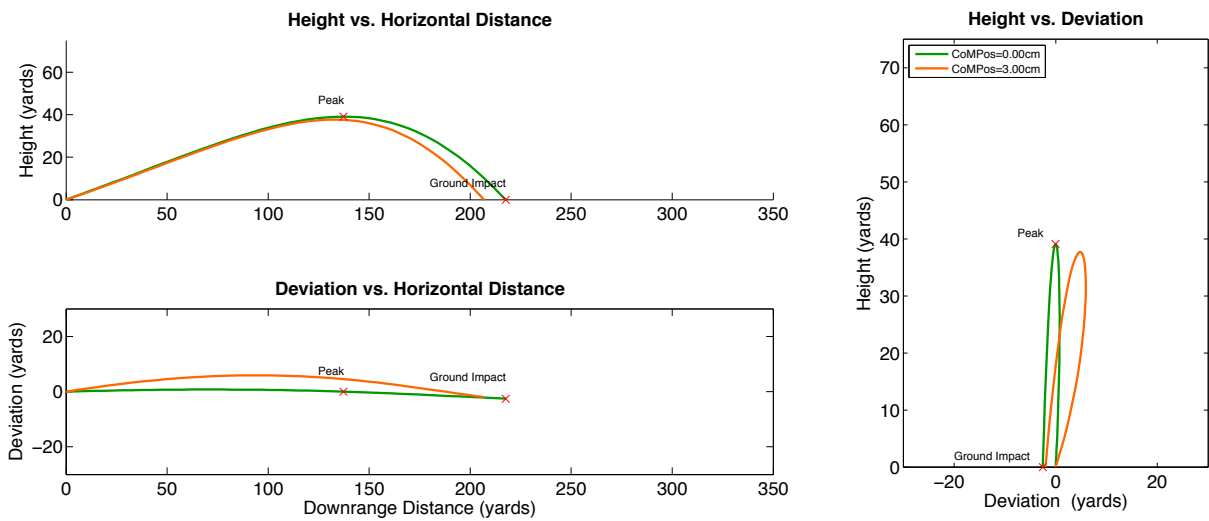

Figure 4.20: Comparison of ball trajectories for different centre of mass positions.
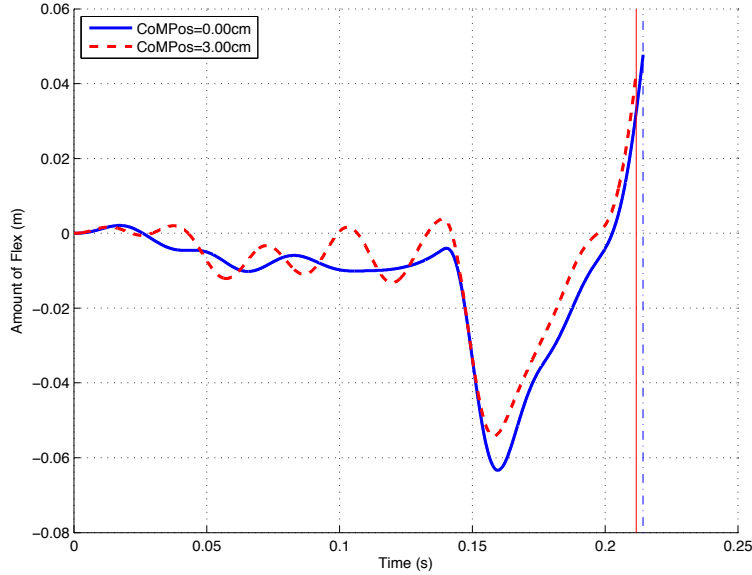
Figure 4.21: Forward/backward flexing of the shaft for clubs with different center of mass positions.

(y_{imp} component of r_{imp} in Figure 3.12). This increases the backwards counter-clockwise rotation of the clubhead after impact. In turn, the gear effect (Equation 3.23) reduces the amount of backspin on the ball.

The clubhead presentation is changed by a change in the amount of flexing of the club during the swing. Examining a plot comparing the forward flex of the club in each case, when the clubhead centre of mass is closer to the face of the club the shaft of the club flexes a few millimetres further forwards at impact (See Figure 4.21). This slightly increases the dynamic loft of the club and helps reduce the spin of the ball. This effect is likely secondary to the change in the moment arm of the impact.
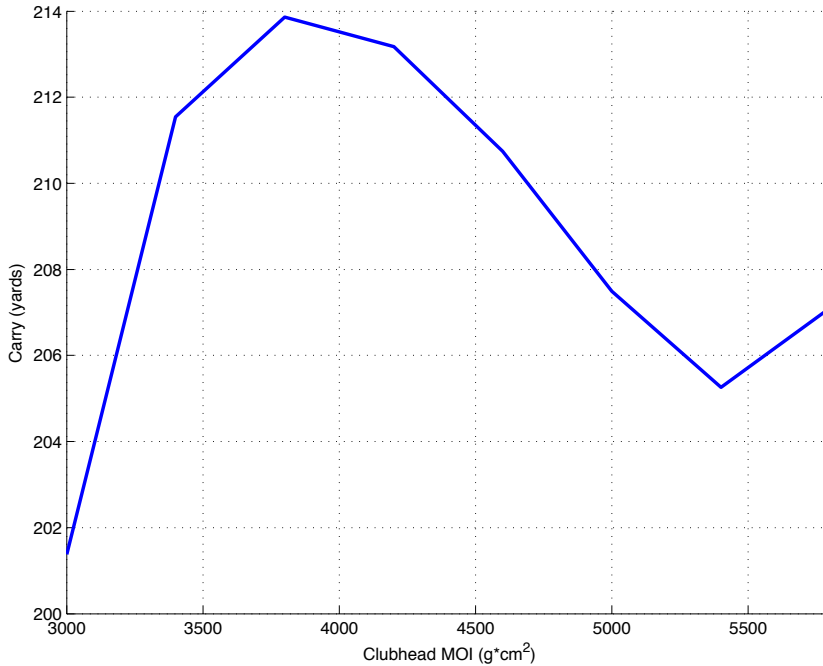
102

Figure 4.22: Comparison of ball trajectories for different clubhead MOI.

4.5 Effect of Clubhead Moment of Inertia

The clubhead moment of inertia (MOI) about its vertical axis (when in address position) was varied from $3000\,\mathrm{g\,cm^2}$ to $5800\,\mathrm{g\,cm^2}$. Having a low MOI increases the amount that the clubhead will spin during an impact which is not perfectly aligned with the centre of mass, increasing side spin on the ball. Despite the impact always occurring at the centre of mass of the club, misaligned impacts will occur due to the face angle at impact. Having a high MOI reduces side spin for off-line hits but may hinder the golfer's ability to close the clubface at impact, reducing the carry. The results showed this effect with a maximum carry distance achieved with an MOI of $3800\,\mathrm{g\,cm^2}$. These results can be seen in Figure 4.22.

Comparing the simulation results at $3000\,\mathrm{g\,cm^2}$ to the results at $3800\,\mathrm{g\,cm^2}$ shows very similar golfer kinematics and very similar club speed and shaft kinematics. There is a small reduction in clubhead speed from $41.4\,\mathrm{m/s}$ to $40.8\,\mathrm{m/s}$ for the $3000\,\mathrm{g\,cm^2}$ club which is caused by the ball being struck slightly later in the swing after the club has begun to move upwards and slow down. The main reason for the change in carry distance is difficulty in controlling the orientation of the clubhead.

In general, when the MOI of the clubhead is low, the optimization process has a difficult time selecting the correct timing for the forearm torque to provide the best impact conditions. Since the MOI is low, the system will respond quickly to this torque causing the club to be in the optimal orientation for striking the ball for only a very brief period of time. This problem is compounded by the effect mentioned at the beginning of this Section where a low MOI causes increased side spin for an off-alignment hit. Using a torque generator that can only provide an on/off activation timing for the forearm muscle may not give us the granularity required to swing well for every MOI configuration.

When the MOI of the clubhead is high, the golfer is not able to square the clubface properly for impact and the resulting shots are of lower quality.

4.6 Effect of Shaft Flexibility

Four different flexible shafts provided by a club manufacturer were studied within the model. By changing the polynomials representing the area, moment of inertia, stiffness, and torsional stiffness of the club, the four different clubs can be included in the model and the golfer's swing optimized for each club. The four clubs have differing stiffness profiles as summarized here in Figure 4.23 and shown in detail in Appendix A.
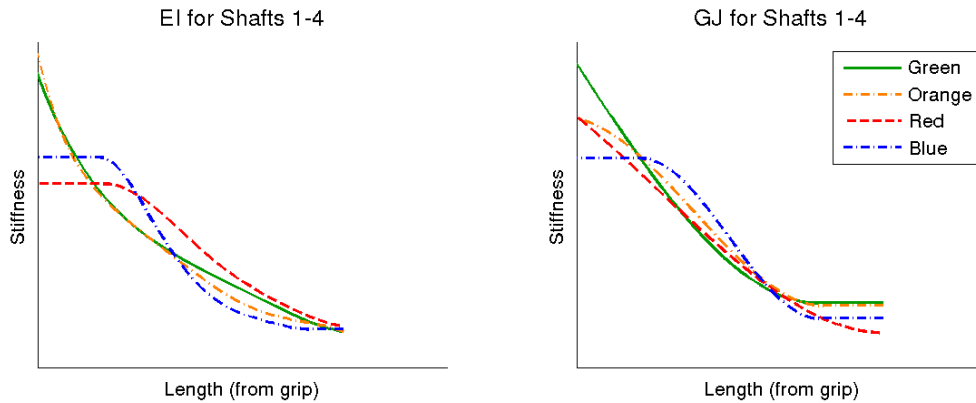
Figure 4.23: EI and GJ curves for flexible shafts used in the study.

It is difficult to determine any trends in whether a particular stiffness profile is better or worse based on the results presented here. While we can determine what club is best for a golfer that swings exactly like the model, the stiffness profile is likely a factor that should be fit to a particular golfer rather than using a 'one-size-fits-all' approach. In this section, the results for each shaft as compared to the default (green) shaft will be presented and any interesting differences from the default behaviour will be noted.

First in terms of carry, the green shaft produced the longest carry (this is why it was selected as the default shaft). The carry results for the four clubs are shown in Figure 4.24. The shortest hitting club is the blue club, followed by the red club and then the orange club. So the question becomes where does this change in carry come from? What changes occur in the golfer's swing as the shaft changes? The first thing to examine is the clubhead speed as the carry distance is mostly influenced by the clubhead speed. As can be seen in Figure 4.25, the clubhead speed for the two shortest carrying clubs (red and blue) is slightly lower than the clubhead speed for the green club. A loss of $0.5\,\mathrm{m/s}$ of clubhead leads to about 3.5 yards of lost carry in the model so while this is a contributing factor, it is not sufficient to explain the whole difference in carry.
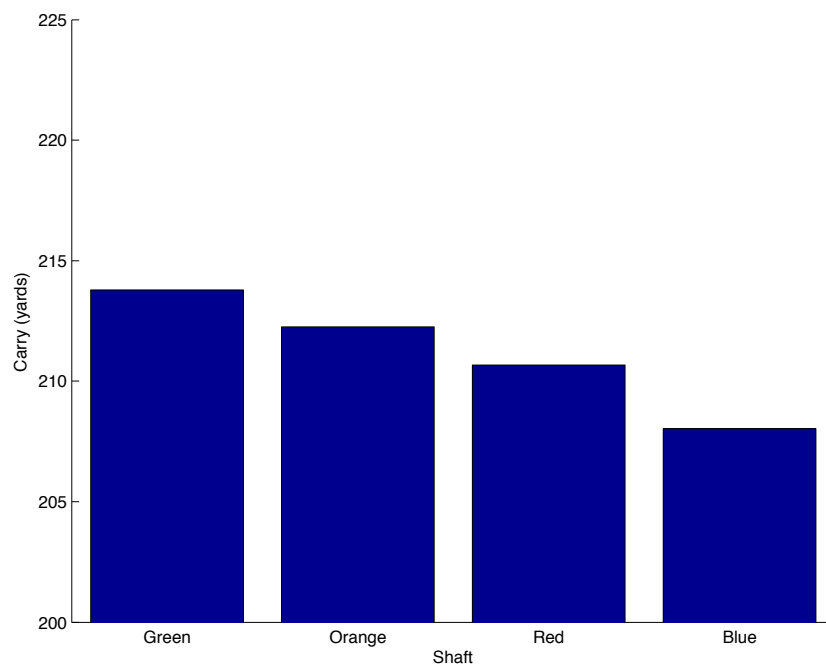
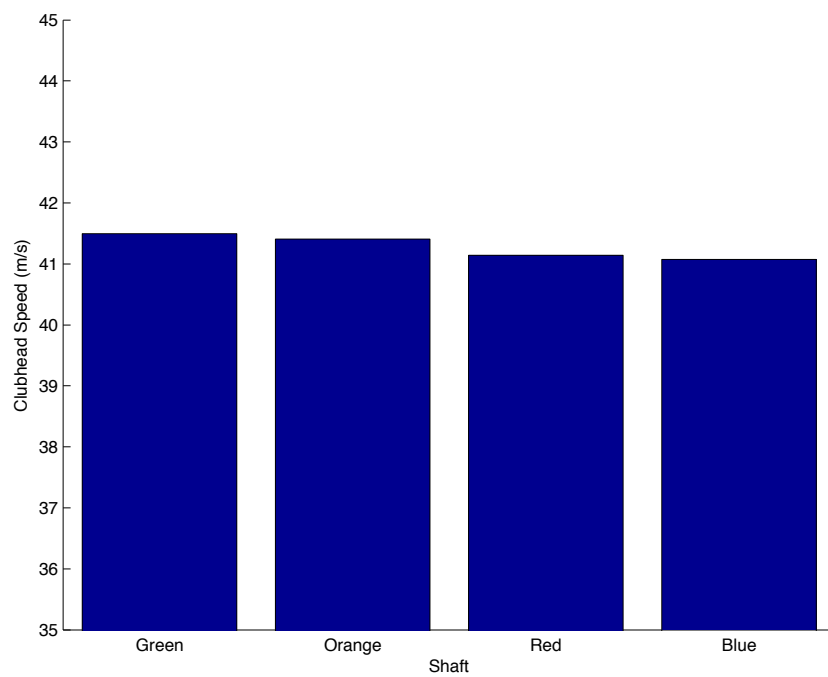Figure 4.24: Ball carry for different flexible shafts.

Figure 4.25: Clubhead speed for different flexible shafts.

Figure 4.26 shows the backspin of the ball struck with each of the flexible shafts. Based on this figure, the orange and blue shafts have higher backspin than the green and red shafts which would lead to reduced ball carry. This explains the differences in carry between the green and orange and red and blue shafts that have very similar clubhead speeds. Looking more closely at the simulation results, it was difficult to determine what is causing the change in backspin. Likely, small differences in the shaft flexibility profiles are leading to slightly different clubhead characteristics at impact and changing the ball launch conditions. In particular the dynamic loft may be affected. This further stresses the importance of selecting the correct flexible shaft for a particular golfer rather than using a 'one-size-fits-all' approach to club fitting. It is also possible that the changes to the flexibility of the shaft stress the optimizer in different ways, leading to less optimal solutions depending on the shaft selected.

4.7   Effect of Club Aerodynamics

Club aerodynamics has the effect of slowing down the swing and reducing the carry distance. There are two types of club aerodynamics included in the model, clubhead aerodynamics and shaft aerodynamics. This Section looks at the effect of removing each aerodynamic force and examines the resulting carry and clubhead speed.

By removing all of the aerodynamic effects on the club, the downrange carry increases by 4 yards from 214 yards to 218 yards (see Figure 4.27). More interesting though is the change in the trajectory of the ball. Without aerodynamic effects, the ball is lifted much higher in the air as significantly more backspin is imparted to the ball. As the launch angle of the ball is nearly unchanged between the scenarios, the increase in the backspin from 3180 RPM to 4149 RPM causes the change in the trajectory of the ball and reducing the
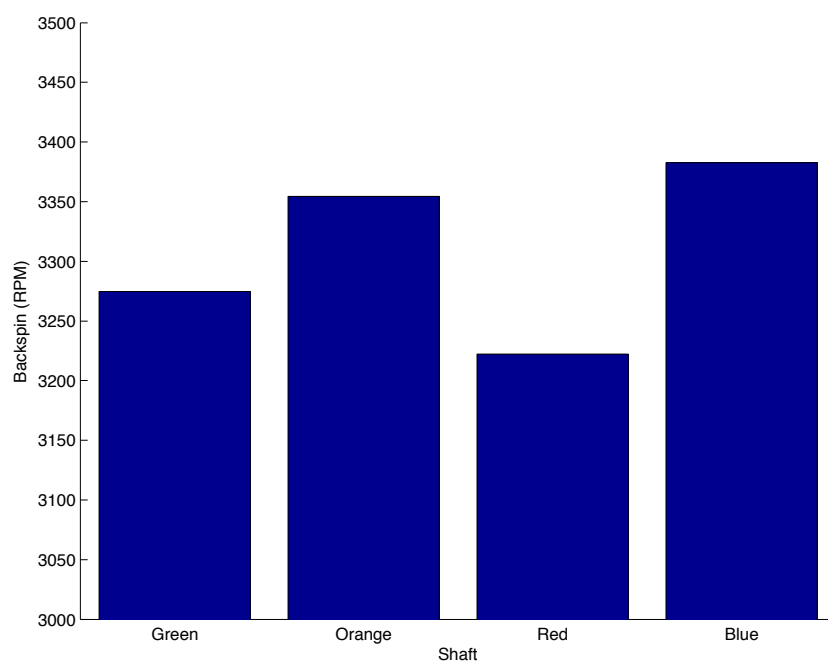
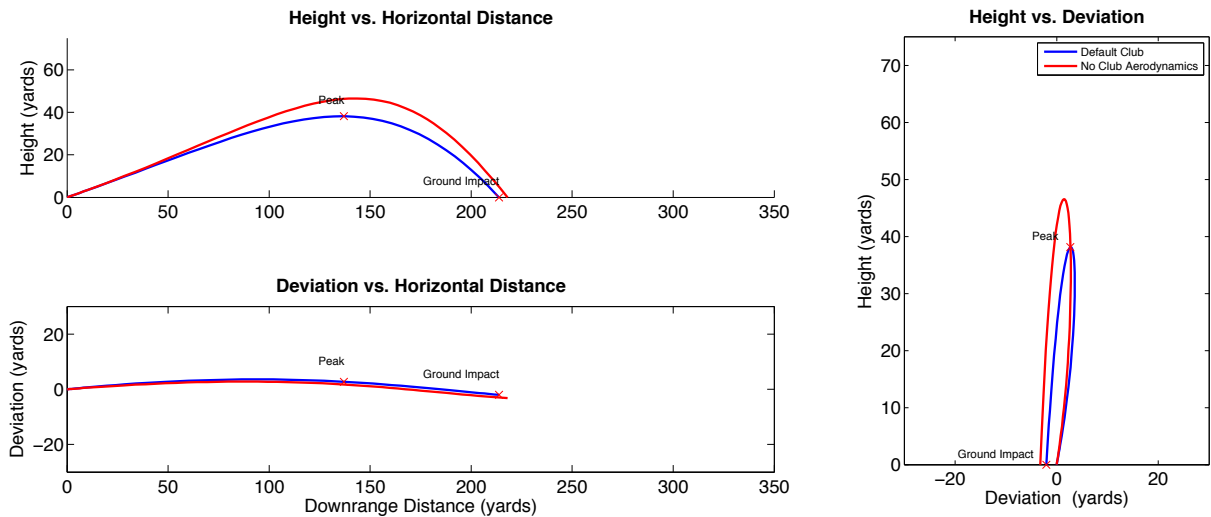Figure 4.26: Backspin of the ball for different flexible shafts.

Figure 4.27: Comparison of the ball trajectories with and without club aerodynamic drag.

improvement in the carry that was expected for higher clubhead speeds.

One possible reason for the change in the backspin is a change in the amount of flexing of the shaft of the club. In the results including club aerodynamics, the shaft is bent forwards 3.8 cm at the time of impact while in the results without aerodynamics the shaft is only bent forwards 0.6 cm. The smaller amount of forward flex reduces the dynamic loft (by about 1°) of the clubhead at impact and increases the amount of backspin on the ball.

4.8   Model Limitations

While the model that has been presented in this work captures many details of the golf drive that have not been addressed before and can be used to answer many interesting club design questions, there are still a few areas in which the model is limited in what it can simulate. This Section will describe the limitations of the model, grouping them under the

four sections described in Chapter 3.

4.8.1   Limitations of the Golfer Model

Model Structure

There are many elements of the golf swing that have been intentionally left out of the golfer model to decrease its complexity. The most obvious omission is the entire lower body of the golfer. The omitted degrees of freedom include the horizontal shifting of the hips and the independent rotation of the hips with respect to the torso. In the context of this model, the removal of horizontal shifting is reasonable because the modern golf swing is primarily a rotational movement. While the golfer feels a significant shift of weight from one leg to the other during the swing, the actual translation of the hips is quite small during the swing [50].

The independent rotation of the hips has been cited as an indicator of golfer excellence [51] but it is not a degree of freedom that is required to capture the kinematics of the hands of the golfer gripping the club. The rotation of the shoulders will have to start earlier if the hip rotation is missing, but the motion of the shoulder joint will remain the same. If the goal of the model was to determine what portion of the power is generated by different joints this degree of freedom would be important, but since the goal is to evaluate club performance, hip rotation can be lumped in with torso rotation. This same simplification will also lead to a higher torque for the torso of the golfer as this torque must provide all of the required angular acceleration of the arms.

The elbow joint in the leading arm of the golfer is not included in the model reducing the degrees of freedom of the model. This joint is not included as most expert golfers keep

111

their leading arm straight throughout the swing. In future versions of the model, it may be interesting to include this joint and see if the optimization process keeps the elbow straight throughout the swing or not.

The final omission from the mechanical structure of the model is the omission of the trailing (right) arm of the golfer. The inclusion of this arm would have resulted in a closed kinematic loop within the model and complicated the equations that must be solved to determine its motion by introducing algebraic constraints to the differential equations. So instead, it is assumed that the golfer's trailing arm plays a negligible role in providing power to the swing and is simply used for stabilization. Since the model golfer does not need to stabilize the swing (the joints used are inherently stable), the second arm is unnecessary. Since the trailing arm has been removed from the golfer, any power production from it must be lumped into the leading arm and its strength has been slightly increased. In particular, the pronation-supination strength is required to be larger to close the clubface.

Finally, the interaction between the hand of the golfer and the grip of the golf club is modeled as a rigid weld. In reality there is some compliance in this joint but this was considered as too difficult to model within the scope of this work.

Joint Torques

The joint torque model described in Section 3.1.1 describes how the golfer model is activated in a way that approximates the muscles of a real golfer. This approximation of the muscle activity of the golfer simplifies the model and reduces the number of parameters that must be optimized to control the swing. A higher fidelity alternative would be to build a model that included individual muscles attached to a skeletal model of the golfer [7]. The obvious question here is: why use joint torques instead of a combination of muscles to power the

model?

When answering this question, important to considering the purpose of the model is important. The primary goal of this project was to build a model that can be used for evaluating golf club design decisions so the primary role of the golfer portion of the model is to deliver the correct forces and kinematics to the golf club grip. For this purpose, active joint torque generators are sufficient as they can provide realistic motions and torques to the joints without the added complications of multiple muscles. The inclusion of multiple muscles for each of the joints would require the solution of the muscle redundancy problem [52] and greatly increase the length of time for simulations. This would be necessary if the goal of the model was to determine which muscles are used most during the swing but it is not necessary for determining the club motion. The muscular joint torques are able to show the relative timing of the golfer's motion, which is sufficient for the analysis in this work.

A second assumption of the joint torque model is that the muscles which power each of the joints are activated to their maximum potential as soon as the torque is turned on and remain fully activated until they are turned off. This leads to the torque profile represented by Equation 3.1 which ramps up from 0 to a maximum value with first-order dynamics. This activation profile is only correct if the golfer is attempting to deliver the maximum torque at the joint. This is a reasonable assumption since the golf drive is a motion which attempts to deliver the maximum amount of power to the swing. Therefore the golfer's muscles should be maximally activated once they start to be used.

In the results Section (Section 4.5) it was found that the model was very sensitive to changes in the moment of inertia of the clubhead and it was hypothesized that this was because the forearm torque generator was unable to be activated partially when the load it must rotate is small. A biomechanic model that modulated the forearm torque may be

113

able to achieve more consistent swing results.

Finally, the joint torque equation ignores the effect of the muscle force-length relationship on the active torques applied. This relationship is unlikely to be important since the muscle sarcomeres are unlikely to be brought outside the normal range of force production during the golf swing [17].

4.8.2   Limitations of the Club Model

The club model represents the shaft of the club as a flexible Rayleigh beam which allows for motion in the transverse directions as well as axial twist. The shaft properties can vary along the length of the shaft but only as 6th-order polynomials. This representation should be sufficient for most golf shafts, but as can be seen in Appendix A, there are several properties which could not be well represented. It's unlikely that this had a significant effect on the results, and even a model which follows the trends as the shaft properties change is an improvement on previous lumped parameter efforts.

The inertia matrix of the clubhead is represented only by the moments of inertia about the three axes shown in Figure 3.8. These are not necessarily principal axes of the clubhead and there should also be products of inertia included. This simplification was made because it was difficult to measure the products of inertia for the clubhead and it is likely that they have minimal effects on the outcome of the swing. This also makes the results of the experiment performed in Section 4.5 easier to interpret.

4.8.3 Limitations of the Impact Model

The impact model used for this work is simple because it was required to be very fast as part of the optimization process. The assumptions required for the impact model outlined in Section 3.4 are not necessarily true, but similar impact models have been used before [24] with good agreement in trends to more sophisticated models. The model likely over-estimates the amount of spin on the ball after impact as there is no deformation of the ball against the surface of the club. In addition, the golfer model always assumes that the golfer would be able to place the ball so that a center impact occurs (e.g., by raising or lowering the tee or shifting their feet). For some joint angle combinations and clubhead orientations this is probably not true. A model which dynamically sets the golfer and ball location as part of the optimization process may be able to achieve more realistic results.

4.8.4 Limitations of the Ball Aerodynamic Model

The ball aerodynamic model used in this paper is a simple and effective one that has been used to model the flight of many types of flying balls. There are more complicated golf ball aerodynamics models that incorporate the Reynold's number of the ball flight and kinematic viscosity of the air when calculating the lift and drag coefficients for the ball, but its unclear whether this increase in complexity results in significant changes to the ball flight path. What might have a larger effect on the final carry distance would be the incorporation of a more modern golf ball in the model. The equations for C_L and C_D found in Section 3.5 are based on experiments performed on golf balls which are no longer current technology. Newer golf balls have led to longer drives and changing the model in this way could lead to longer carry distances. In addition, the aerodynamic model does not include the roll of the golf ball. If the role were included, flatter trajectories (which lead to longer

115

roll) might become preferable within the optimization.

Chapter 5

Conclusions and Future Work

This Chapter will summarize the work completed in this thesis and outline the main recommendations based on the results presented in Chapter 4. Finally, suggestions for future research directions will be made.

5.1   Project Summary

This project consists of three sections. In the first section, a thorough review of the physics of the golf swing and previous golfer models was undertaken. This portion of the project concluded that there was a need of a physics-based simulation of the golf swing that takes into account golfer biomechanics and can be used for evaluating golf drivers based on ball carry distance.

The second portion of the project consisted of the development of a golfer, club, impact and aerodynamic model that can be used for evaluating golf drivers. The golfer portion of the model is a 4 degree of freedom model of the torso, left arm, and hand of the golfer

that includes both passive and active joint torques. The active joint torques are calculated by parameterized joint torque equations that have been carefully designed to mimic the actions of human muscles acting on the joints in question, and can be turned on and off during the swing. The club portion of the model consists of a flexible shaft modeled using Rayleigh beam theory and a rigid clubhead. The shaft is able to accommodate bending in the transverse directions and axial rotation. Is also has varying stiffness properties along its length which are set using polynomial representations of the E, I, G, and J curves. The third section of the model is an impulse-momentum impact model that is able to calculate the ball launch conditions given the clubhead speed, orientation, and angular velocity. Finally, the ball carry is calculated using a conventional aerodynamic model for golf ball flight.

The model is controlled by manipulating the active joint torques of the golfer in an optimization process that selects the correct times to turn the joint torques on and off during the swing to achieve the maximum ball carry. After optimization, the model using the default parameters was found to hit the ball 214 yards. To show that the algorithm successfully optimizes the swing of the golfer, the strength of the modeled golfer was varied and the muscle timings of the golfer were observed to change as the ball carry increased from 209 yards to 255 yards.

Finally, the model was used to perform experiments on some of the parameters involved in the design of a golf driver. The clubhead mass, clubhead centre of mass location, clubhead moment of inertia, club aerodynamics, and shaft flexibility were all manipulated within the model and the obtained carry results presented in Chapter 4. The recommendations for golf club design from these experiments are summarized here.

5.2   Recommendations

Based on the experiments performed in Chapter 4 the following recommendations can be made with regards to the design of golf clubs.

1. The mass of the clubhead should be around $200\,g$ for optimal carry distance.

2. The clubhead centre of mass should be located as close to the face of the club as possible along a horizontal line.

3. Different flexible shafts allow the golfer to hit the ball different distances and shaft stiffness should therefore be tuned for the golfer that is purchasing the club.

4. The aerodynamics of the club have a small effect on the carry and reducing the aerodynamic drag would allow golfers to hit the ball further. To accommodate for reduced drag force bending the club and reducing the dynamic loft, a more aerodynamic clubhead may need to be combined with a more flexible club.

5.3   Future Research

Continuing this line of research there are at least three different directions which could be taken. First, there are many more experiments which could be performed using the current model to examine the effect of different club and golfer parameters on the swing. Here are a few ideas, but there are probably many more questions that could be investigated using this model.

1. Using a stronger golfer (to simulate higher clubhead speeds) perform the same set of club experiments again to see if the experiments yield the same results for stronger

119

golfers. It may be that a more powerful golfer would be able to accommodate a larger clubhead more easily, or requires a different flexible shaft than the default golfer simulated in this model.

2. Allow the start point of the swing to start in more wound and less wound positions and change the passive strength properties of the golfer to simulate more or less flexible golfers.

3. Experiment with the loft of the golf club to investigate the effect of driver loft on carry distance.

4. Modify the shaft flexibility directly to produce flexibility profiles that follow certain desired trends and examine their effect on the golfer performance.

This is just a small number of the many studies that could be performed using this model. Another interesting approach might be to change the parameters that are varied in the optimization process from the golfer control parameters to the golf club parameters. Instead of adapting the swing to the chosen club, the optimization process would then adapt the club to the golfer's swing. To make this work, it would probably be necessary to perform a rotation of optimizations back and forth between the club and the golfer to find good swings for the new club. Attempting to optimize both the golfer and club parameters at the same time would probably be too many parameters for the current techniques to find a good solution.

Second, the current model would benefit from significant experimental work being performed to validate the model and confirm that the generated swings are possible by real golfers. While this model was based on other models that have been validated experimentally, and each individual component has been validated in previous work, the complete

model has not been experimentally confirmed. An experimental study in which a number of golfers are examined and compared to the swings found by this model should be undertaken to confirm the findings of this work. In particular, it would be interesting to compare the maximum torques found through an inverse dynamic analysis with the torques generated during the swing by the model in this work.

There are many ways that the model of the swing could be expanded to increase the range of experiments that can be investigated through its use or to improve its fidelity.

1. Replace the joint torque generators with muscles like those used in other biomechanical models [7] [53]. This should not have a large effect on the torques that can be generated at each joint, but the model could then be used to determine which muscles contribute most to the golf swing.

2. Include the hips of the golfer as both a torsional and translational degree of freedom. This would improve the ability of the model to match the kinematics of a real golfer at the cost of increased complexity in the model.

3. Similarly, the inclusion of the elbow joint could be used to determine whether the optimized golfer would choose to keep their arm straight throughout the swing or to start with it bent and straighten at some point during the swing.

4. The inclusion of joint torques that could be activated partially to allow the pronation of the arm to happen more slowly during the swing could improve the ability of the model to strike the ball and decrease the sensitivity of the swing to changes in the joint torques timing.

5. The impact model which is used in this work could be replaced with a model that accounts for the deformation of the ball and club during impact using a finite element

modeling approach, a volumetric contact model, or some other modeling technique that improves the accuracy of the ball launch conditions.

6. Modern aerodynamic coefficients for the ball aerodynamic model could be obtained by experiment to improve the results of the carry model.

7. Place the ball at a location relative to the torso before the swing begins, detect the impact point, and calculate the ball launch conditions based on the clubhead orientation at that time. This would remove the constraint that the ball be struck at the centre of face of the club and allow for the possibility of applying the impact impulses backwards into the club and golfer. The location of the ball would probably need to be included as part of the optimization parameters to achieve good swings, and would require significant computing time and resources.

8. Include the backswing of the golfer so that the flexible club starts the swing with the correct curvature due to the dynamic loads of the backswing.

These improvements to the model would increase the range of experiments that can be performed with it and improve the accuracy of the results.

References

[1] B.M. Nigg and W. Herzog, *Biomechanics of the Musculo-skeletal System*, John Wiley & Sons, Chichester, 3rd edition, 2006.

[2] G.T. Yamaguchi, *Dynamic Modeling of Musculoskeletal Motion*, Springer Science and Business Media, New York NY, 2006.

[3] A.E. Engin and S.-M. Chen, "Statistical Data Base for the Biomechanical Properties of the Human Shoulder Complex - II:Passive Resistive Properties Beyond the Shoulder Complex Sinus", *Journal of biomechanical engineering*, vol. 108, no. 3, pp. 222–227, 1986.

[4] P. Shi and J. McPhee, "Dynamics of flexible multibody systems using virtual work and linear graph theory", *Multibody System Dynamics*, vol. 4, pp. 355–381, 1999.

[5] HSBC, "Golf's 2020 Vision : The HSBC Report", Tech. Rep., HSBC, 2012.

[6] D. Coate, "Driving Distance on the PGA and LPGA Tours, 1993-2012", Tech. Rep. June 2013, PGA Tour, Newark, NJ, 2013.

[7] N. Mehrabi, R. S. Razavian, and J. McPhee, "A Physics-Based Musculoskeletal Driver Model to Study Steering Tasks", *Journal of Computational and Non-Linear Dynamics*, 2014.

[8] A. Cochran and J. Stobbs, *Search for the Perfect Swing*, Triumph Books, Chicago, 2nd edition, 2005.

[9] C. I. Egret, O. Vincent, J. Weber, F. H. Dujardin, and D. Chollet, "Analysis of 3D kinematics concerning three different clubs in golf swing.", *International Journal of Sports Medicine*, vol. 24, no. 6, pp. 465–469, 2003.

[10] P. A. Hume, J. Keogh, and D. Reid, "The Role of Biomechanics in Maximising Distance and Accuracy of Golf Shots.", *Sports Medicine*, vol. 35, no. 5, pp. 429–449, 2005.

[11] A. Vena, D. Budney, T. Forest, and J. Carey, "Three-dimensional kinematic analysis of the golf swing using instantaneous screw axis theory, Part 2: golf swing kinematic sequence.", *Sports Engineering (Springer Science & Business Media B.V.)*, vol. 13, no. 3, pp. 125–133, 2011.

[12] R. Neal, R. Lumsden, M. Holland, and B. Mason, "Body Segment Sequencing and Timing in Golf.", *International Journal of Sports Science & Coaching*, vol. 2, no. 0, pp. 25–36, 2007.

[13] S. G.S. Coleman and A. J. Rankin, "A three dimensional examination of the planar golf swing", *Journal of Sports Science*, vol. 3, no. 23, pp. 227–234, 2005.

[14] T. Iwatsubo, K. Adachi, and T. Kitagawa, "A study of link models for dynamic analysis of swing motion", in *Engineering of Sport 4*, S Ujihashi and S J Haake, Eds., Kyoto, 2002, pp. 701–707, Blackwell Publishing.

[15] J. M. Mansour and M. L. Audu, "The Passive Elastic Moment at the Knee and its Influence on Human Gait", *Journal of Biomechanics*, vol. 19, no. 5, pp. 369–373, 1986.

[16] S. J. MacKenzie and E. J Sprigings, "A three-dimensional forward dynamics model of the golf swing", *Sports Engineering (Springer Science & Business Media B.V.)*, vol. 11, no. 4, pp. 165–175, 2009.

[17] S. J. MacKenzie, *Understanding the Role of Shaft Stiffness in the Golf Swing*, PhD thesis, University of Saskatchewan, 2005.

[18] R. D. Milne and J. P. Davis, "The role of the shaft in the golf swing.", *Journal of biomechanics*, vol. 25, no. 9, pp. 975–983, 1992.

[19] S. J. MacKenzie and E. J. Sprigings, "Understanding the role of shaft stiffness in the golf swing", *Sports Engineering*, vol. 12, no. 1, pp. 13–19, Oct. 2009.

[20] M. A. Lampsa, "Maximizing Distance of the Golf Drive: An Optimal Control Study", *Journal of Dynamic Systems, Measurement, and Control*, vol. 97, no. 4, pp. 362, 1975.

[21] M.G. Reyes and A. Mittendorf, "A Mathematical Swing Model for a Long-Driving Champion", in *Science and golf III: proceedings of the 1998 World Scientific Congress of Golf*, M. R. Farrally and A. J. Cochran, Eds., St. Andrews, Scotland, 1999, pp. 13–19, Human Kinetics.

[22] R. S. Sharp, "On the mechanics of the golf swing", *Proceedings of the Royal Society A: Mathematical, Physical and Engineering Sciences*, vol. 465, no. 2102, pp. 551–570, Feb. 2009.

[23] S. Sandhu, M. Millard, J. McPhee, and D. Brekke, "3D dynamic modelling and simulation of a golf drive", *Procedia Engineering*, vol. 2, no. 2, pp. 3243–3248, June 2010.

[24] W. Petersen and J. McPhee, "Comparison of Impulse-Momentum and Finite Element Models for Impact between Golf Ball and Clubhead", in *Science and Golf V: Proceedings of the World Scientific Congress of Golf*, Phoenix, USA, 2008.

[25] United States Golf Association, "Rules of Golf: Appendix II - Design of Clubs", 2014.

[26] T. Yamaguchi and T. Iwatsubo, "Optimum Design of Golf Club Considering Mechanical Impedance Matching", in *Science and Golf III: proceedings of the 1998 World Scientific Congress of Golf*, M.R. Farraly and Alastair J Cochran, Eds., St. Andrews, Scotland, 1998, pp. 500–509, Human Kinetics.

[27] L.J. Briggs, "Effect of spin and speed on the lateral deflection (curve) of a baseball; and the Magnus effect for smooth spheres", *American Journal of Physics*, vol. 27, no. 8, pp. 589, 1959.

[28] J. McPhee and G. C. Andrews, "Effect of sidespin and wind on projectile trajectory, with particular application to golf", *American Journal of Physics*, vol. 56, no. 10, pp. 933, 1988.

[29] S. Baek, "Flight Trajectory of a Golf Ball for a Realistic Game", *International Journal of Innovation, Management and Technology*, vol. 4, no. 3, pp. 346–350, 2013.

[30] T. Cunneff, "Get in Gear - Drivers Long Distance Calling", `http://www.linksmagazine.com/best_of_golf/get-in-gear-drivers`, Accessed: 2014-10-30.

[31] Golf Digest, "Lighter is better: Equipment Q&A with Nate Radcliffe, Cleveland Golf", 2011.

[32] S. M. Nesbit, "A three dimensional kinematic and kinetic study of the golf swing", *Journal of Sports Science & Medicine*, vol. 4, pp. 499–519, 2005.

[33] S. M. Nesbit and M. Serrano, "Work and Power Analysis of the Golf Swing", *Journal of Sports Science & Medicine*, vol. 4, pp. 520–533, 2005.

[34] N. F. Betzler, *The Effect of Differing Shaft Dynamics on the Biomechanics of the Golf Swing*, PhD thesis, Edinburgh Napier University, 2010.

[35] I. C. Kenny, A. J. McCloy, E. S. Wallace, and S. R. Otto, "Segmental sequencing of kinetic energy in a computer-simulated golf swing", *Sports Engineering*, vol. 11, no. 1, pp. 37–45, July 2008.

[36] D. Haeufle, J. Worobets, I. Wright, J. Haeufle, and D. Stefanyshyn, "Golfers do not respond to changes in shaft mass properties in a mechanically predictable way.", *Sports Engineering (Springer Science & Business Media B.V.)*, vol. 15, no. 4, pp. 215–220, 2012.

[37] W. M. Pickering and G. T. Vickers, "On the double pendulum model of the golf swing", *Sports Engineering*, vol. 2, pp. 161–172, 1999.

[38] S. J. MacKenzie and E. J. Sprigings, "Understanding the mechanisms of shaft deflection in the golf swing", *Sports Engineering*, vol. 12, no. 2, pp. 69–75, Jan. 2010.

[39] I.E. Brown and G.E. Loeb, "Measured and modeled properties of mammalian skeletal muscle: IV. Dynamics of activation and deactivation.", *Journal of Muscle Research and Cell Motility*, vol. 21, no. 1, pp. 33–47, Jan. 2000.

[40] M.L. Audu and D.T. Davy, "The influence of muscle model complexity in musculoskeletal motion modeling.", *Journal of biomechanical engineering*, vol. 107, no. 2, pp. 147–57, May 1985.

[41] M. Hirashima, K. Ohgane, K. Kudo, K. Hase, and T. Ohtsuki, "Counteractive relationship between the interaction torque and muscle torque at the wrist is predestined in ball-throwing.", *Journal of neurophysiology*, vol. 90, no. 3, pp. 1449–63, Sept. 2003.

[42] S. McGill, J. Seguin, and G. Bennett, "Passive stiffness of the lumbar torso in flexion, extension, lateral bending, and axial rotation. Effect of belt wearing and breath holding.", *Spine*, vol. 19, no. 6, pp. 696–704, 1994.

[43] A.E. Engin, "Passive resistive torques about the long bone axes of major human joints.", *Aviation, space, and environmental medicine*, vol. 50, no. 10, pp. 1052–1057, 1979.

[44] P. Shi, J. McPhee, and G. R. Heppler, "A deformation field for euler-bernoulli beams with applications to flexible multibody dynamics", *Multibody System Dynamics*.

[45] E. Henrikson, P. Wood, and J. Hart, "Experimental investigation of golf driver club head drag reduction through the use of aerodynamic features on the driver crown", *Procedia Engineering*, vol. 72, pp. 726–731, 2014.

[46] M. Sadraey, *Aircraft Performance Analysis*, VDM Verlag Dr. Muller, 2009.

[47] S. J. Quintavalla, "A generally applicable model for the aerodynamic behavior of golf balls", in *Science and Golf IV: Proceedings of the 2002 World Scientific Congress of Golf*, E. Thain, Ed., St. Andrews, Scotland, 2002, pp. 341–348, Routledge.

[48] MapleSim, *Version 7.0*, MapleSoft, Waterloo, ON, 2014.

[49] MATLAB, *Version 8.2.0.701 (R2013b)*, The MathWorks Inc., Natick, Massachusetts, 2013.

[50] D. M. Lindsay, S. Mantrop, and A. A. Vandervoort, "A Review of Biomechanical Differences Between Golfers of Varied Skill Levels", *International Journal of Sports Science and Coaching*, vol. 3, pp. 187–197, 2009.

[51] C. Joyce, A. Burnett, and K. Ball, "Methodological considerations for the 3D measurement of the X-factor and lower trunk movement in golf.", *Sports Biomechanics - International Society of Biomechanics in Sports*, vol. 9, no. 3, pp. 206–21, Sept. 2010.

[52] R. D. Crowninshield and R. A. Brand, "A physiologically based criterion of muscle force prediction in locomotion.", *Journal of Biomechanics*, vol. 14, no. 11, pp. 793–801, 1981.

[53] V. Norman-Gerum and McPhee J., "Comparison of Cylindrical Wrapping Geometries to Via Points for Modeling Muscle Paths in the Estimation of Sit-to-Stand Muscle Forces", in *ASME 2013 International Design Engineering Technical Conferences and Computers and Information in Engineering Conference*, Portland, Oregon, USA, 2013, ASME.

APPENDICES

Appendix A

Shaft Characteristics - Polynomial Fits

The characteristics of the flexible club were modeled using 6th order polynomials to capture the changes in the E,I,G, and J curves. 4 different clubs were modeled using data provided by the manufacturer. While we are unable to provide the actual values due to an agreement with the manufacturer the polynomial fits for each of the four clubs are presented in this appendix.

In general, the fits are quite good but there are a couple cases where the polynomials were unable to match the desired shape exactly.
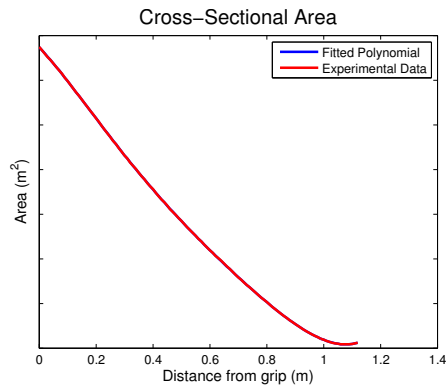
(a) Cross-sectional area vs. Distance
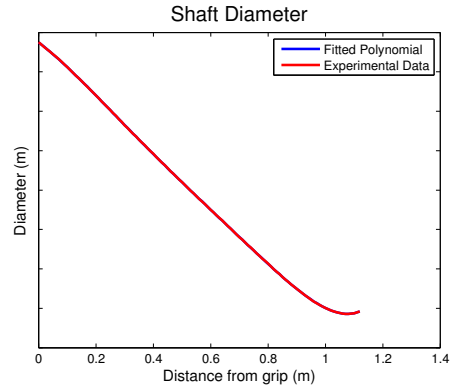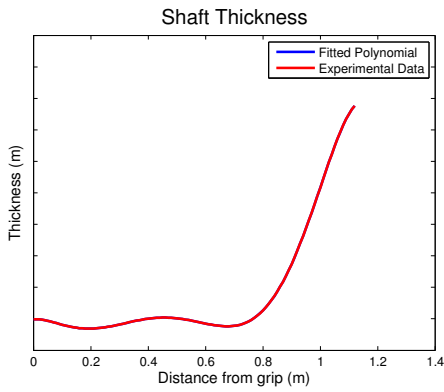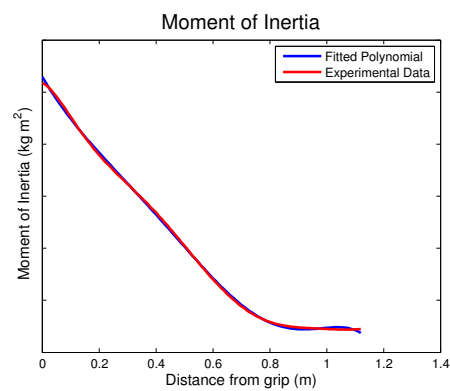
(b) Club shaft diameter vs. Distance

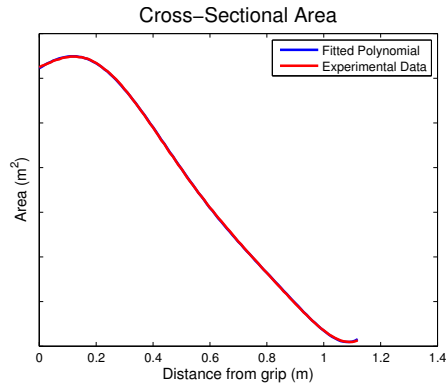(c) Club shaft thickness vs. Distance
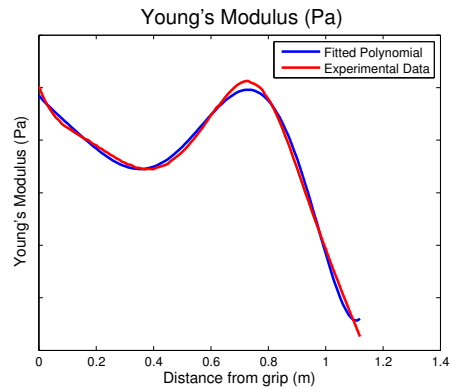
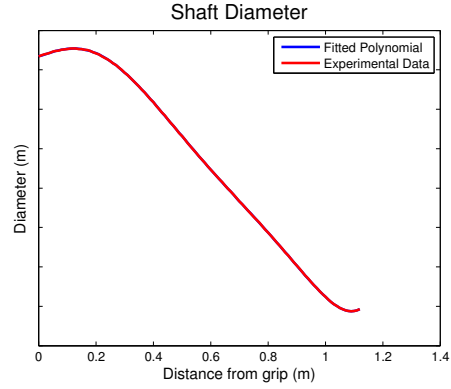(d) Young's Modulus vs. Distance
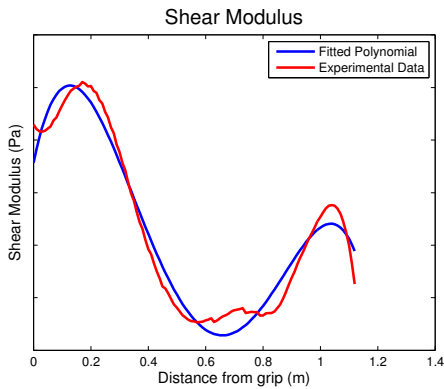
(e) Shear Modulus vs. Distance
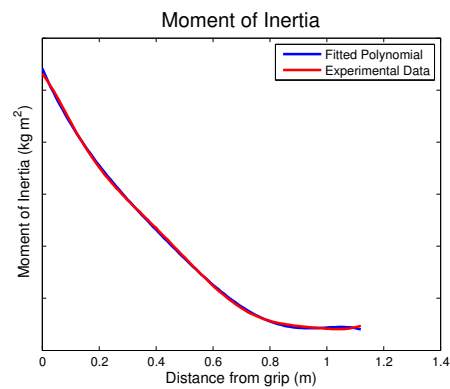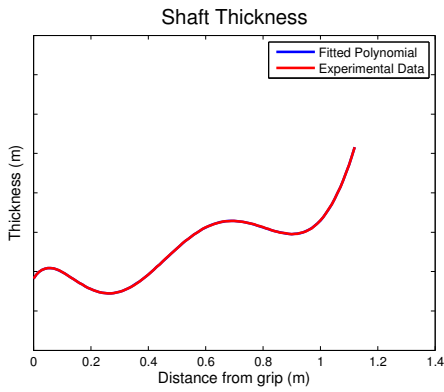
(f) Moment of Inertia vs. Distance

Figure A.1: Green club polynomial fitting comparison.
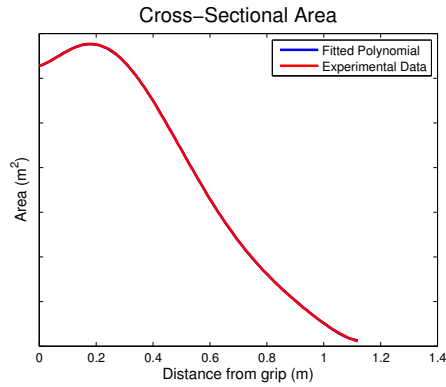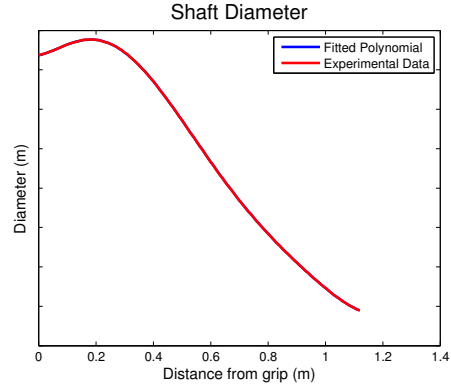
(a) Cross-sectional area vs. Distance

(b) Club shaft diameter vs. Distance
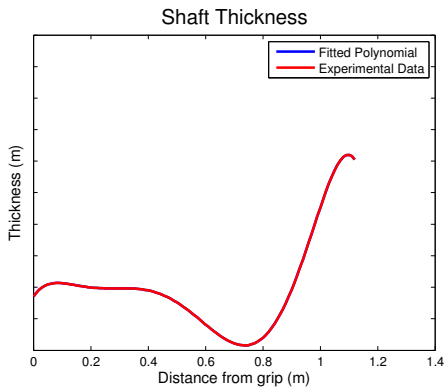
(c) Club shaft thickness vs. Distance
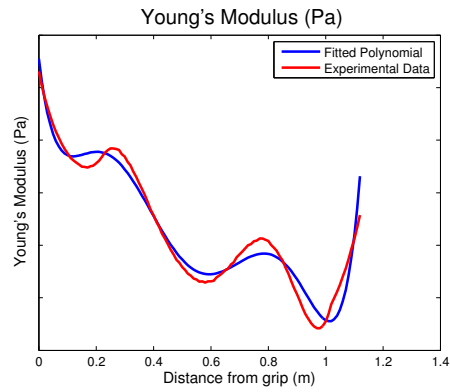
(d) Young's Modulus vs. Distance
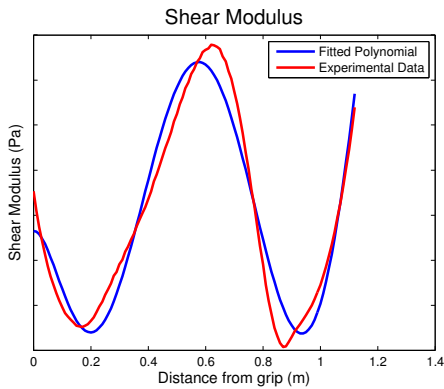
(e) Shear Modulus vs. Distance
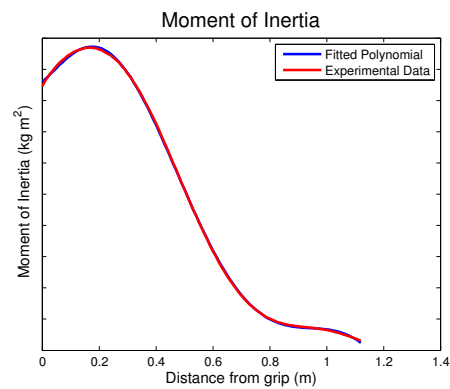
(f) Moment of Inertia vs. Distance

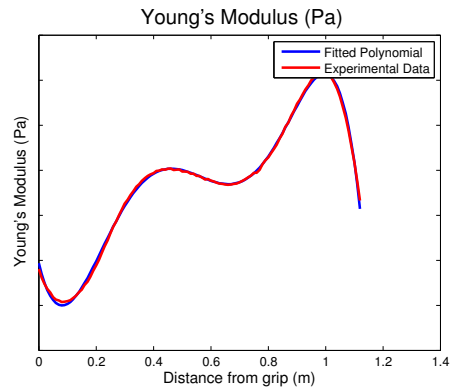Figure A.2: Yellow club polynomial fitting comparison.
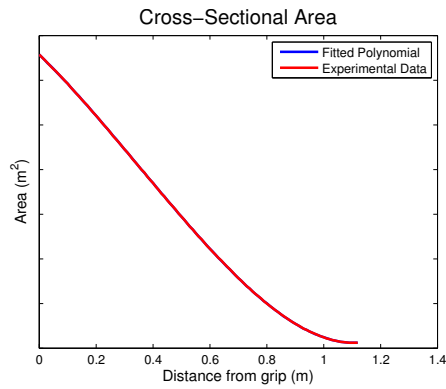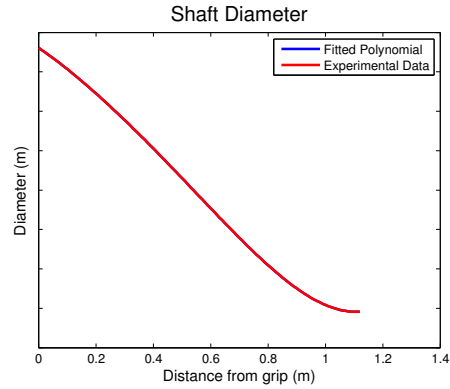
(a) Cross-sectional area vs. Distance

(b) Club shaft diameter vs. Distance
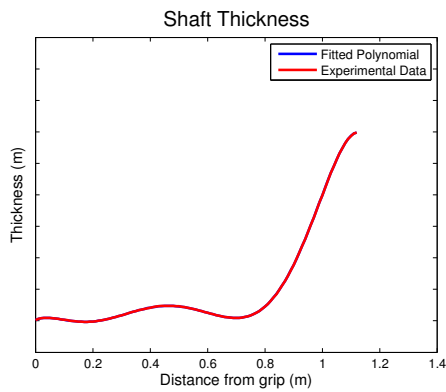
(c) Club shaft thickness vs. Distance
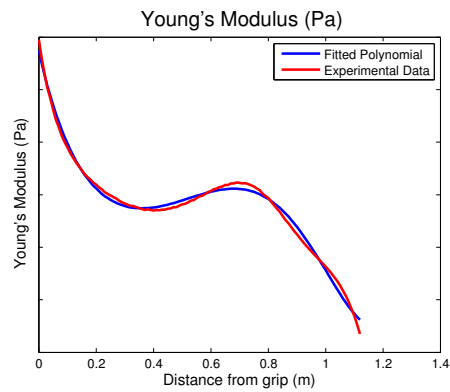
(d) Young's Modulus vs. Distance
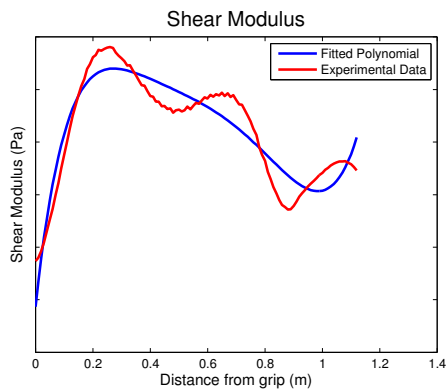
(e) Shear Modulus vs. Distance

(f) Moment of Inertia vs. Distance

Figure A.3: Orange club polynomial fitting comparison

(a) Cross-sectional area vs. Distance

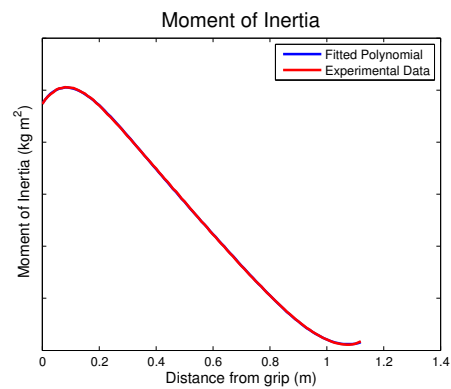(b) Club shaft diameter vs. Distance

(c) Club shaft thickness vs. Distance

(d) Young's Modulus vs. Distance
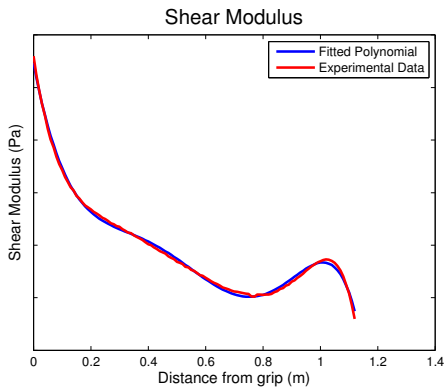
(e) Shear Modulus vs. Distance

(f) Moment of Inertia vs. Distance

Figure A.4: Red club polynomial fitting comparison